Dissertation Thesis

Effect of Elastic Knitted Fabric Construction Parameters on Thermo-physiological Properties

Study programme: P3106 Textile Engineering
Study branch: Textile Technics and Materials Engineering

Author: **Amany Ahmed Salama Khalil, M.Eng.**
Thesis Supervisor: Ing. Pavla Těšinová, Ph.D.
    Department of Textile Evaluation

Liberec 2023

Declaration

I hereby certify, I, myself, have written my dissertation as an original and primary work using the literature listed below and consulting it with my thesis supervisor and my thesis counsellor.

I acknowledge that my dissertation is fully governed by Act No. 121/2000 Coll., the Copyright Act, in particular Article 60 – School Work.

I acknowledge that the Technical University of Liberec does not infringe my copyrights by using my dissertation for internal purposes of the Technical University of Liberec.

I am aware of my obligation to inform the Technical University of Liberec on having used or granted license to use the results of my dissertation; in such a case the Technical University of Liberec may require reimbursement of the costs incurred for creating the result up to their actual amount.

At the same time, I honestly declare that the text of the printed version of my dissertation is identical with the text of the electronic version uploaded into the IS/STAG.

I acknowledge that the Technical University of Liberec will make my dissertation public in accordance with paragraph 47b of Act No. 111/1998 Coll., on Higher Education Institutions and on Amendment to Other Acts (the Higher Education Act), as amended.

I am aware of the consequences which may under the Higher Education Act result from a breach of this declaration.

April 22, 2023   Amany Ahmed Salama Khalil, M.Eng.

Abstract

To enhance the dimensional stability of knitted fabrics, spandex is incorporated in the knitting machine in form of core spun yarn or by plaiting technique. The thermo-physiological properties of the fabric are one of the most important properties that affect on the human comfort. Therefore, the proposed study aims to investigate the effect of construction parameters of elastic single jersey knitted fabric (*SJKF*), namely yarn count, loop length, spandex weight percent (*SWP*), and plaiting technique on the geometrical and thermo-physiological properties. The elastic SJKF were produced at two levels of yarn count (25 and 35 Ne), five levels of loop length (2.7, 2.9, 3.1, 3.3, 3.4 mm), and five levels of *SWP* (4, 5, 6, 7, 8%) with full and half plaiting techniques. For comparison, the 100% cotton samples were produced at the same levels of yarn count and loop length. The geometrical and thermo-physiological properties, fabric stretch, fabric growth, and thermal properties at two levels of extension (15 and 30%) were measured.

The results showed that Adding spandex leads to stitch overlapping; therefore, the elastic *SJKF* thickness was ranged between 3.6*d to 4.4*d where *d* is yarn diameter. The thermal conductivity and absorptivity, water vapor resistance, stitch density, and fabric weight of full and half plaited *SJKF* decreased when the loop length and *SWP* increased. While the thermal resistance and fabric thickness of the elastic *SJKF* increased with the loop length increasing, and decreased with *SWP* increasing. The thermal conductivity of full plaited knitted fabric was higher than half plaited fabric, and the thermal resistance of half plaited *SJKF* was higher than full plaited *SJKF*. The fabric growth of the full plaited *SJKF* was less than 100% cotton samples, while the fabric stretch of the elastic *SJKF* was higher than 100% cotton samples. When the fabric extension increased from 15 to 30%, the fabric thickness and the thermal conductivity, resistance, and absorptivity of full plaited decreased. The spandex incorporating in the weft knitting machine had a good impact on the geometrical and thermo-physiological properties.

Also, this study aims to present an innovated 3D geometrical model of the stitch overlapping, maximum set structure, and open structure to calculate the pore size and pore distribution through the SJKF structures by using AutoCAD software. A 3D multifiber model was developed based on actual construction parameters, such as loop length 2.9 mm, and yarn diameter 0.1662 mm. It was noticed that the overlapping structure had the smallest pore volume, followed by the maximum set, followed by the open structure.

The last aim of this study is to derive a new model that can be used to predict the

thermal conductivity of the elastic *SJKF* based on the geometrical parameters of the loop and fibers direction to the heat flow direction. It was marked that the predicted values of the thermal conductivity from the new model were very close to the experimental values, and model is prepared to be used for prediction of thermal properties of *SJKF*.

Keywords:

Elastic knitted fabric; full plaited; half plaited; thermo-physiological properties; water vapor resistance; thermal conductivity; stitch overlapping; geometrical model.

Abstrakt

Pro zvýšení rozměrové stability je do pletacího stroje při pletení přiváděn spandex ve formě jádrové příze nebo technikou kladení. Termo-fyziologické vlastnosti plošných textilií jsou jednou z nejdůležitějších vlastností, které ovlivňují pohodlí člověka. Navrhovaná studie si proto klade za cíl prozkoumat vliv konstrukčních parametrů elastické jednolícní pleteniny (SJKF), konkrétně jemnosti příze, délky oček, hmotnostního podílu spandexu (SWP) a techniky kladení spandexu na geometrické a termo-fyziologické vlastnosti. Pleteniny byly vyrobeny ve dvou jemnostech příze (25 a 35 Ne), pěti délkách očka (2,7; 2,9; 3,1; 3,3; 3,4 mm), pěti podílech spandexu (4, 5, 6, 7 a 8 %) a s plným a polovičním kladením spandexu. Pro srovnání byly vyrobeny vzorky ze 100% bavlny se stejnými jemnostmi příze a délky očka. Byly naměřeny geometrické a termo-fyziologické vlastnosti, statické a trvalé prodloužení pleteniny a tepelné vlastnosti v relaxovaném stavu a na dvou úrovních roztažení (15 a 30 %).

Výsledky ukázaly, že přidání spandexu vede k výraznému překrývání oček, proto se tloušťka SJKF pohybovala v násobcích průměru příze *d* mezi 3,6*d až 4,4*d. Tepelná vodivost a nasákavost, výparný odpor, hustota oček a hmotnost pleteniny plně a polovičně kladené SJKF se snížily, když se délka očka a SWP zvětšily. Zatímco tepelný odpor a tloušťka pleteniny rostly s rostoucí délkou očka a klesaly s rostoucím SWP. Tepelná vodivost pleteniny plně kladeného spandexu byla vyšší než pleteniny polovičně kladeného spandexu. Tepelný odpor pleteniny polovičně kladeného spandexu byl vyšší než pleteniny plně kladeného spandexu. Trvalé prodloužení u plně kladených SJKF bylo menší než u vzorků ze 100% bavlny, zatímco statické prodloužení u elastických SJKF bylo vyšší než u vzorků ze 100% bavlny. Když se roztažení pleteniny zvýšilo z 15 na 30 %, tloušťka pleteniny, tepelná vodivost, tepelný odpor a nasákavost plně kladeného materiálu se snížily. Začlenění spandexu do pletacího stroje mělo pozitivní vliv na geometrické a termo-

fyziologické vlastnosti.

Tato studie si také klade za cíl prezentovat inovované 3D geometrické modely s překrýváním oček, strukturou maximálního zaplnění a otevřenou strukturou pro výpočet velikosti pórů a distribuce pórů ve strukturách SJKF pomocí softwaru AutoCAD. Byl vytvořeny původní 3D modely zohledňující i vlákna na základě skutečných konstrukčních parametrů, jako je délka očka 2,9 mm a průměr příze 0,1662 mm. Bylo potvrzeno, že překrývající se struktura měla nejmenší objem pórů, následovaný modelem s maximální dostavou a modelem s otevřenou strukturou.

Posledním cílem této studie bylo odvodit nový model, který lze použít k predikci tepelné vodivosti elastického SJKF, na základě geometrických parametrů očka a poloze vláken ke směru tepelného toku. Bylo ověřeno, že predikované hodnoty tepelné vodivosti z nového modelu byly velmi blízké experimentálním hodnotám a model je tedy možné úspěšně aplikovat na predikci tepelné vodivosti SJKF.

Klíčová slova:
Elastická pletenina; plné kladení; poloviční kladení; termo-fyziologické vlastnosti; výparný odpor; tepelná vodivost; překrývání oček; geometrický model.

List of Figures

List of Tables

Number	Table description	Page
4.1	SJKF specifications	11
4.2	Factors information of factorial design	17
5.1	The results of variance analysis (P value at significant level 95 %)	20
5.2	The significant levels of yarn count and SWP on fabric growth and stretch	43
6.1	Actual loop geometrical parameters	56
6.2	Theoretical pore's volume values of different fabric structures at different sections	61
7.1	Curve fitting equations for the relation between thermal conductivity and loop length	77

All other tables were listed in chapter 10 (Appendices) from table 10.1 to 10.28.

Content

Table of Contents

List of Abbreviations and Nomenclature

Symbol	Description	Unit
ε	Fabric porosity	%
ρ_f	Fibre density	$Kg.m^{-3}$
ρ_c	Cotton fibre density	$Kg.m^{-3}$
ρ_s	Spandex fibre density	$Kg.m^{-3}$
ρ_{fabric}	Fabric density	$Kg.m^{-3}$
W	Fabric weight per unit area	$g.m^{-2}$
h	Fabric thickness	mm
b	Thermal absorptivity	$W. s^{1/2} m^{-2}. K^{-1}$
α_e	Twist factor	-
d	Yarn diameter	mm
c	Course spacing	mm
w	Wale spacing	mm
l	Loop length	mm
C	Specific heat capacity	$J. kg^{-1}. K^{-1}$
λ	Thermal conductivity coefficient	$W. m^{-1}. K^{-1}$
λ_{fab}	Fabric thermal conductivity coefficient	$W. m^{-1}. K^{-1}$
λ_f	Fibres thermal conductivity coefficient	$W. m^{-1}. K^{-1}$
λ_c	Cotton fibres thermal conductivity coefficient (0.5)	$W. m^{-1}. K^{-1}$
λ_s	Spandex fibres thermal conductivity coefficient (0.15)	$W. m^{-1}. K^{-1}$
λ_a	Thermal conductivity of air (0.026)	$W. m^{-1}. K^{-1}$
λ_{cotton}	Thermal conductivity of cotton fibres in one repeat	$W. m^{-1}. K^{-1}$
$\lambda_{spandex}$	Thermal conductivity of spandex in one repeat	$W. m^{-1}. K^{-1}$
λ_{air}	Thermal conductivity of air in one repeat	$W. m^{-1}. K^{-1}$
λ_{ser}	Thermal conductivity of fibres in series	$W. m^{-1}. K^{-1}$
λ_p	Thermal conductivity of fibres in parallel	$W. m^{-1}. K^{-1}$
F_c	Cotton fibres volume fraction	-
F_s	Spandex volume fraction	-
F_f	Total fibres volume fraction	-
F_a	Air volume fraction	-
A	Original distance between bench marks (100 mm)	mm

B	Distance between bench marks measured after 1 min of tension release	mm
D	Distance between bench marks measured after 60 min of tension release	mm
E	Distance between bench marks measured while specimen is under tension force	mm
$SJKF$	Single jersey knitted fabric	-
SWP	Spandex weight percent	%
fp	Full plaited	-
hp	Half plaited	-
WVR	Water vapour resistance	Pa. m^2. W^{-1}
FGW	Fabric growth in wales direction	%
FGC	Fabric growth in courses direction	%
FSW	Fabric stretch in wales direction	%
FSC	Fabric stretch in courses direction	%
$ME\ 2$	Maxwell- Eucken 2 model	-
N	total number of fibres in yarn cross-section	-
T	Yarn count	tex (g/km)
t	Cotton fibre fineness	tex (g/km)
D	Cotton fibre diameter	mm
A	Cotton fibre cross-section area	mm^2
TPI	Number of twists per inch	t/in
Nm	Yarn metric count	Nm (m/g)
Ne	English yarn count	Ne (yd/Ib)
V_{pi}	Pores volume at ith section	mm^3
V_{xi}	Enclosure volume of the ith section	mm^3
V_{fi}	Fibre volume of the ith section	mm^3
ε_i	Theoretical porosity in the ith section	%

1. CHAPTER 1: INTRODUCTION

The human body tries to maintain a constant core temperature of about 37°C where a rise or fall of 5°C can be fatal. The human body continuously generates heat by its metabolic processes. The heat is lost from the body by conduction, convection, radiation, evaporation, and respiration [1]. Body heat balance varies with the climate; in hot climates, the problem is one of heat dissipation, whereas in cold climates, it is one of heat conservation. Clothing plays an important role in the maintenance of heat balance as it modifies the heat loss from the skin surface and at the same time, has the secondary effect of altering the moisture loss from the skin [2]. The general clothing assemblies approximately covers around 90% of the human body. Therefore, the heat and moisture transmission behaviour of the fabric plays a very important role in maintaining thermo-physiological comfort [1].

The thermo-physiological properties of fabrics have a significant impact on the human thermal comfort [3], which is defined as a state of satisfaction with the thermal conditions of the environment [4]. The thermal comfort properties study the way in which the heat, air and water vapour are transmitted through a fabric which is heterogenous mixture of solid fibres and air. The fabric's thermo-physiological properties depend on the temperature difference between environment and skin, construction parameters of fabrics, yarns structure, yarn properties, fibre's properties, fibre's type, fabric thickness, porosity, areal density, number of fabric layers, and trapped air [5].

Textile fabrics have varying degrees of flexibility based on structural parameters [6]. Knitted fabrics are characterized by comfort compared to woven fabrics due to their high extensibility (compression and elongation of individual stitch), air permeability, and heat retention, but the dimensional stability after repeated washing especially single jersey knitted fabrics (*SJKF*) is considered the main disadvantage. To enhance the dimensional stability and maintain the dimensions during use and after repeated stresses of knitted fabrics, the spandex on form of plaiting technique or core-spun yarn are used. In plaiting technique, spandex is incorporated with cotton yarns by using a separate feeder for spandex. If the spandex and cotton yarn are knitted side-by-side in every course, with the spandex yarn always kept on one side of the cotton yarn, this is called full plaiting. When the spandex is incorporated in alternating courses, the method is called half plaiting [7].

Lycra is the trade name of elastane (spandex) yarns and has an extension-at-break greater than 200 %, and shows high recovery after unloading. These fibres exhibit rubber-like behaviour with high reversible extension as high as 400 - 800 %. Chemically, spandex is a synthetic linear macromolecule with a long chain containing at least 85 % of segmented polyurethane along with the alternating hard and soft segments linked by urethane bonds – NH – CO – O – [8][9][10][11]. Soft segment gives elasticity (stitch rearrangement), while the hard segment gives molecular interaction force to the fibre and which ensures a certain level of strength of the fibre and long-term stability. Spandex improves the dimensional stability, body fit of weft knitted fabric and freedom of body movements. Spandex proportion is one of the most important parameters of single jersey plaited fabrics and influences fabric characteristics [12].

So, there is a need to investigate the effect of spandex weight percent on the thermo-physiological comfort properties of elastic *SJKF*. The aim of this thesis is firstly, to estimate the effect of construction parameters of elastic *SJKF*, namely yarn count, loop length, and spandex weight percent on the geometrical and thermo-physiological comfort properties. Secondly a mathematical model is presented to predict thermal conductivity of elastic *SJKF*. Thirdly, a new approach to investigate the pore size and pore distribution inside the *SJKF* structure is proposed.

2. CHAPTER 2: OVERVIEW OF THE CURRENT STATE OF THE PROBLEM

In the last decades, a lot of researchers have been concerned with the thermo-physiological properties of knitted fabrics. The thermal properties of plain, rib and interlock produced from cotton-bamboo blended yarns were investigated [13]. It was included that the thermal conductivity of knitted fabric decreased when the yarn count increased (became finer). The thermal conductivity and thermal resistance values of interlock fabric was the maximum followed by the rib and plain fabrics. The effect of fabric parameters on the thermal properties of polyester/cotton double layer knitted interlock fabrics was analysed [14]. The results showed that the thermal resistance depended on the percentage of fibre that had higher specific heat and thermal resistance was in direct proportion with the yarn count, loop length and fabric thickness. The thermal absorptivity of the fabric decreased with fabric weight decreasing and cotton content increasing. The effect of stitch length and fabric structure on the dimensional and thermo-physiological properties of knitted fabrics made of Seacell and elastane yarns were investigated [15]. Single Jersey, Single Piqué and Double Piqué were produced from yarns composed of 20% SeaCell pure/10% SeaCell Active/70% Combed Cotton, 12 tex and bare elastane 4.4 tex at loop lengths 2, 2.5, and 3 mm. It was concluded that the thermo-physiological properties can be changed by fabric construction and the loop length had a significant effect on the thermo-physiological properties, especially the thermal conductivity and air permeability. The effect of fibre, yarn and fabric parameters was investigated on heat and moisture transport properties of single jersey plated fabrics [16]. Twelve single jersey plated knit samples were produced from cotton, polyester, nylon, and viscose yarns at three levels of loop length. Cotton yarn was used in the outer layer while filament yarns of three varying fibre types were used in the inner (next to skin). It was found that as the loop length increased, the thermal resistance, conductivity, and absorptivity decreased while the relative water vapour permeability, air permeability and water absorbency increased. The thermo-physiological properties of double-layered weft fabrics knitted from cotton or man-made bamboo yarns and synthetic polyamide, polypropylene, and polyester yarns were studied [17]. The results showed that It was established that thermal properties of double-layered knitted fabrics depend on raw material, structural parameters and knitting pattern of the fabric.

Others have been concerned with the effect of spandex on the geometrical and

physical properties of elastic knitted fabric. The dimensional and physical properties of cotton/spandex single jersey fabrics were investigated and compared to 100% cotton knitted fabrics. The presence of spandex increased the fabric weight and thickness, on the contrary, it decreased air permeability, pilling grade, and spirality [18][19]. The geometrical characteristics of core-spun cotton/spandex interlock structures with high, medium and low tightness factors were studied under dry, wet, and full relaxation conditions. The elastic interlock samples had higher dimensional constants compared to 100 % cotton samples, and core cotton/spandex yarns increased tightness factors during relaxation states [20]. The effect of spandex type, the tightness factor of the base, and spandex yarn on the dimensional and physical properties of cotton/spandex single jersey fabrics were investigated. The fabrics knitted with spandex yarns that have the largest tension values under a constant draw ratio give the highest weight, courses per cm, stitches per cm^2, thickness, and lowest air permeability values [21]. The relation between spandex consumption and fabric dimensional and elastic behaviour of cotton/spandex plaited plain knitted fabrics was studied. The results showed that spandex proportion inside fabric has an incidence on fabric width, weight, and elasticity [12]. The effect of spandex yarn input tension, yarn loop length, and spandex yarn linear density on the elastic properties of spandex knitted fabrics was studied. The stitch density, fabric weight and thickness of spandex fabrics were higher, and fabric growth was lower than the knitted fabric without spandex. As the fabric loop length increased, the fabric stretch increased in both wale and course directions [22]. The effect of the extension percent of bare spandex yarns during loop formation on the geometrical, physical, and mechanical properties of plain jersey fabrics was studied. Results showed that for the full plaited (*fp)* and half plaited (*hp)* fabrics, the stitch density, fabric thickness and weight increased, while air permeability, initial elasticity modulus, and the breaking load and extension decreased considerably compared to 100% cotton knitted fabric [7]. The impact of the raw material, count of yarn, pattern and elastomeric yarn ratio on the performance and physical properties of the plain, pique, double-pique and fleeced elastic knitted fabrics was found out. Test results showed that raw material, yarn count, and elastane ratio had a significant effect on bursting strength [23]. The physical, dimensional, and mechanical properties of back plaited cotton/spandex *SJKF* were investigated and are compared to knitted fabrics made from 100% cotton, and the effect of spandex percentage was also studied. It was found that the presence of spandex in *SJKF* increased course density, fabric thickness, and fabric recovery, while fabric width, fabric porosity, and extension were decreased [24]. Plain and rib fabrics produced from

100% cotton, half-plaited and full-plaited were investigated for physical, dimensional, geometrical, and some comfort properties and compared to each other. The results showed that transfer wicking ratios of the half-plaited fabrics were the highest, whereas the transfer wicking ratios of the full-plaited fabrics were the lowest, and extension under constant load and residual deformation ratios decreased with the addition of spandex and the increase of spandex content [25]. Based on the previous research, spandex has a significant effect on the dimensional, physical and mechanical properties of knitted fabrics.

A few researchers have been concerned with the thermal comfort properties of elastic knitted fabrics. The artificial neural network (ANN) was used to predict the global thermal comfort index of stretched knitted fabric from the structural parameters as inputs [26]. The results showed that ANN was in good agreement with target and calculated input data. The thermal comfort properties of some Egyptian stretch knitted fabrics made from synthetic and spandex yarns based single jersey were statistically investigated. The results showed that both the thermal conductivity and resistance of all the selected fabric samples increased with the increase of fabric density, and the fabric temperature variation decreased with fabric thickness increasing [27]. The physical properties, strength and thermal comfort characteristics of the interlock knitted fabric produced from cotton and elastane yarns (full and half plaited) were investigated and compared to 100% cotton fabrics. It was included that the elastic fabrics produced from coarser elastane yarn had higher weight, thickness, bursting strength and puncture resistance. In terms of thermal comfort, the fabrics including coarser elastane yarn provided higher thermal conductivity and thermal absorptivity, lower air and relative water vapour permeability. As the elastane rate increased, fabric weight, thickness, bursting strength, puncture resistance, and thermal absorptivity increased, while air permeability decreased as well, and the fabrics knitted using elastane yarns presented higher thermal conductivity [28]. Based on the previous research, spandex has a significant effect on the dimensional, physical and mechanical properties of knitted fabrics. It was noticed that more researches are required to investigate and study the effect of spandex percent, loop length and spandex state (full and half plaited) on thermo-physiological properties of elastic knitted fabrics in details. Also, some data base about the thermo-physiological of elastic *SJKF* is needed to be available to the manufacturers and designers of fabrics.

3. CHAPTER 3: THE AIMS OF THE THESIS

The thermal comfort properties are one of the most important parameters that affect the human comfort. Last decades, researchers are interested in the thermal properties of textiles and try to find the parameters that affect consumer comfort. Based on the literature review, it was necessary in the current work to:

1. Investigate the effect of construction parameters of elastic *SJKF* (yarn count, loop length, spandex weight percent and plaiting technique) on the geometrical and thermo-physiological properties.

2. Analyse the effect of spandex percent on fabric growth and fabric stretch of *SJKF*.

3. Present a theoretical 3D model of stitch overlapping, maximum set, and open structures by using AutoCAD software to investigate the pore size and distribution for different *SJKF* structures.

4. Apply three simple mathematical models (Maxwell–Eucken 2, Schuhmeister, Militky) of thermal conductivity to investigate if these models can be used to predict the thermal conductivity of elastic *SJKF*.

5. Derive a new equation that describes the thermal conductivity of the elastic *SJKF* based on the loop geometry and the yarn and fibres inclination on the direction of heat flow.

6. To assist the manufacturers and designers to predict the thermo-physiological properties of elastic *SJKF* produced from cotton yarns.

4. CHAPTER 4: STUDIED MATERIAL AND USED METHODS

4.1 Studied materials

In order to investigate the effect of fabric construction parameters, two different combed yarn counts were produced (25 and 35Ne) from Egyptian cotton fibres Giza 86 (fibre fineness: 172 mtex, staple length: 32 mm) and with twist factor α_e=3.6 (838 and 709 turns per meter for yarn count 35 and 25 Ne, respectively). Then full and half plaited *SJKF* were produced with two yarn counts and five levels of spandex weight percent (*SWP)* (4, 5, 6, 7, and 8%) and five levels of the loop length (2.7, 2.9, 3.1, 3.3, and 3.4 mm) as shown in table 4.1. Spandex count was 30 and 70 dtex for full and half plaited respectively to get the same *SWP*. Spandex yarns (bare spandex) were incorporated by the plaiting technique (feeding spandex yarn at different tension with cotton yarn) where spandex yarns have a separate feeding system, plaiting roller and guide eye, as shown in figure 4.1. The adjustment of spandex percentage is obtained by adjusting and optimizing the speed of spandex delivery system. To increase spandex weight percent, the tension on spandex yarns decreased and vice versa. *SJKF* without spandex were produced at the same levels of yarn count and loop length. All samples were produced on VIGNONI SJ-B (number of feeders: 57, diameter: 19-inch, machine gauge: 24 needles/inch), and were treated according to the elastic knitted fabric finishing recipe. First, heat setting at 185 °C was applied, followed by dyeing at 95 °C and finally compacting at 90 °C.

Table 4.1: *SJKF* specifications

Yarn count		100% cotton	Full plaited					Half plaited				
	SWP (%)	0	4	5	6	7	8	4	5	6	7	8
25 Ne	Loop length (mm) 2.7	√	√	√	√	√	√	√	√	√	√	√
	2.9	√	√	√	√	√	√	√	√	√	√	√
	3.1	√	√	√	√	√	√	√	√	√	√	√
	3.3	√	√	√	√	√	√	√	√	√	√	√
	3.4	√	√	√	√	√	√	√	√	√	√	√
35 Ne	Loop length (mm) 2.7	√	√	√	√	√	√	√	√	√	√	√
	2.9	√	√	√	√	√	√	√	√	√	√	√
	3.1	√	√	√	√	√	√	√	√	√	√	√
	3.3	√	√	√	√	√	√	√	√	√	√	√
	3.4	√	√	√	√	√	√	√	√	√	√	√

Guide eye of cotton yarn

Plaiting roll

Latch needle

Guide eye of elastane yarn

Figure 4.1. Plaiting technique in knitting machine

4.2 Used methods

4.2.1 *Yarn diameter*

Yarn diameter was measured by taking images of the yarns by the camera (ProgRes-CT3) attached to a microscope under transmitted light. The captured images were analysed by using NIS-elements software. The threshold of binary images was adjusted then binary image processing was applied, such as erosion and dilation for 70 images for each count, as shown in figure 4.2. and the yarn diameter was calculated by inserting 70 images.
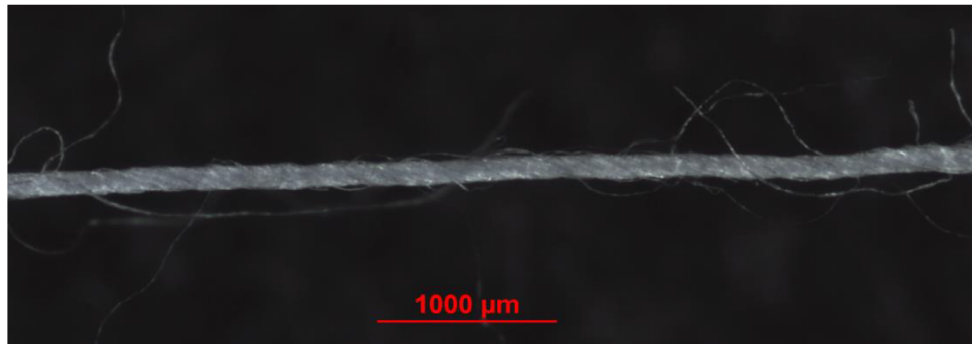
a- Yarn image before processing
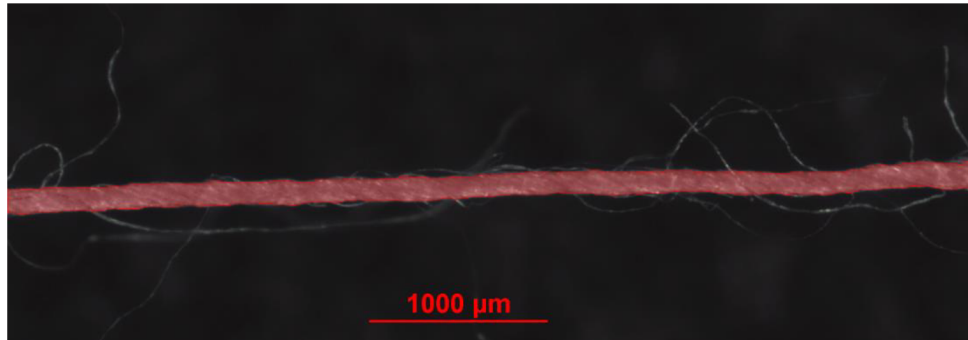
b- Yarn image after processing

Figure 4.2. Yarn images before and after binary processing

4.2.2 *Yarn bending rigidity*

The bending rigidity of yarns was measured according to internal standard No.22- 201- 01/01 [30]. Figure 4.3 shows the device used for testing, where one end of the yarn was fixed and another end was free under the yarn weight. Then the image of yarn bending was captured and analysed by using LUCIA image analysis software, as shown in figure 4.4, and the bending rigidity of yarn was obtained by applying the differential equation of the bending line [31].
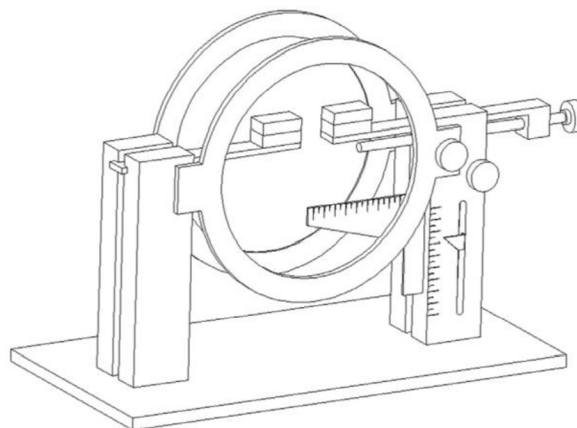
Figure 4.3 the device used for measuring yarn bending stiffness [30]
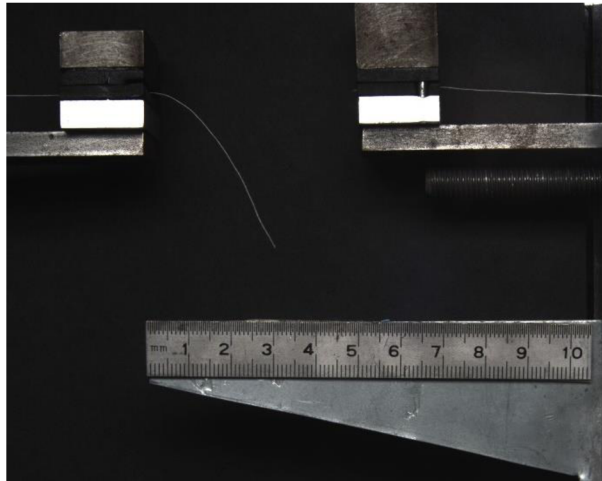
Figure 4.4 captures image of yarn bending

4.2.3   *Fabric porosity*

The fabric density (ρ_{fabric}) and fabric porosity (ε) were calculated from the following equations [32]:

$$\text{Fabric density, } \rho_{fabric} = \frac{W}{h} \qquad\qquad \dots\dots\dots\dots\dots \quad (4.1)$$

$$\text{Fabric porosity, } \varepsilon(\%) = \left(1 - \frac{\rho_{fabric}}{\rho_f}\right) * 100 \qquad \dots\dots\dots\dots\dots \quad (4.2)$$

Where W: fabric weight per unit area (g.m^{-2}), h: fabric thickness (mm) and ρ_f: fibre density (kg.m^{-3}). ρ_f for 100% cotton is equal to 1520 kg.m^{-3}, but ρ_f for elastic knitted fabric was calculated from equation 3.3 [33].

$$\rho_f = \frac{\rho_s\,\rho_c}{\frac{SWP}{100}\,\rho_c + \left(1 - \frac{SWP}{100}\right)\rho_s} \qquad \dots\dots\dots\dots\dots \quad (4.3)$$

Where ρ_s : spandex fibre density (kg.m^{-3}), ρ_c: cotton fibre density (kg.m^{-3}).

4.2.4   *Thermo-physiological properties*

Thermal conductivity, resistance and absorptivity and fabric thickness were measured by using Alambeta tester (non-destructive instrument) [34] according to the standard ISO 8301 [35]. Relative water vapour permeability was tested by Permetest instrument, which is the so-called skin model that simulates dry and wet human skin in terms of its thermal feeling [36][37] according to ISO 11092 [38]. Air permeability was measured by FX 3300-20 Labotester III according to EN ISO 9237 [39]. Fabric growth and fabric stretch were

measured according to ASTM D2594 – 04 [29] as follows:

4.2.5 *Fabric growth and fabric stretch*

Flexi-frame was designed according to the standard, as shown in figure 4.5. Fabric samples were cut with the dimension of 125 mm*400 mm, folded in half lengthwise forming a loop and sewed, then bench marks 100 mm were placed on samples. Fabric sample was hanged on rods of flexi-frame, as shown in figure 4.6, then extensions 15% and 30% were applied in wales and course direction, respectively, by moving a movable board down. After an extension was applied for 2 hrs. ±5 min, the sample was free from flexi-frame and put on the table, and the length between bench marks was measured after 1 min and 60 min. To measure the fabric stretch, the tension force (10, 15, 20, and 25 N) were applied, as shown in figure 4.7, and the length between bench marks was measured after applying weight by a ruler or from monitor.
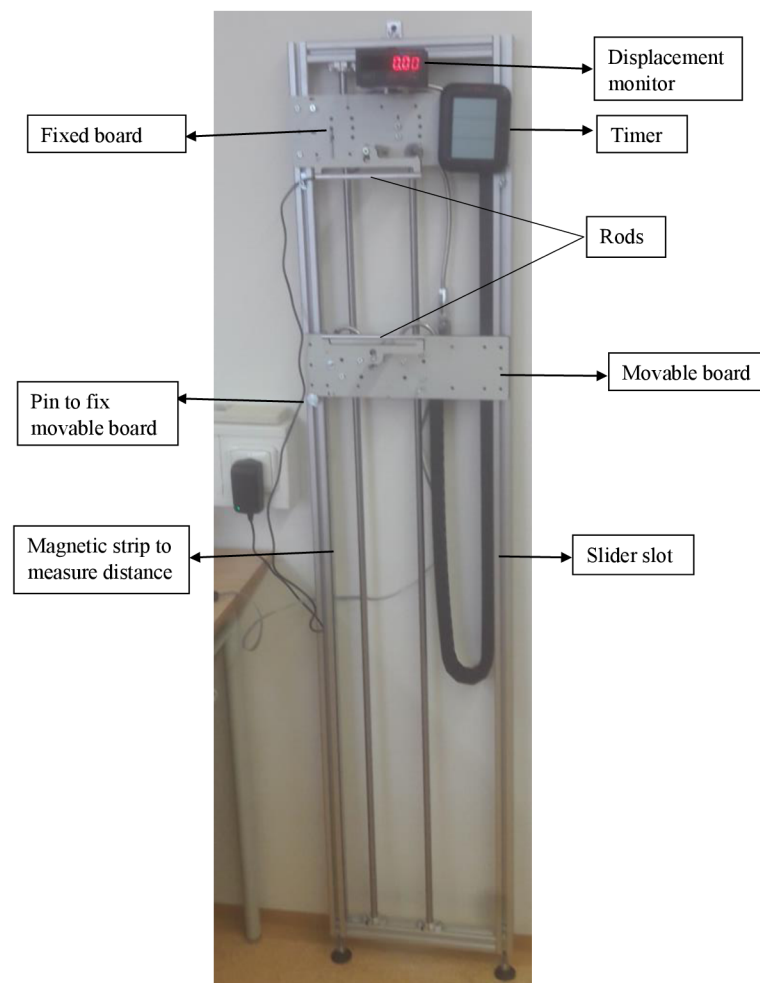
Figure 4.5. Flexi-frame
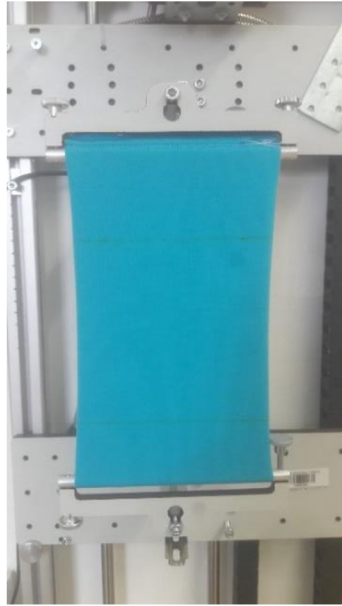
Figure 4.6. Hanged sample

Figure 4.7. Applied tension force

The Fabric growth and fabric stretch were calculated from the following equations:

$$Fabric\ Growth_{1\ min}\ (\%) = \frac{B - A}{A} * 100 \qquad \dots \dots \dots \dots [4.4]$$

$$Fabric\ Growth_{60\ min}\ (\%) = \frac{D - A}{A} * 100 \qquad \dots \dots \dots \dots [4.5]$$

$$Fabric\ Stretch\ (\%) = \frac{E - A}{A} * 100 \qquad \dots \dots \dots \dots [4.6]$$

Where A is the original distance between bench marks (100 mm), B is the distance between bench marks measured after 1 min of tension force release, D is the distance between bench marks measured after 60 min of tension release. Recovery, E is the distance between bench marks measured while the specimen is under tension force.

4.2.6   *Thermal properties under extension*

Thermal properties (thermal conductivity, resistance and absorptivity) and fabric thickness were measured under two levels of extension 15 and 30% for loose fitting knitted fabric as mentioned on the standard test method ASTM D2594 – 04. The thermal properties of compression knitted fabric under extensions ranged between 0 to 60% was investigated [40][41]. The extensions were applied by embroidery frame of diameter 15 cm, as shown in figure 4.8. To obtain 15 and 30% extension, two circles with diameters

13 and 11.5 cm were marked respectively on the samples. Then the samples were extended to get the desired extension.
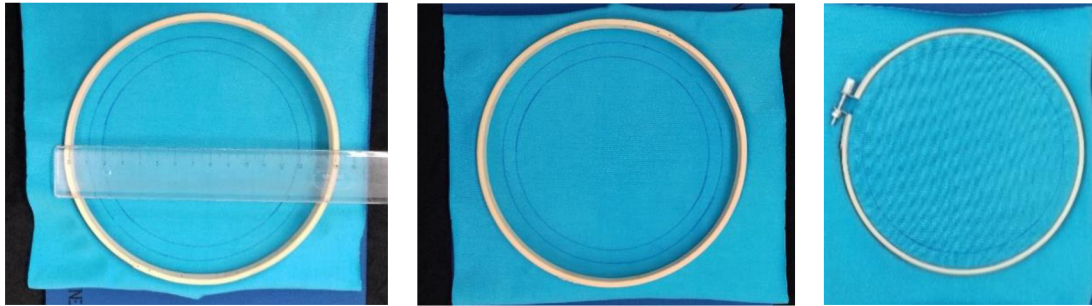
Figure 4.8. Applied extension by using embroidery frame

To determine the significance effects of the yarn count, loop length, *SWP* and plaiting technique on all tested properties of elastic *SJKF* at 95% significant level, the general factorial analysis was applied by using Minitab program. Table 4.2 shows the factors information. Multi-way ANOVA was applied to investigate the effect of *SWP*, relation time, and direction of applied tension on fabric growth and stretch also, to investigate the effect of extension percent on the thermal conductivity.

Table 4.2. Factors information of factorial design

Factor	Levels	Values
Plaiting technique	2	full plaiting, half plaiting
Yarn count (Ne)	2	25 - 35
Loop length (mm)	5	2.7 - 2.9 - 3.1 - 3.3 - 3.4
Spandex weight percent (%)	5	4- 5 - 6 - 7 - 8

5. CHAPTER 5: SUMMARY OF THE ACHIEVED RESULTS

In order to investigate the effect of loop length and *SWP* on the geometrical and thermo-physiological properties, the produced *fp* and *hp SJKF* from yarn count 35 Ne at five levels of loop length and *SWP* will be shown. The same effects and trends were found for samples produced from yarn count 25 Ne (according to appendix (I)).

5.1 Geometrical properties

5.1.1 Stitch density

Figure 5.1 shows the effect of loop length on the stitch density of *SJKF* at five levels of *SWP*. Generally, the stitch density went down with loop length increasing. The stitch density of elastic knitted fabric was higher than 100% cotton by 80% and 59% at loop length 2.7 mm and *SWP* 4% for *fp* and *hp,* respectively. Spandex yarn in knitted fabric works on the convergence of course and wales; therefore, stitch density increases.

Increasing *SWP* means that the feeding tension of spandex yarn in the knitting machine decreases during the production process, so the compression effect of spandex reduces and the wales and courses density decrease. Therefore, the stitch density of *fp* and *hp* knitted fabric decreased with *SWP* increasing.

The stitch density of *fp* was a bit higher than *hp* due to the plaiting technique. The stitch density of *SJKF* produced from yarn count 35 Ne was higher than samples produced from yarn count 25 Ne (according to table 10.1, appendix I). it could be interpreted that all samples were produced on the same knitting machine therefore samples produced from yarn count 35 Ne had the ability to close the wales and courses to each other due to finer count.
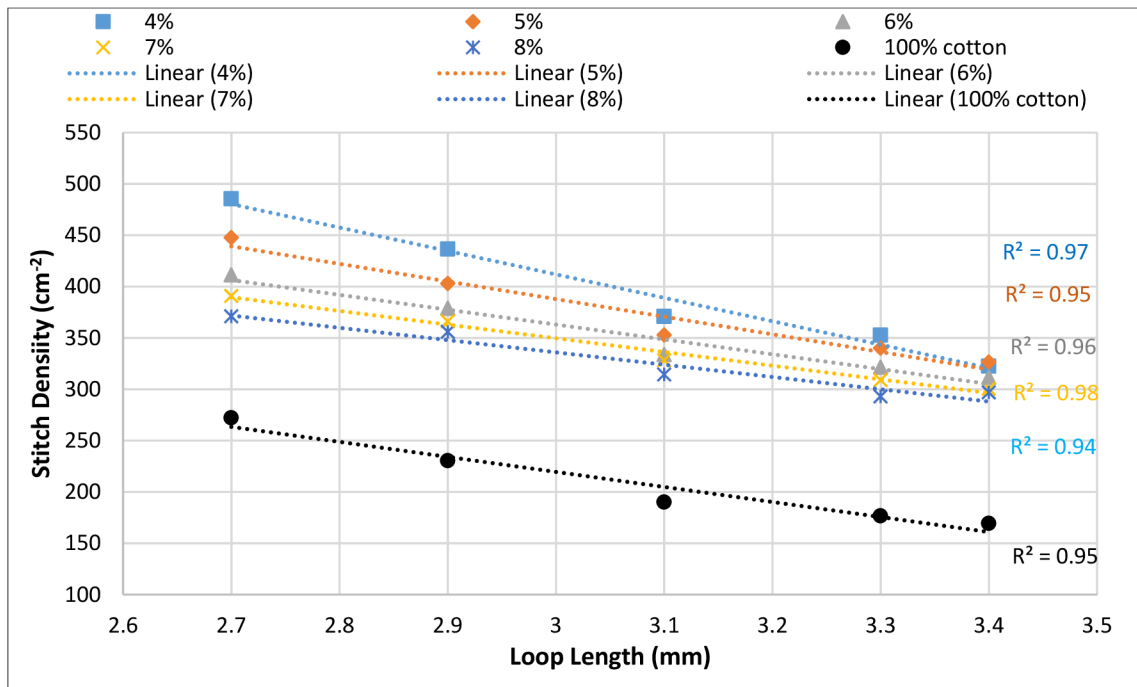
a- Full plaited (35 Ne)
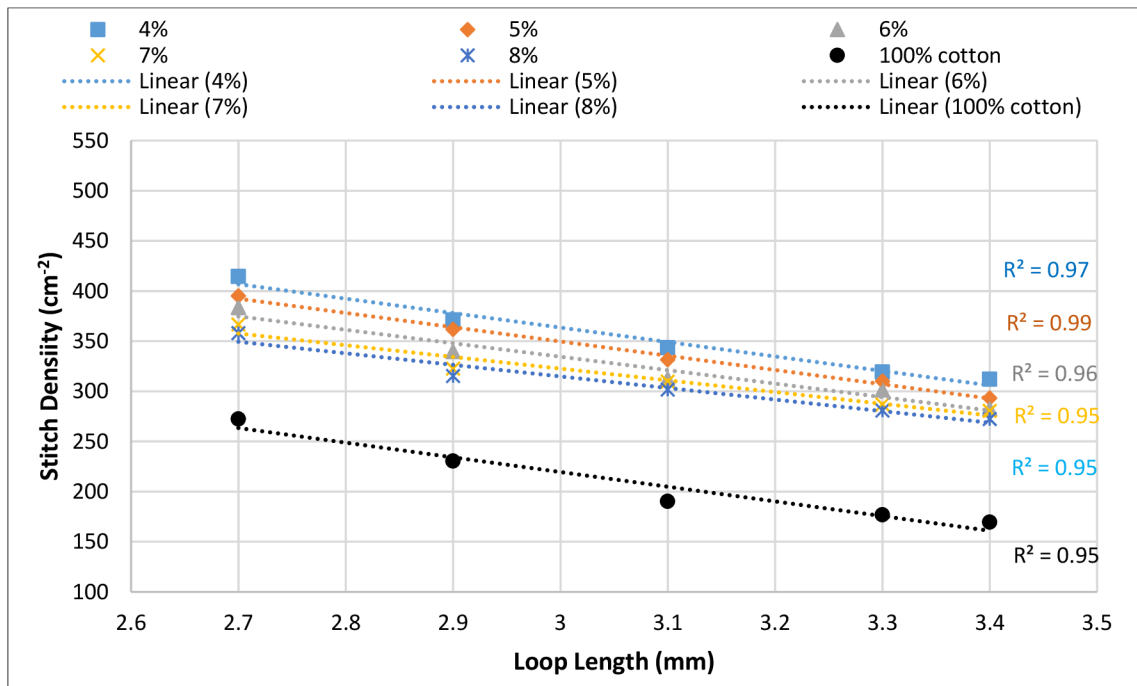
b- Half plaited (35 Ne)

Figure 5.1. Effect of loop length on the stitch density (35 Ne)

The statistical analysis showed that *SWP,* loop length, plaiting technique and yarn count had a significant effect on the stitch density, as shown in table 5.1.

Table 5.1. The results of variance analysis (P value at significant level 95 %)

Dependent property	P value, Independent variables			
	Loop length (mm)	SWP (%)	Plaiting technique	Yarn count (Ne)
Fabric thickness (mm)	< 0.001	< 0.001	0.047	< 0.001
Thermal conductivity (W. m^{-1}. K^{-1})	< 0.001	< 0.001	< 0.001	< 0.001
Thermal resistance (m^2. K. W^{-1})	< 0.001	< 0.001	< 0.001	< 0.001
Thermal absorptivity (W.m^{-2}. s$^{1/2}$. K^{-1})	< 0.001	< 0.001	< 0.001	< 0.001
WVR (Pa.m^2. W^{-1})	< 0.001	< 0.001	< 0.001	< 0.001
Air permeability (mm.s^{-1})	< 0.001	< 0.001	< 0.001	< 0.001

5.1.2 *Fabric weight*

The weight of *SJKF* decreased with the increase of loop length and the fabric weight of the elastic knitted fabric was higher than 100% cotton by 97 and 69 % at loop length 2.7 for *fp* and *hp* respectively. For both *fp* and *hp* knitted fabric, the weight per unit area went down when *SWP* went up. The fabric weight of *fp* was higher than *hp* due to the reduction of stitch density, as shown in figure 5.2 therefore, the number of fibres decreased. The fabric weight of samples produced from the yarn count of 25 Ne was higher than 35 Ne (according to table 10.2, appendix I).
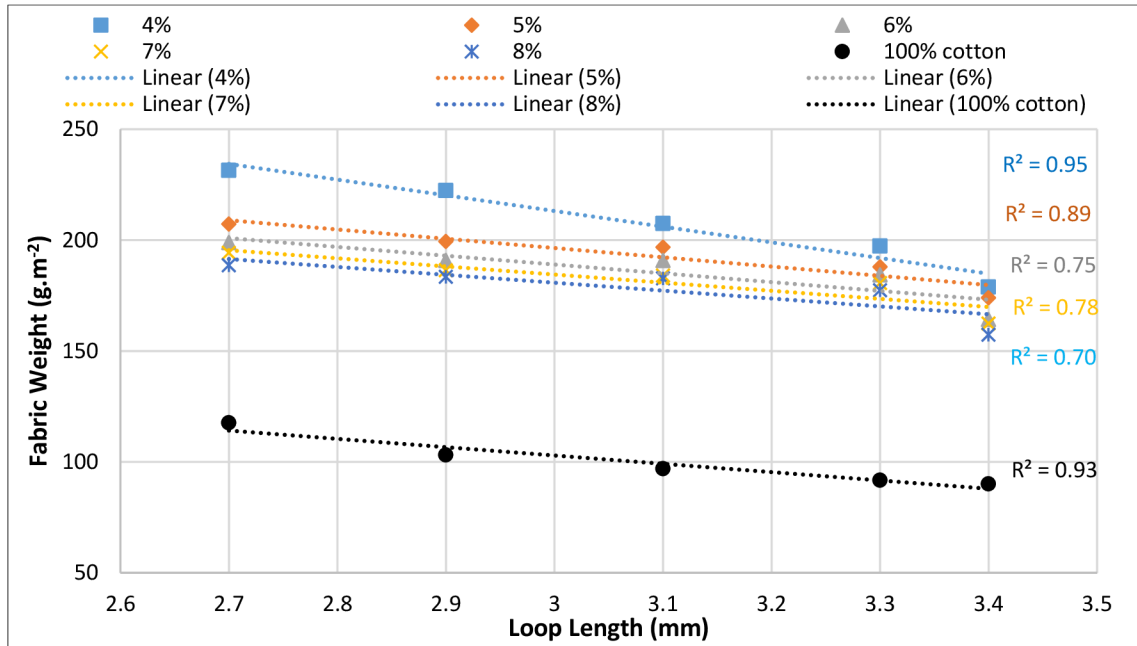
a- Full plaited (35 Ne)
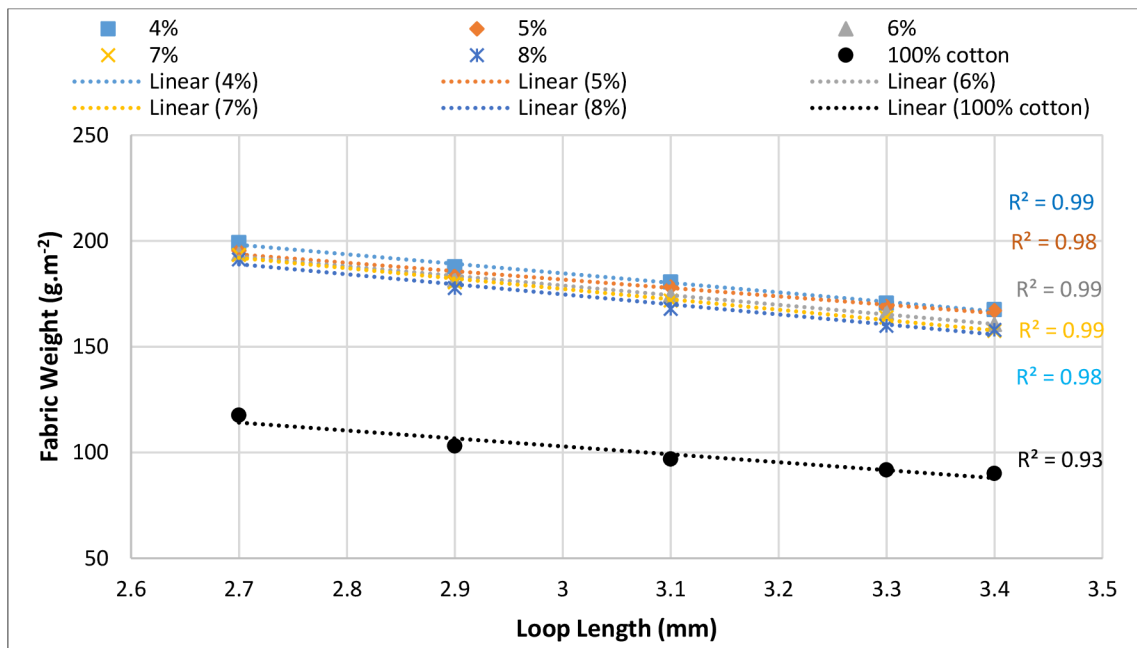
b- Half plaited (35 Ne)

Figure 5.2. Effect of loop length on the fabric weight (35 Ne)

5.1.3   *Fabric thickness*

Figures (5.3-a) and (5.3-b) display the effect of loop length on fabric thickness of full and half plaited *SJKF,* respectively, at five levels of *SWP* (4, 5, 6, 7, and 8%). The theoretical fabric thickness equals twice the yarn diameter for open and normal structures (jamming condition or maximum set), as shown in figure (5.4-a:d). For open structure, wale spacing (*w*) is more than 4 *d*, and course spacing (*c*) is more than $2*\sqrt{3}*d$ where *d* is the yarn diameter (mm). While for normal structure, *w* is equal to 4*d, and *c* is equal to $2*\sqrt{3}*d$. The elastic fabric thickness of experimental samples ranged between 3.58*d (0.596 mm) to 4.44*d (0.739 mm). So, it could be interpreted that spandex leads to stitch overlapping ($c < 2*\sqrt{3}*d$, $w < 4*d$, but it was assumed to be equal to 4*d for geometrical modelling), as shown in figure (5.4-e:g). Also, adding spandex leads to stitch legs overlapping, as shown in figure (5.4-h), which significantly increases the fabric thickness. The fabric thickness of *fp* knitted samples was higher than 100% cotton by 47% at loop length 2.7 mm and *SWP* 4% and 69% at loop length 3.4 mm and *SWP* 8% as shown in figure (5.3-a) and figure 5.5.

In general, for *fp* and *hp*, the fabric thickness decreased with the increase of the *SWP* from 4 to 8% by 17% at loop length 2.7mm for *fp* and by 7% at the loop length 2.7mm for *hp*. It could be interpreted as the increase of *SWP* reduced the stretch ability as well as the compression effect of spandex on loops, as shown in figures (5.4-f) and (5.4-g), and reduced the stitch density as well, as shown in figure 5.1. The increase of loop length increased the loop's overlapping; therefore, the fabric thickness increased consequently. The thickness of *fp* samples was higher than *hp* samples, and this may be due to the spandex plaiting in all courses and alternative courses.

The fabric thickness of 100% cotton knitted fabric decreased with the increase of stitch length due to the reduction of stitch density, and there is no stitch overlapping, as shown in figure (5.4-b).
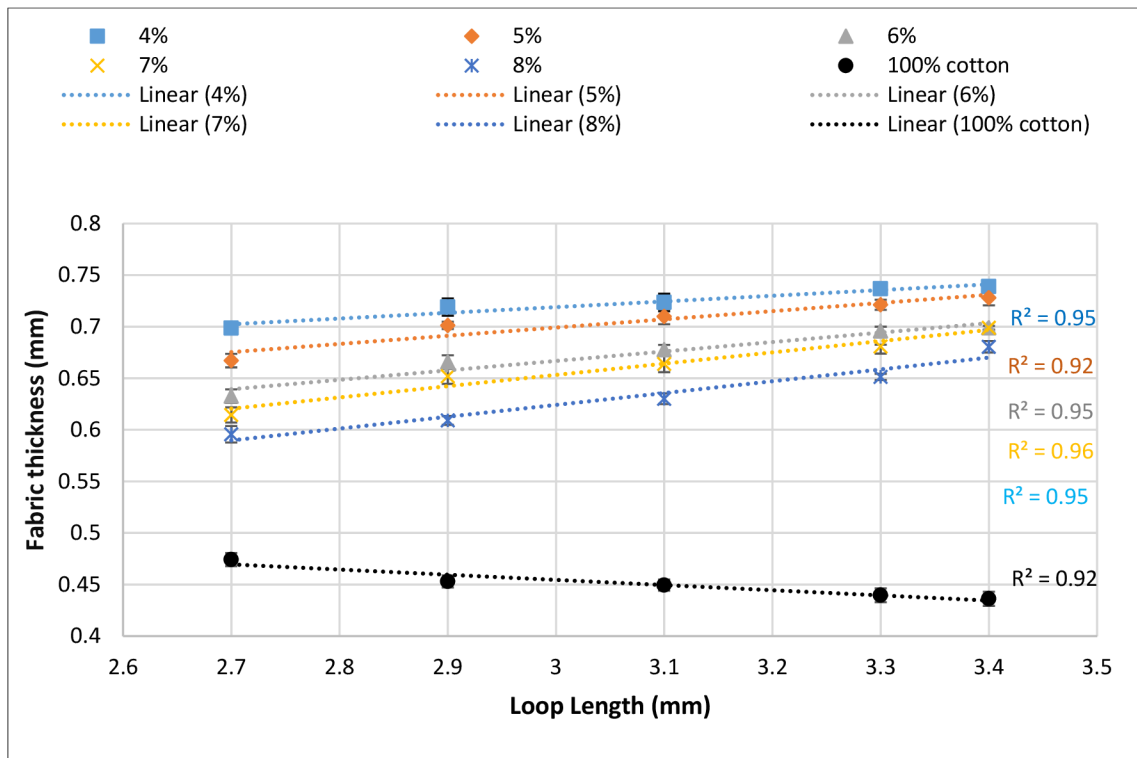
a- Full plaited (35 Ne)
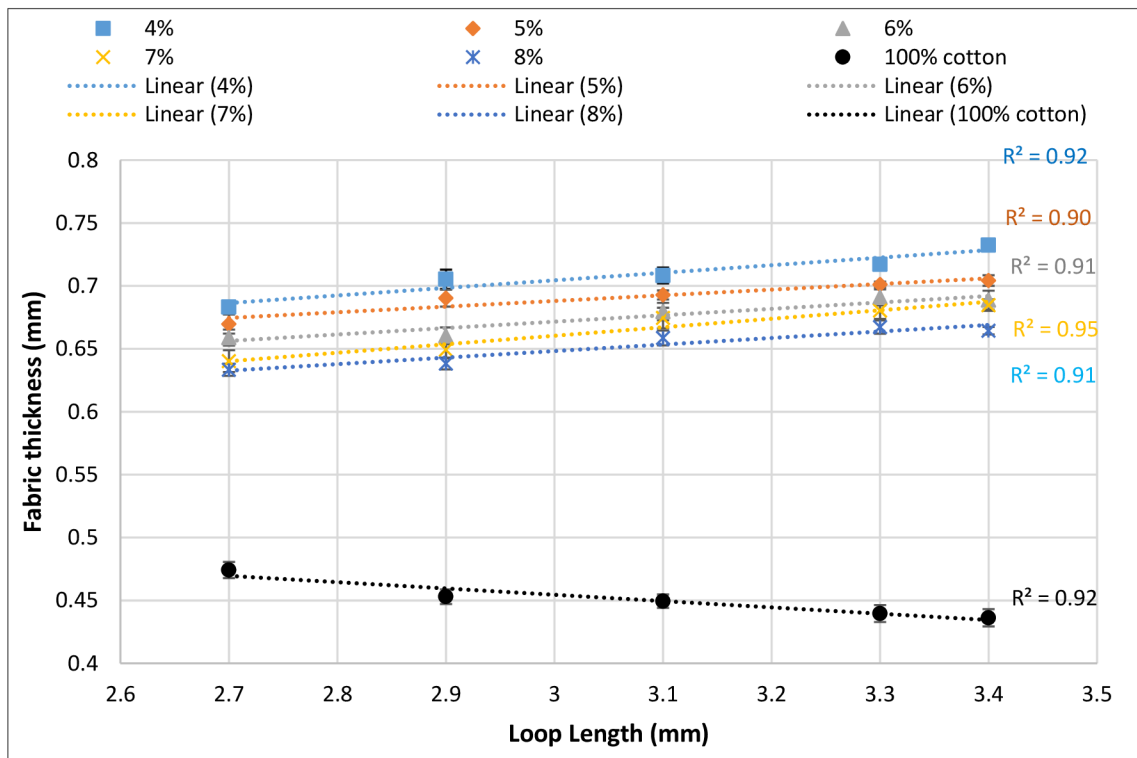
b- Half plaited (35 Ne)

Figure 5.3. Effect of loop length on the fabric thickness (35 Ne)
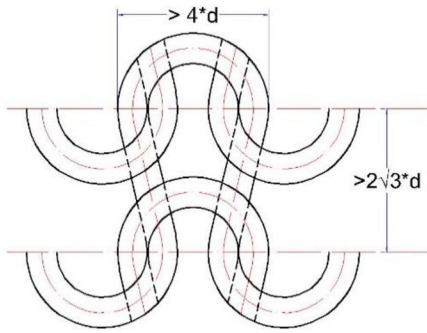
(a) Theoretical geometry of open structure
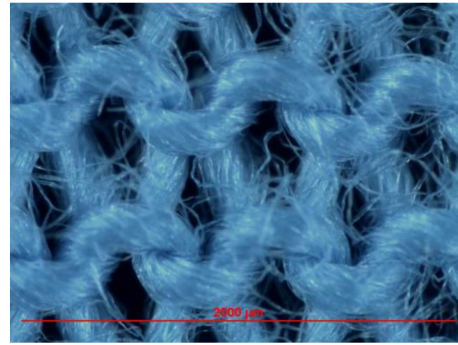
(b) Microscopic image of open structure at 35 Ne
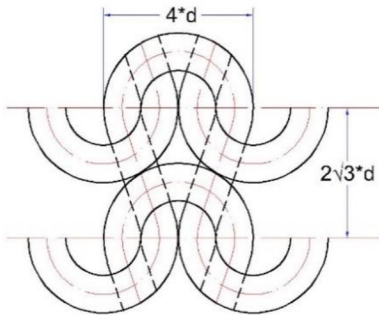
(c)Theoretical geometry of normal structure
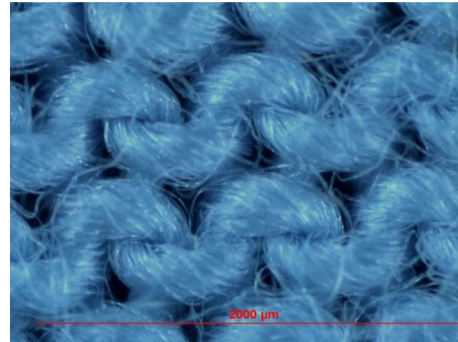
(d) Microscopic image of normal structure at 25 Ne
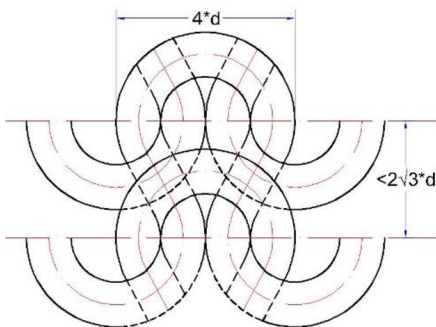
(e) Theoretical geometry of stitch overlapping
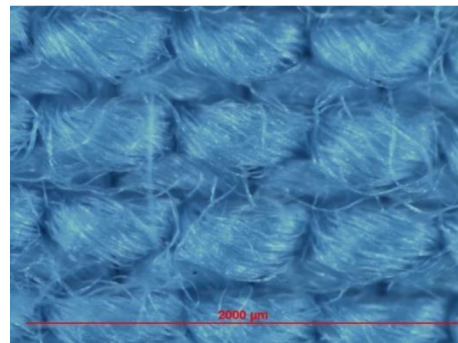
(f) Microscopic image of stitch overlapping at *SWP* 4% and 35 Ne
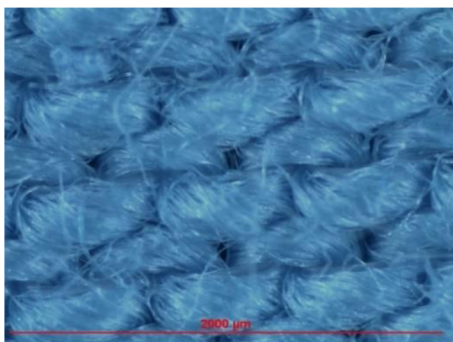
(g) Microscopic image of overlapping at *SWP* 8% and at 35 Ne

(h) Microscopic image of legs overlapping at *SWP* 4% and 35 Ne

Figure 5.4. Single jersey loop structure, all microscopic images at loop length 2.9 mm.
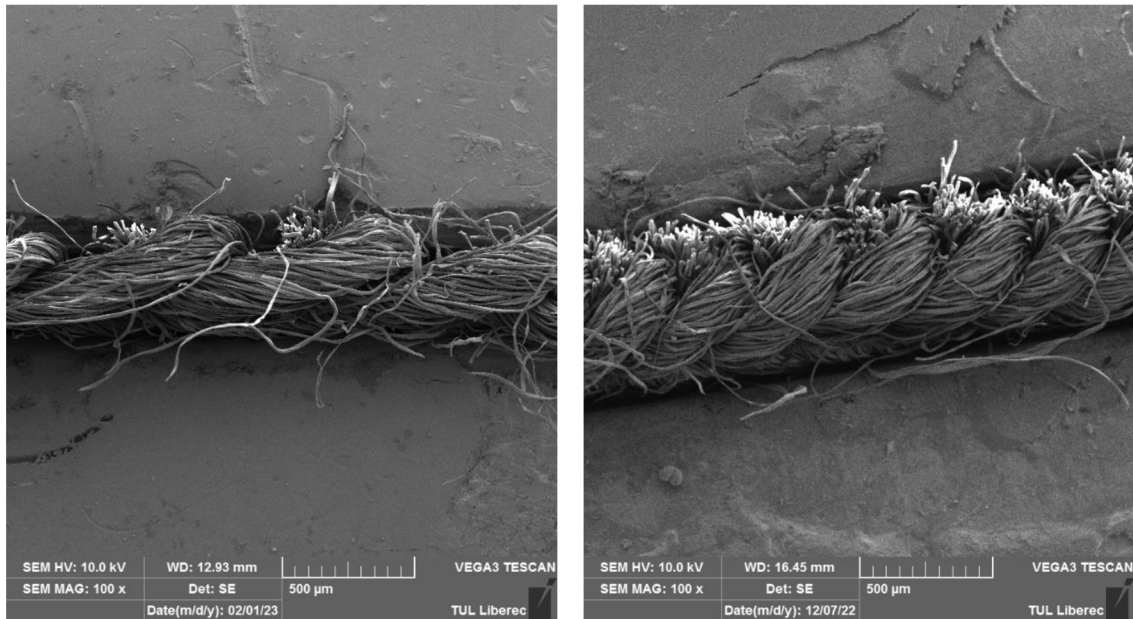
| a-   100% cotton | b-   Elastic knitted fabric at *SWP* 4% |

Figure 5.5. SEM of images *SJKF* by SEM at loop length 2.7 mm and 35 Ne

All trends for *SJKF* produced from yarn count 25 Ne were the same of *SJKF* produced from yarn count 35 Ne as shown in figure in 5.6. The thickness of fp was higher than 100% cotton samples by 37 % at loop length 3.4 mm and *SWP* 8%.

Fabric thickness of samples produced from yarn count 25 Ne was higher than 35 Ne that is because yarn count 25 Ne had higher diameter than yarn count 35 Ne as shown in figure 5.7, and also bending rigidity of yarn 25 Ne was higher than yarn 35 Ne as shown in figure 5.8. The statistical analysis showed that *SWP*, loop length, plaiting technique and yarn count had a significant effect on the fabric thickness, see table 5.1. Therefore, the increase of fabric thickness may lead to an increase in the thermal resistance of the tested samples.
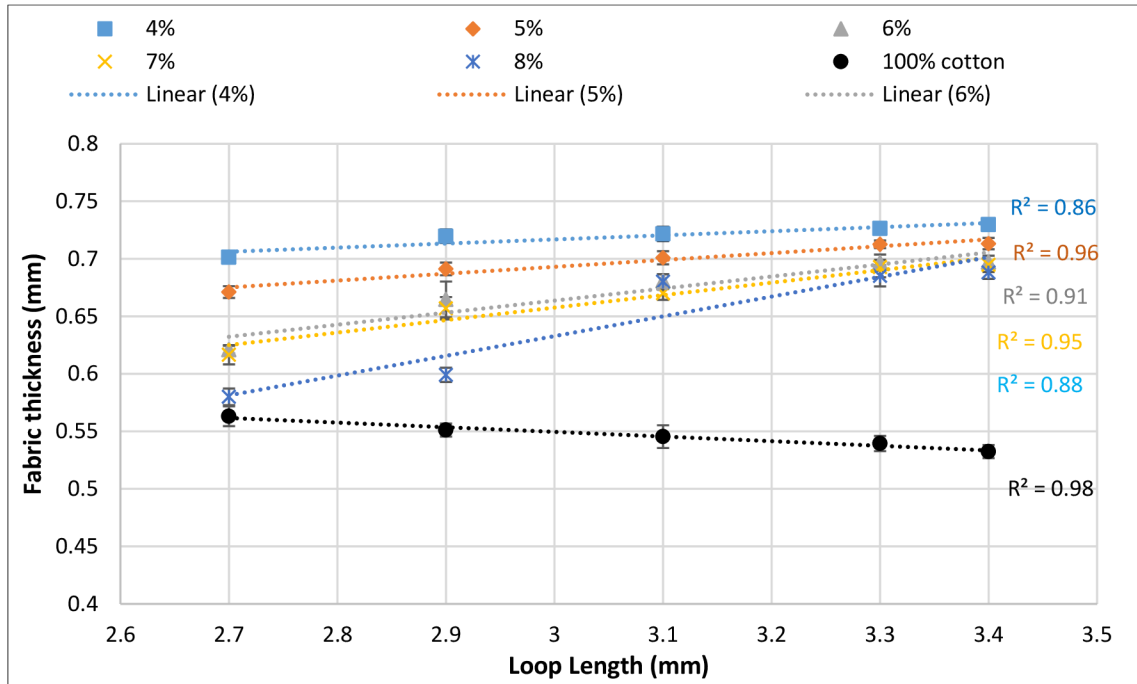
a-   Full plaited (25 Ne)
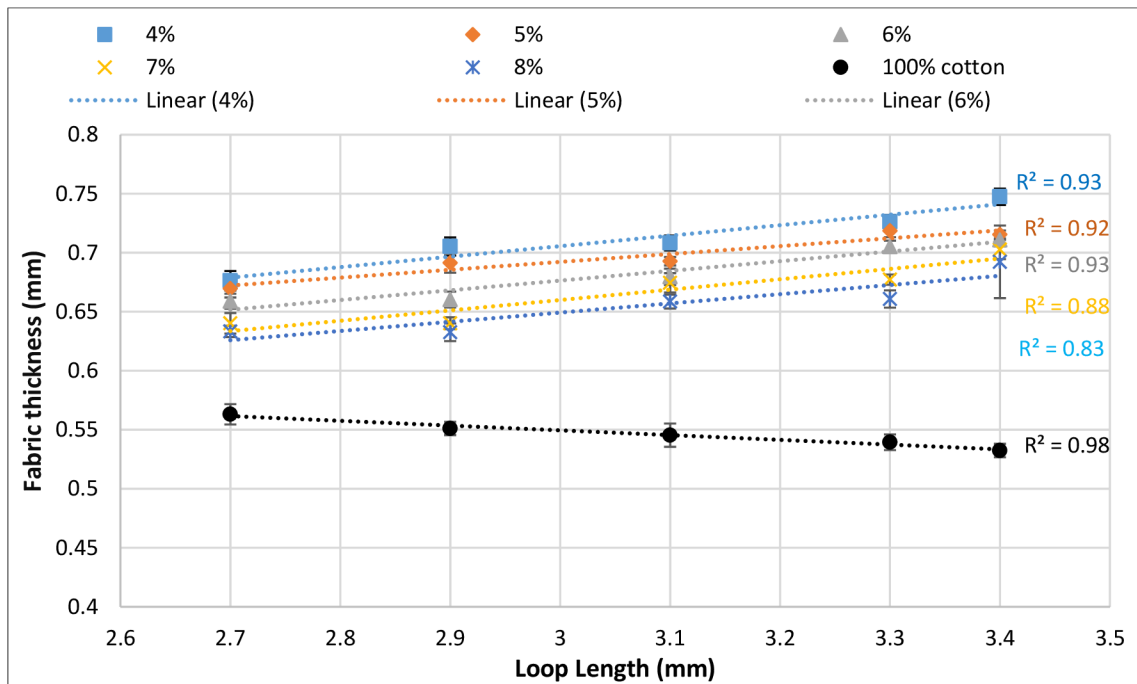
b-   Half plaited (25 Ne)

Figure 5.6. Effect of loop length on the fabric thickness (25 Ne).
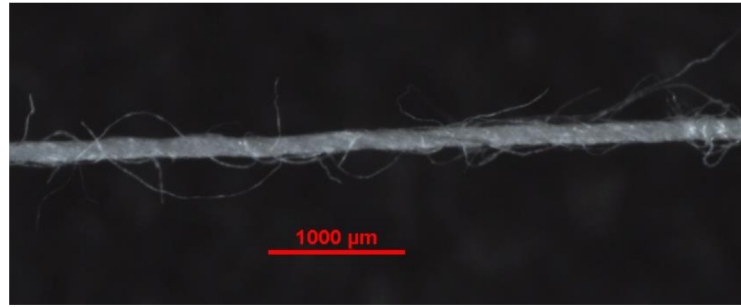
a-   Image of yarn count 35 Ne (d=.1664mm)
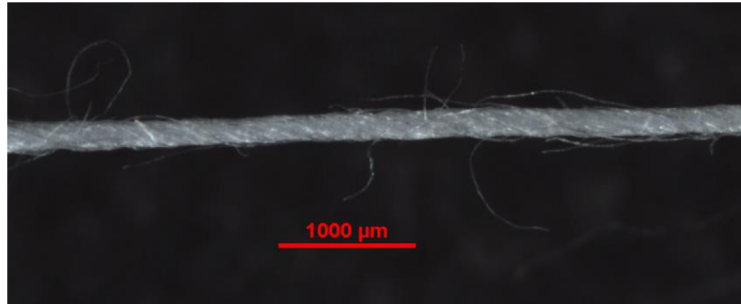
b-   Image of yarn count 25 Ne (d=.2053 mm)

Figure 5.7. Images of yarns
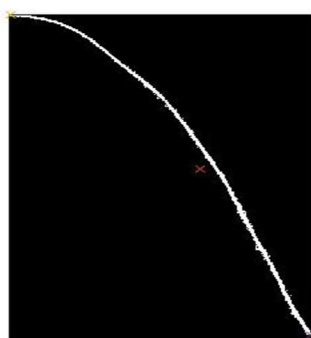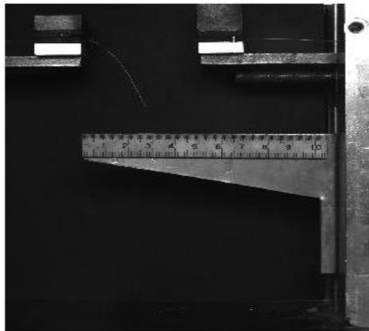
EI = 1.9538e-09N.m^2

a-   Yarn 35 Ne
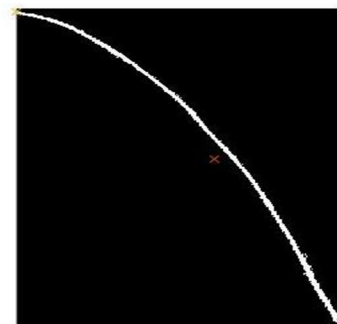
EI = 3.1538e-09N.m^2

b-   Yarn 25 Ne

Figure 5.8. yarn bending rigidity

5.1.4   *Fabric porosity*

The fabric porosity of *fp* was lower than 100% cotton samples by just 7 and 2% at loop length 2.7 and 3.4 mm, respectively, and *SWP* 4%, as shown in figure (5.9-a). Also, the fabric porosity of *hp* was lower than 100% cotton by 4 and 1% at loop length 2.7 and 3.4 mm respectively and *SWP* 4%, as shown in figure (5.9-b).
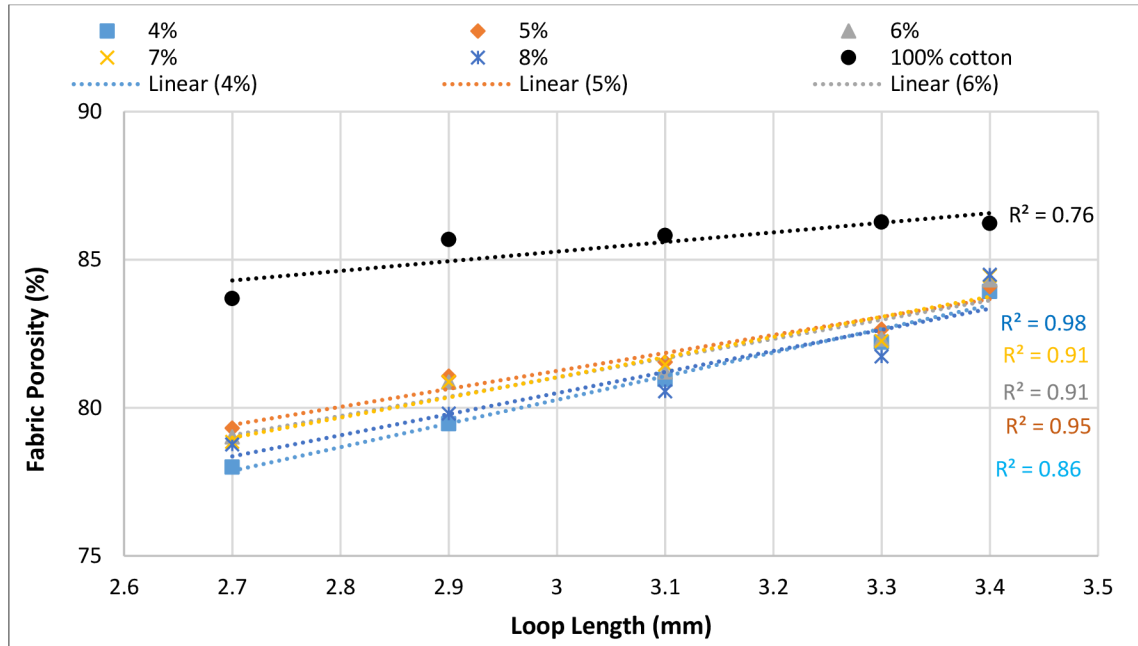
a-   Full plaited (35 Ne)
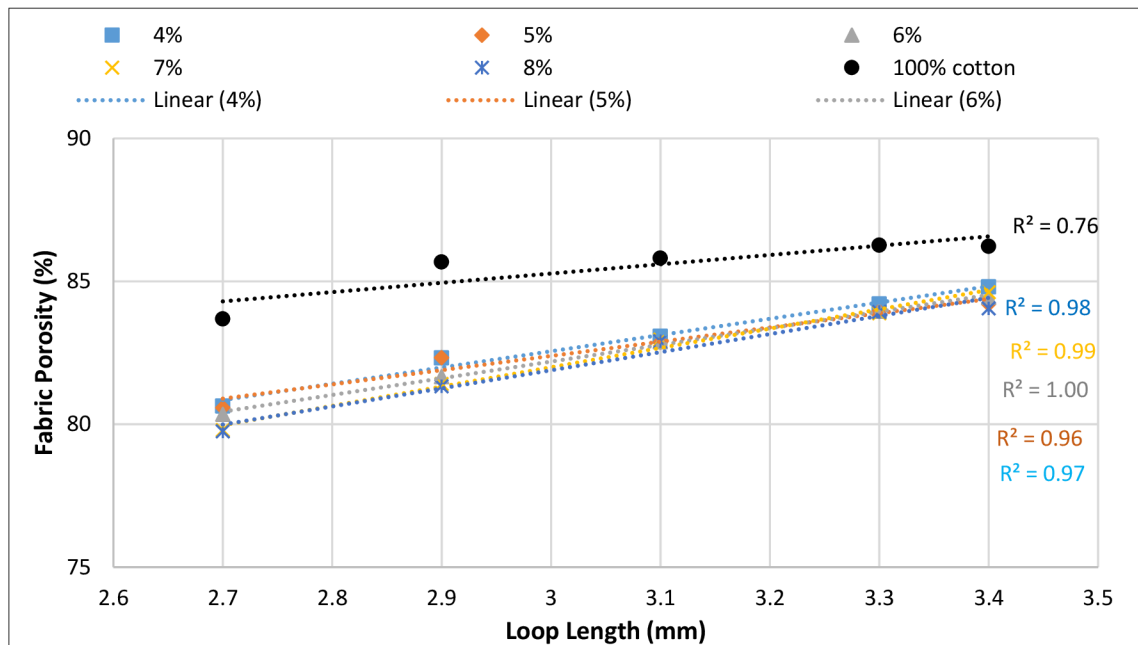
b-   Half plaited (35 Ne)

Figure 5.9. Effect of loop length on the fabric porosity (35 Ne).

The fabric porosity of *fp* and *hp* produced from yarn count 25 Ne were lower than 100% cotton by 6 and 4% respectively at loop length 2.7 mm and *SWP* 4%, as shown in appendix (I), table 10.4. the stitch density of elastic *SJKF* was higher than 100% cotton samples, and there was no a big difference between the porosity of 100% cotton and elastic *SJKF*, the pores size and distribution inside the structure plays an important role in thermo-physiological properties. The fabric porosity of *hp* was slightly high than *fp* due to the ridges formed on the hp fabric surface. The fabric porosity of *SJKF* went up with the increasing of the loop length due to the stitch density decreasing.

5.2 Thermo-physiological properties

5.2.1 Thermal conductivity

The thermal conductivity coefficient (λ) presents the amount of heat which passes from $1m^2$ area of material through the distance 1m within 1s and the temperature difference 1K [6]. It is the fabric ability to transfer heat from body to environment and vice versa depending on the temperature difference between the body and environment[14]. The thermal conductivity can be expressed by the following equation.

$$\lambda = \frac{Q * h}{A * \Delta T * 1000} \qquad ...\,...\,...\quad (5.1)$$

Where λ is the thermal conductivity coefficient (W.m^{-1}.K^{-1}), Q is the amount of heat (W), h is the fabric thickness (mm), A is the fabric tested area (m^2), and ΔT is the temperature difference (K).

In general, the thermal conductivity of elastic knitted fabric decreased with increasing of *SWP* for both *fp* and *hp*, as illustrated in Figures (5.10-a) and (5.10-b) respectively. It could be interpreted that the stitch overlapping decreases with increasing of *SWP* and the stitch density decreases, as shown in figure 5.1. So, the number of fibres per unit area decreased; therefore, the number of paths which the heat transferred through the fibres by conduction decreased. Increase *SWP* means to increase in the number of spandex fibres and a reduction in the number of cotton fibres. The thermal conductivity of spandex and cotton fibres is 0.15 and 0.5 W. m^{-1}. K^{-1}, respectively [42], so the average thermal conductivity of fibres decreased according to the following equation.

$$\lambda_{\mathrm{f}} = \frac{SWP}{100}\,\lambda_{\mathrm{s}} + \left(1 - \frac{SWP}{100}\right)\lambda_{\mathrm{c}} \qquad ...\ ...\ ...\quad (5.2)$$

Where λ_f is the thermal conductivity of fibres (W.m^{-1}.K^{-1}), λ_s is the thermal conductivity of spandex (0.15 W.m^{-1}.K^{-1}), and λ_c is the thermal conductivity of cotton fibres (0.5 W.m^{-1}.K^{-1})
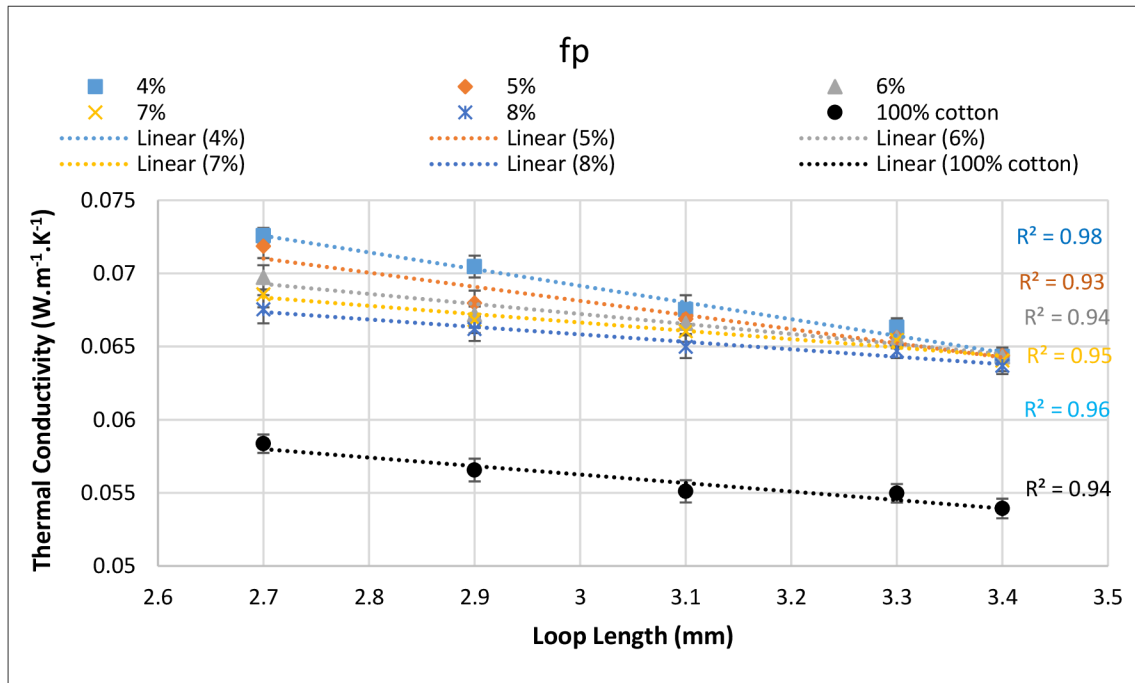
a-   Full plaited (35 Ne)
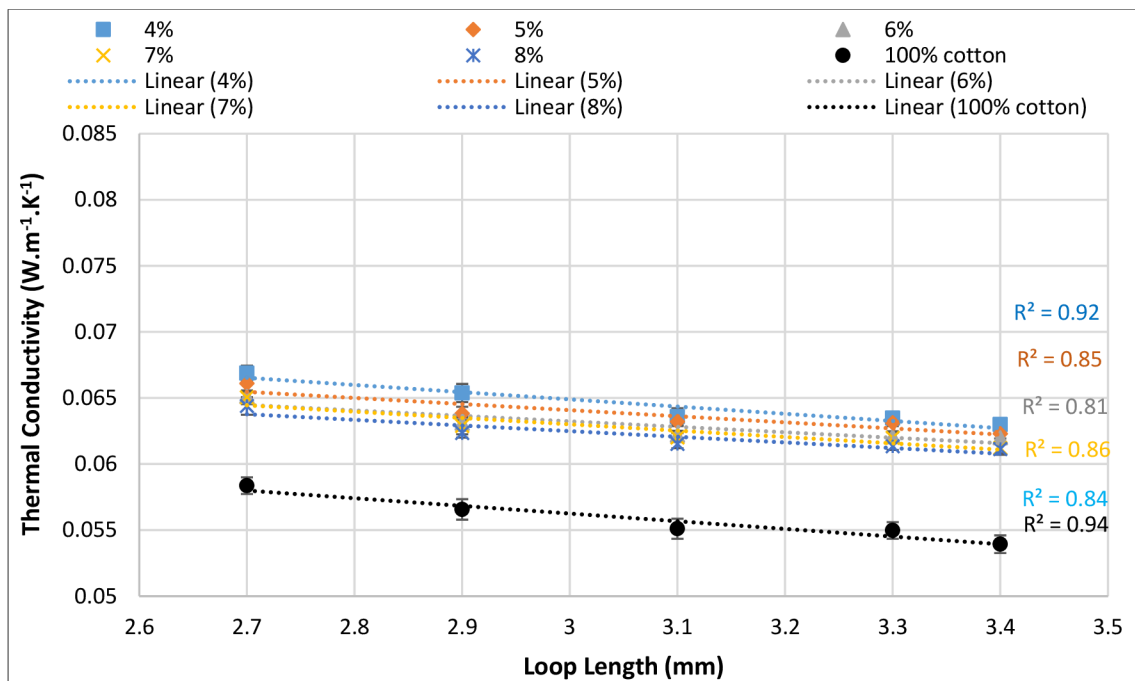
b-   Half plaited (35 Ne)

Figure 5.10. Effect of loop length on the thermal conductivity (35 Ne)

The thermal conductivity of *SJKF* went down with the increase of loop length [43] it may be due to the increase of loop length leads to decrease the stitch density, as shown in figure 5.1. So, the number of fibres per unit area decreases and the number of paths which the heat is transferred through the fibres by conduction decreases.
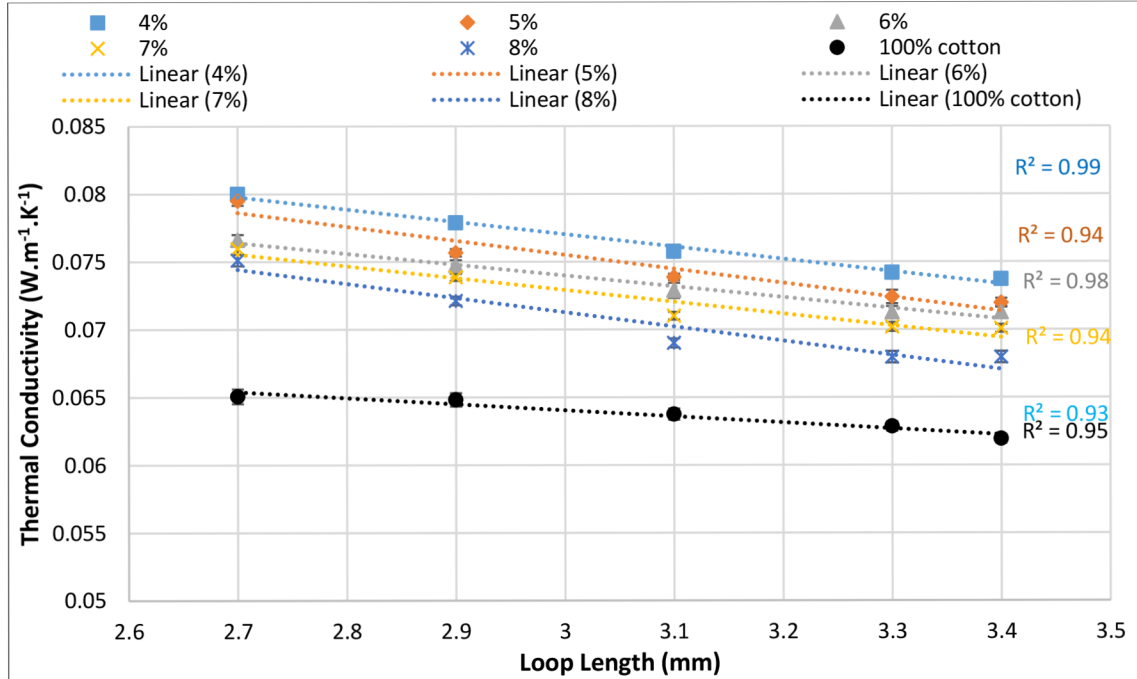
Full plaited (25 Ne)
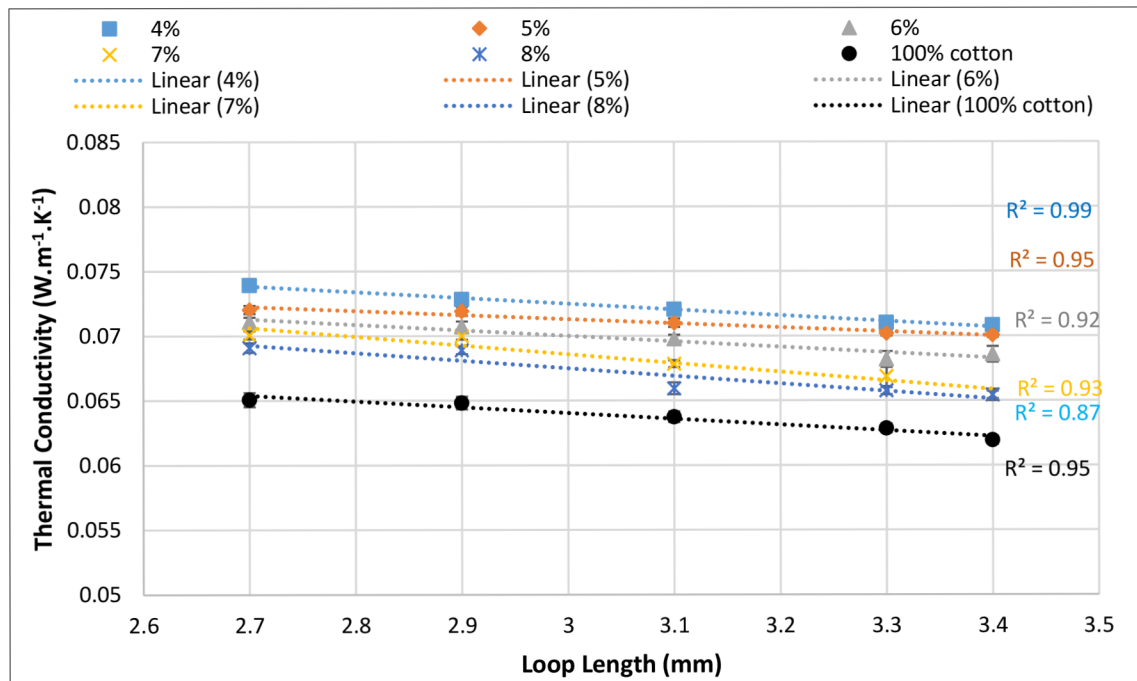
Half plaited (25 Ne)

Figure 5.11. Effect of loop length on the thermal conductivity (25 Ne)

The thermal conductivity of elastic *SJKF* samples was higher than the 100% cotton samples by 24 and 15% at loop length 2.7 mm and *SWP* 4% for *fp* and *hp,* respectively, due to stitch density increase. The thermal conductivity of *fp* was higher than *hp* due to decrease in stitch density of *hp* because of the plaiting technique.

For knitted samples produced from yarn count 25 Ne, the same trends were found as knitted samples produced from yarn count 35 Ne, as shown in figure 5.11. The thermal conductivity of fp was higher than 100% cotton samples by 23 % at loop length 2.7 mm and *SWP* 4%. The thermal conductivity of knitted samples produced from yarn count 25 Ne was higher than 35 Ne [43] due to the increase of number of fibres in the yarn cross-section. The statistical analysis showed that *SWP*, loop length, plaiting technique and yarn count had a significant effect on the thermal conductivity, as shown in table 5.1.

5.2.2   *Thermal resistance*

Figure 5.12 illustrates the effect of loop length on the thermal resistance of *SJKF* produced from yarn count 35 Ne. Generally, the thermal resistance of elastic *SJKF* went up with the increase of loop length because the fabric thickness increased and thermal conductivity decreased when the loop length went up, as shown in figures 5.8 and 5.4, which matches with the heat transfer through conduction theory, as in Eq. (5.3). Also, the fabric porosity increased with the increase of loop length, as shown in figure 5.9 and the stitch density decreased with the loop length increasing. The stitch density and loop length had a significant effect on the thermal resistance of weft structures [44].

$$R = \left(\frac{h}{\lambda * 1000}\right) \qquad \ldots \ldots \ldots \ldots \ldots \ldots \ldots \ldots \ldots \ldots \ldots \quad (5.3)$$

where R is thermal resistance ($K.m^2.W^{-1}$), λ is thermal conductivity ($W.m^{-1}.K^{-1}$), and *h* is the fabric thickness (mm). Also, the thermal resistance of elastic *SJKF* went down when *SWP* went up because the fabric thickness decreased with increase of *SWP*.

The thermal resistance of 100% cotton samples decreased with the increase of loop length due to the decrease of fabric thickness when the loop length increased. The thermal resistance of elastic *SJKF* was higher than 100% cotton fabric by 60 and 52% for both *fp* and *hp,* respectively, at loop length 3.4 mm and *SWP* 4%.
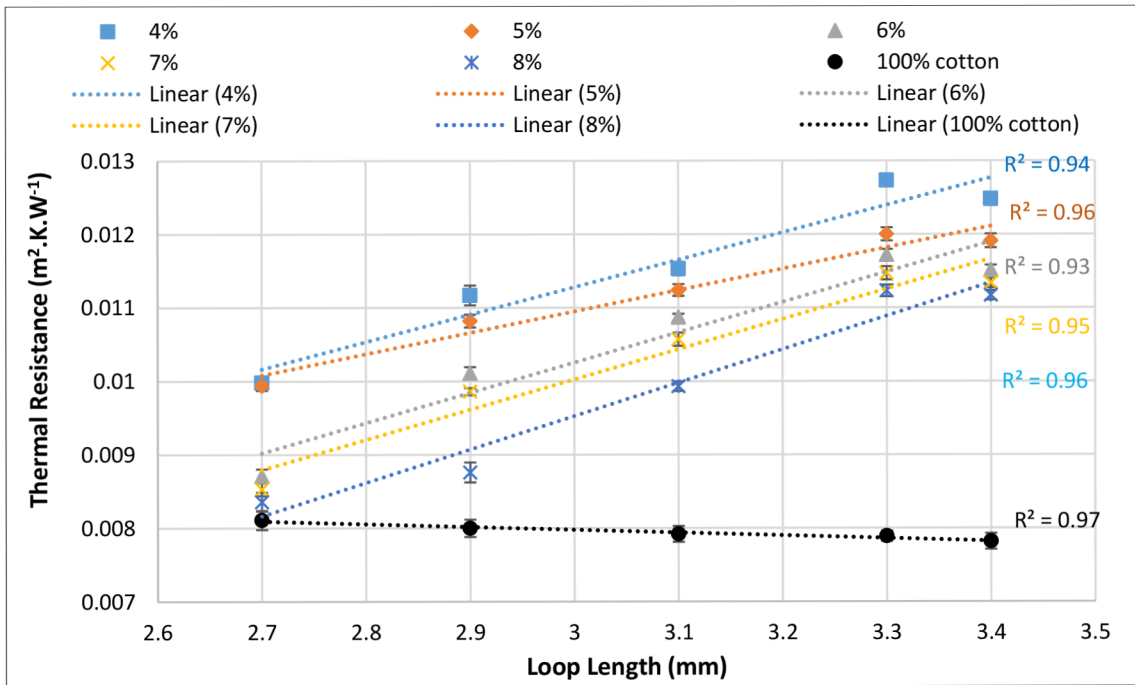
a-   Full plaited (35 Ne)
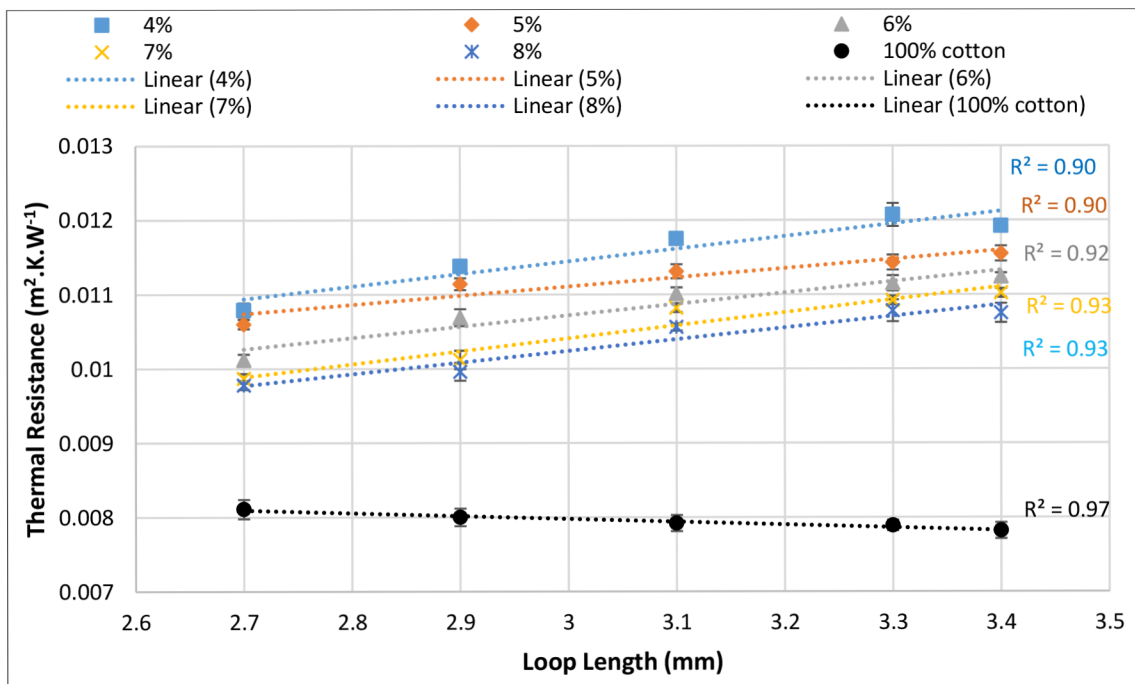
b-   Half plaited (35 Ne)

Figure 5.12. Effect of loop length on the thermal resistance (35 Ne)

5.2.3   *Thermal absorptivity*

Thermal absorptivity is the objective measurement of the warm cool feeling of a fabric. Fabrics with a lower thermal absorptivity value have a warm feeling and vice versa [45]. The thermal absorptivity increases with the thermal conductivity increasing and fabric density according to the following equation [46].

$$b = (\lambda_{fab} \, \rho_{fabric} \, C)^{1/2} \qquad\qquad .... \qquad\qquad (5.4)$$

Where b: thermal absorptivity ($W. s^{1/2} m^{-2}. K^{-1}$), λ: thermal conductivity ($W.m^{-1}. K^{-1}$), ρ: fabric density ($kg.m^{-3}$), C: specific heat capacity ($J.kg^{-1}.K^{-1}$).

The thermal absorptivity has a strong correlation with fabric structure, fibre type, surface roughness and contact points [47][48], and the contact area is perpendicular to the normal line of heat flow.

The thermal absorptivity of both *fp* and *hp* went down with the increase of *SWP* and loop length, as shown in figure 5.13; this may be due to the reduction of contact points at a very short time and a decrease in thermal conductivity because of the decrease in stitch density with the increase of *SWP,* as shown in figure 5.1. The thermal absorptivity of *fp* was higher than *hp*, it may be due to the ridges formed on the *hp* fabric surface due to the spandex plating technique in alternative courses, as shown in figure 5.14. So, the number of contact point in *hp* is less than *fp,* and the effective contact heat flow will be lower, and the thermal conductivity of *fp* was higher than *hp* as shown in figure 5.10. The thermal absorptivity of 100% cotton samples decreased with the loop length increasing, it was lower than *fp* and *hp* by up to 42 and 41%, respectively, at loop length 3.4 mm and *SWP* 4%, so 100% cotton samples give a warmer feeling compared to *fp* samples.
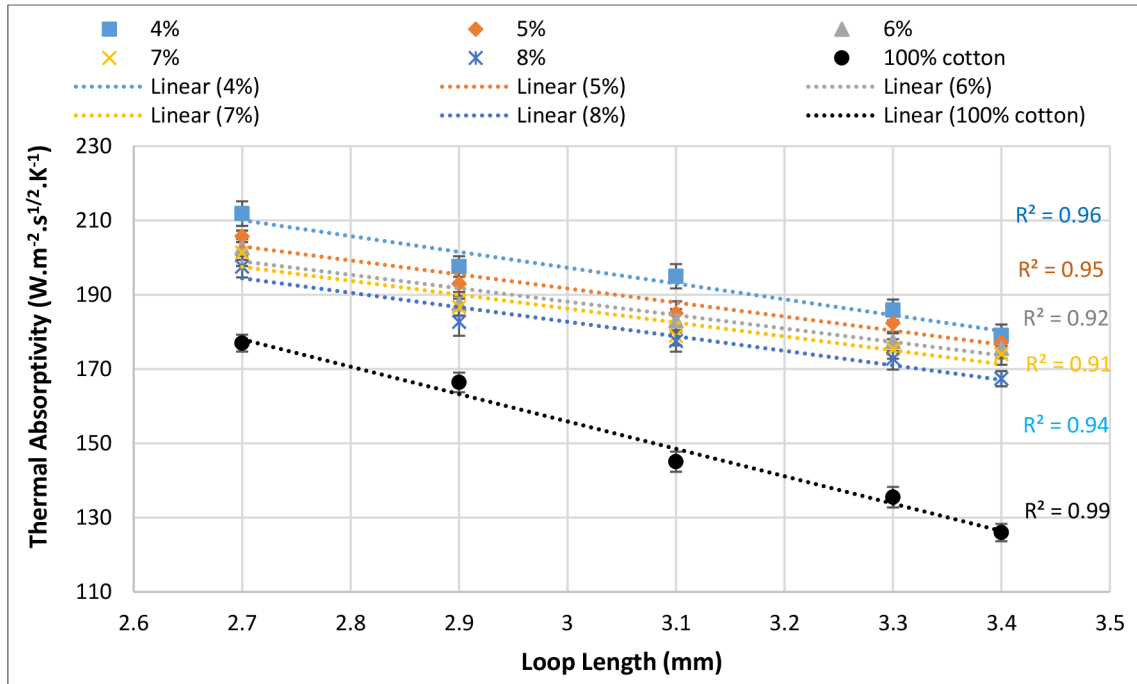
a- Full plaited (35 Ne)
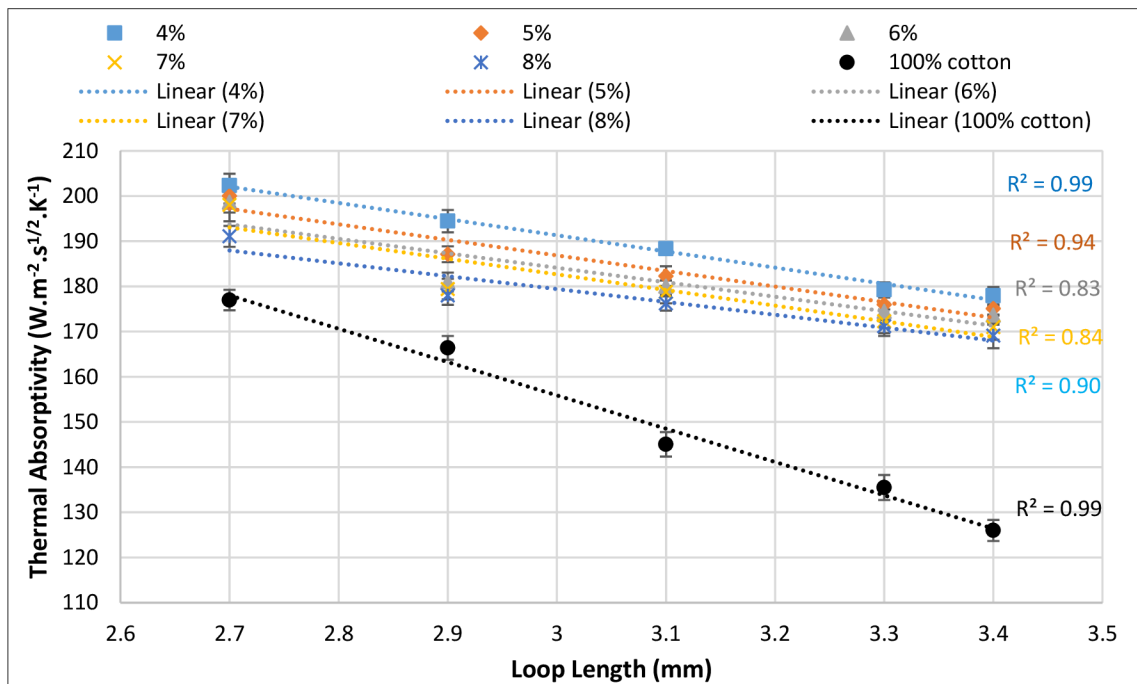
b- Half plaited (35 Ne)

Figure 5.13. Effect of *SWP* on the thermal absorptivity (35 Ne)

a
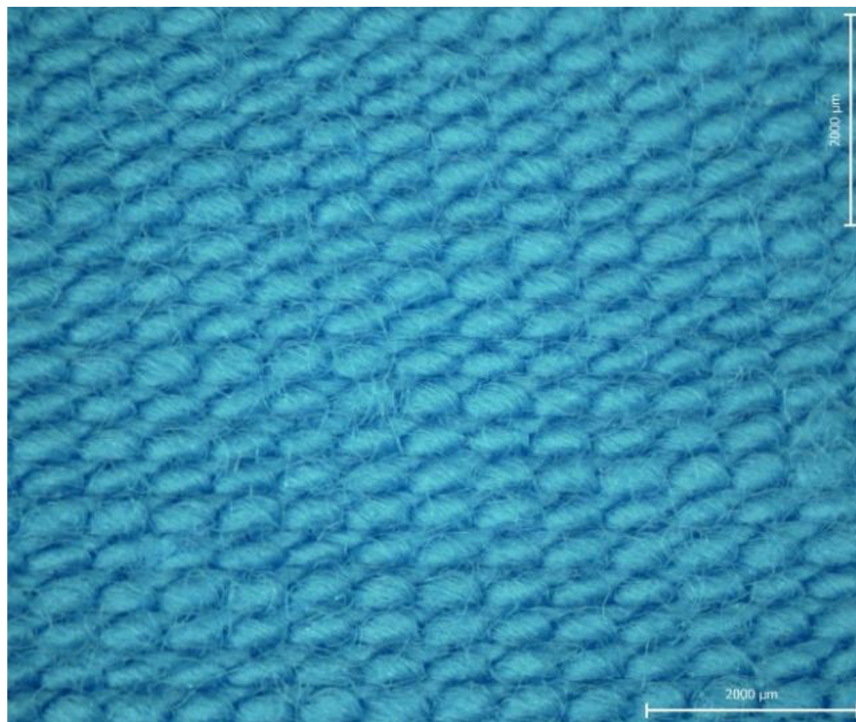
b

Figure 5.14. Microscopic back images of elastic knitted fabrics at 2.7 mm loop length and 5% *SWP*: a- half plaited, b- full plaited

The thermal absorptivity of the samples produced from yarn count 25 Ne had the same trends as the samples produced from yarn count 35 Ne, as shown in figure 5.15. The thermal absorptivity of *SJKF* produced from yarn count 25 Ne was higher than samples

produced from yarn count 35 Ne because the produced samples from yarn count 25 Ne had higher thermal conductivity than produced samples from yarn count 25 Ne, as shown in figures 5.10 and 5.11. *SWP*, loop length, plaiting technique, and yarn count had a significant effect on the thermal absorptivity, as shown in table 5.1.
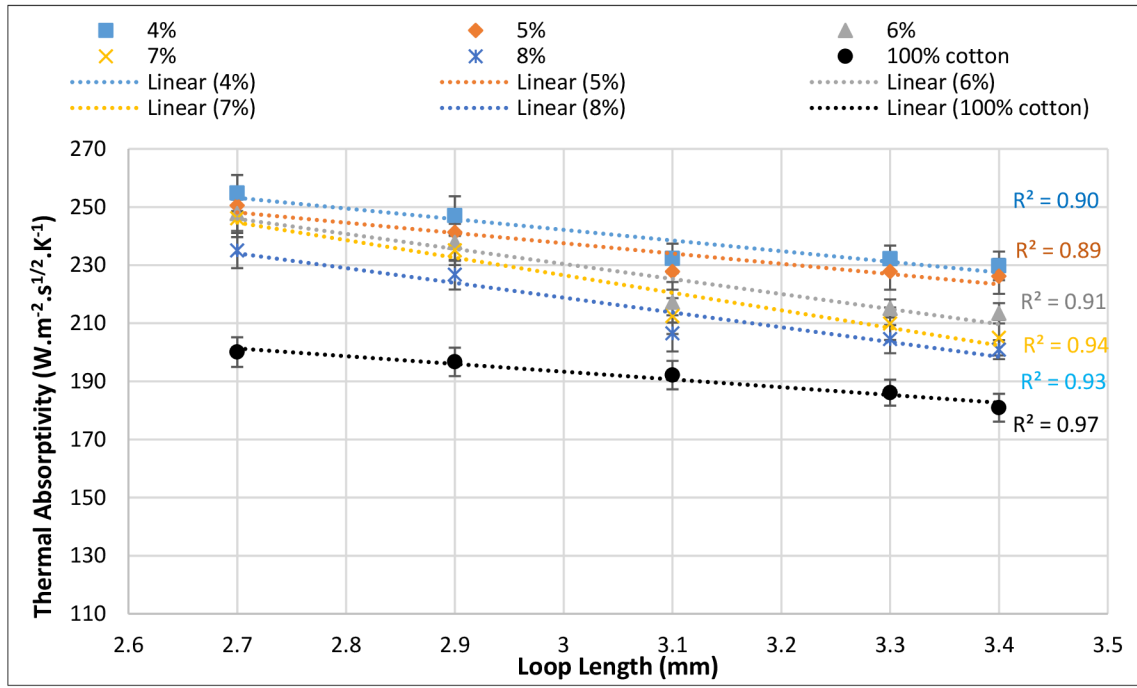
a- Full plaited (25 Ne)
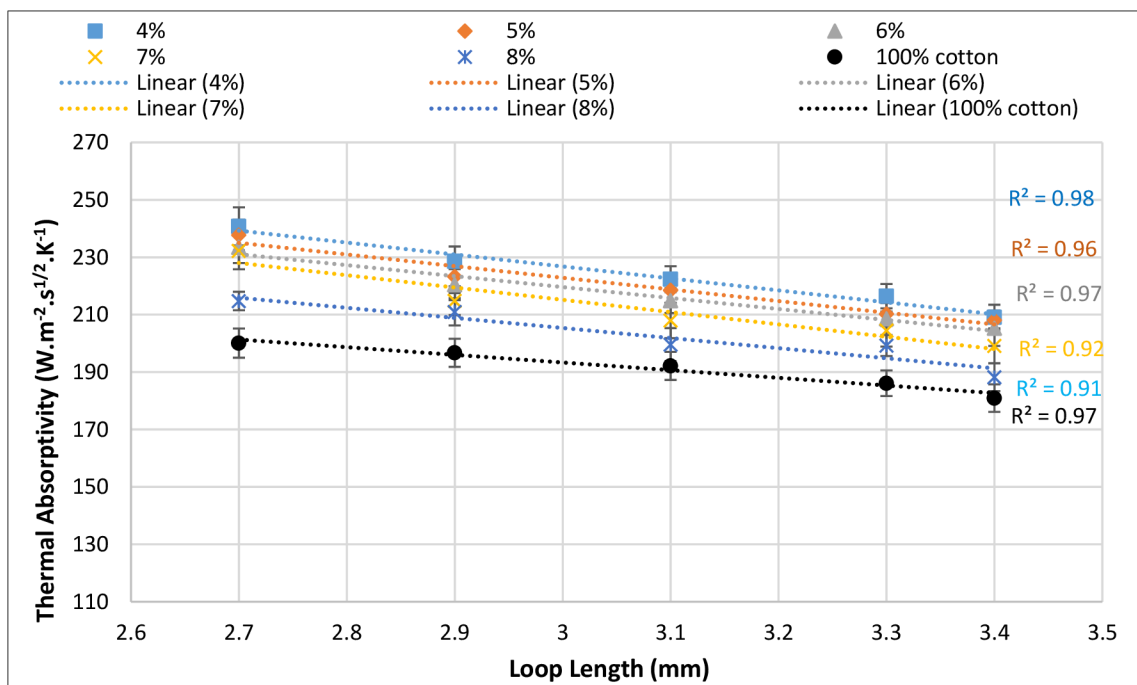
b- Half plaited (25 Ne)

Figure 5.15. Effect of *SWP* on the thermal absorptivity (25 Ne)

5.2.4 *Water vapour resistance*

Figure 5.16 shows the water vapour resistance (*WVR*) of *fp* and *hp* SJKF at different levels of *SWP* and loop length.
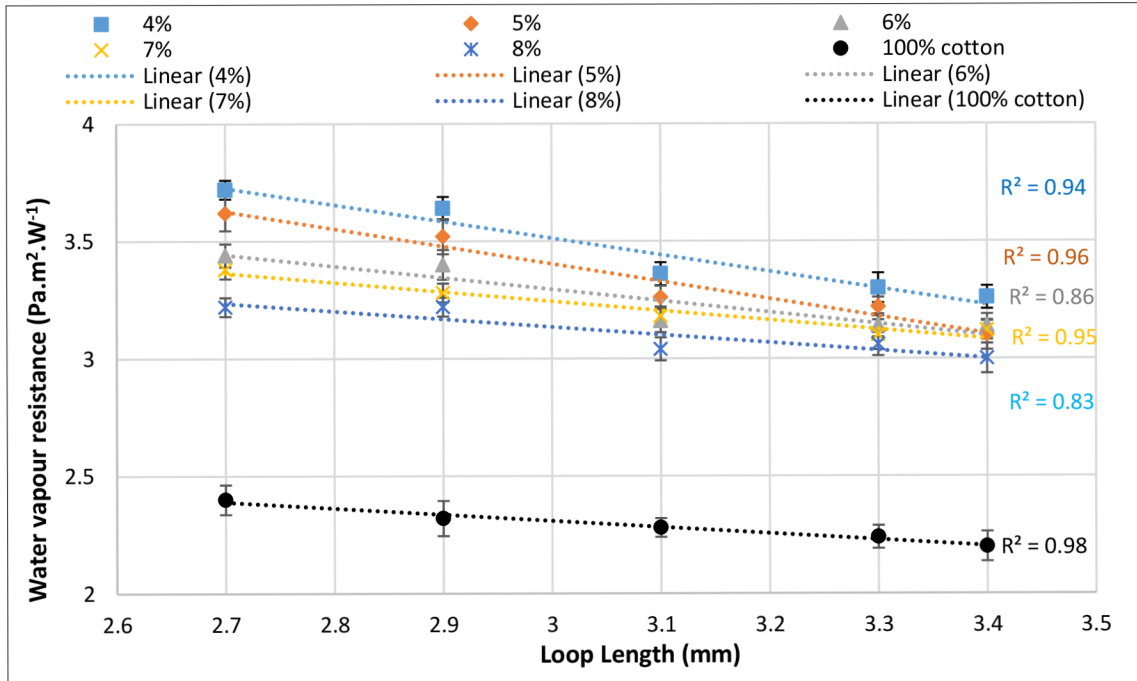
a- Full plaited (35 Ne)
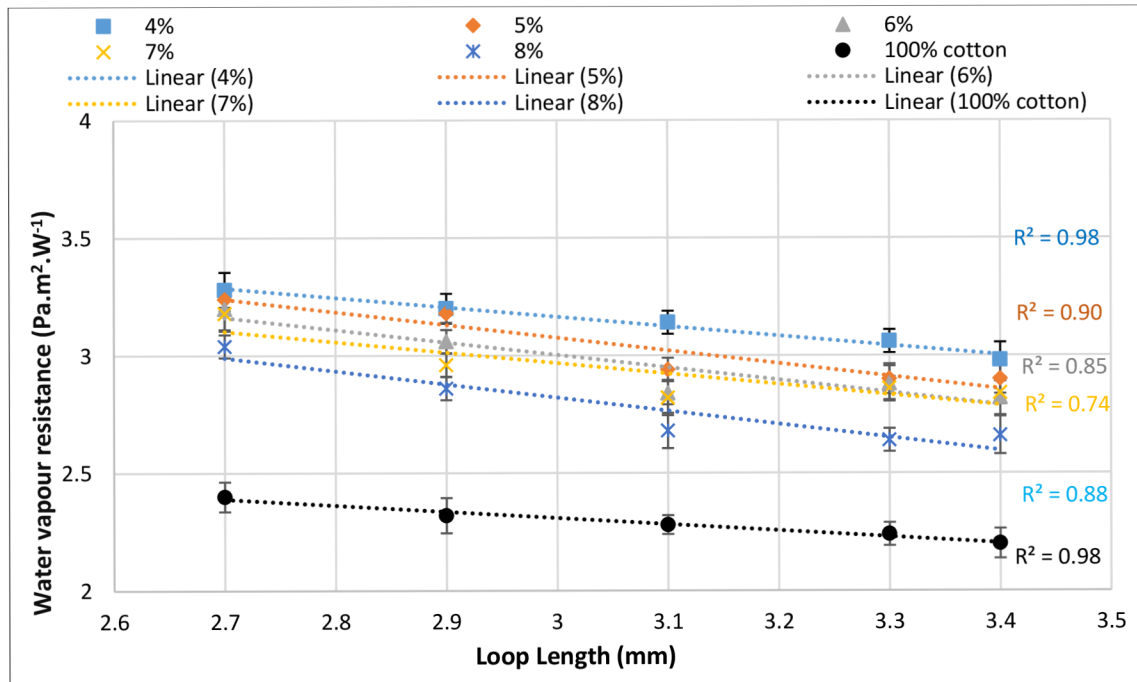
b- Half plaited (35 Ne)

Figure 5.16. Effect of loop length on the water vapour resistance (35 Ne)

The *WVR* decreased with the increase of *SWP* and loop length for both *fp* and *hp* due to the decrease of stitch density as shown in figure 5.1, which leads to an increase in air pore's size and water vapour transfer by diffusion through air gaps. The *WVR* of *fp* was relatively higher than *hp*. The *WVR* values of both *fp* and *hp* were less than 5 so the *WVR* was within an excellent level of water vapour transfer [49]. It could be interpreted that all samples were produced from hydrophilic fibres and absorbed water by capillary phenomena. The *WVR* of elastic *SJKF* samples was higher than 100% cotton samples by 55 and 37% for *fp* and *hp,* respectively, at loop length 2.7 mm and *SWP* 4%.

Also, the *WVR* of elastic *SJKF* produced from yarn count 25 Ne decreased when the loop length and *SWP* increased for both *fp* and *hp,* as shown in figure 5.17. The *WVR* of samples produced from yarn count 25 Ne was higher than the samples produced from yarn count 35 Ne it may be due to the samples produced from yarn count 25 Ne had lower porosity (according to table 10.4, appendix I), therefore; lower pore size. Statistical analysis showed that *SWP*, loop length, yarn count and plaiting technique had a significant effect on *WVR* as shown in table 5.3.
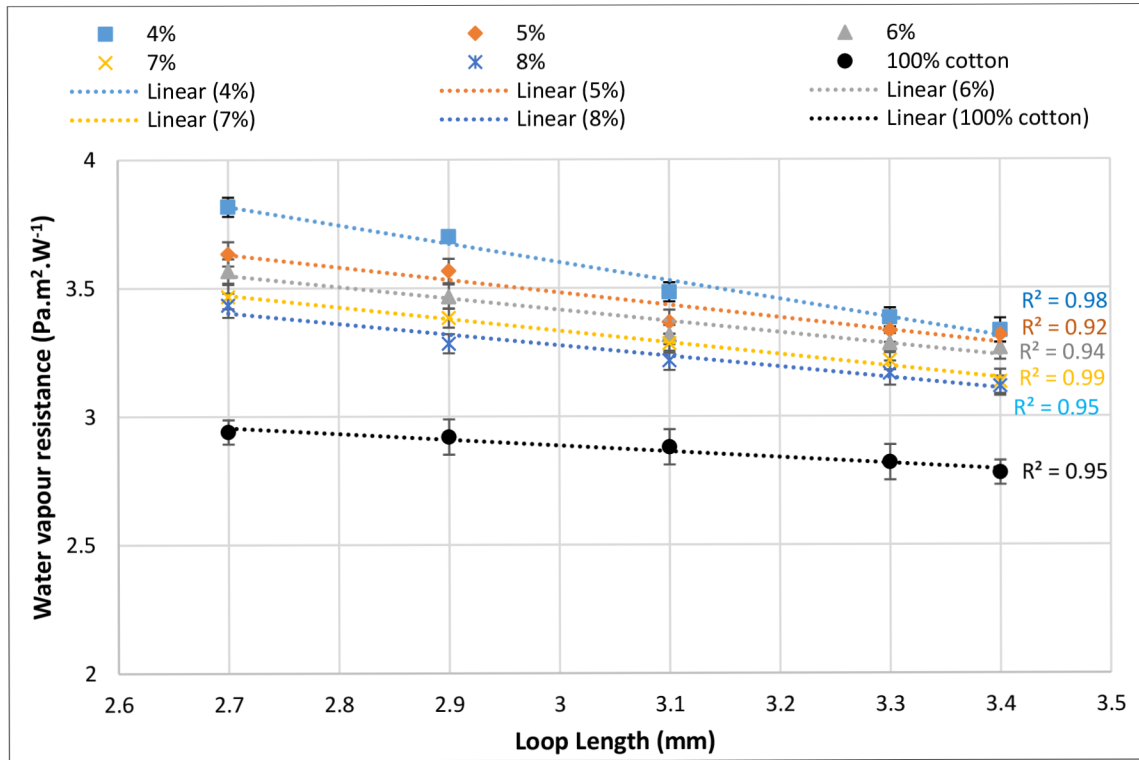
a- Full plaited (25 Ne)
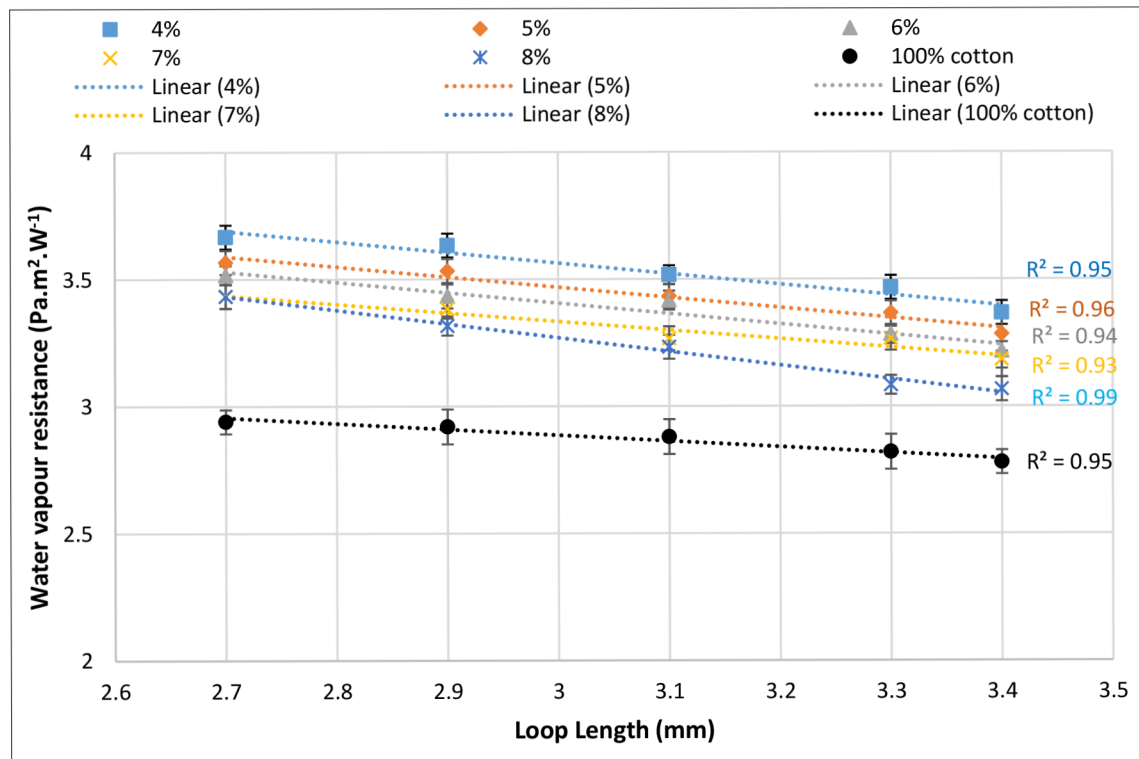
b- Half plaited (25 Ne)

Figure 5.17. Effect of loop length on the water vapour resistance (25 Ne)

5.2.5   *Air permeability*

Air permeability is the rate of airflow through the fabric when subjected to a pressure difference on either surface of the fabric, and it is mostly affected by the fabric porosity in addition to the thickness[6][50].
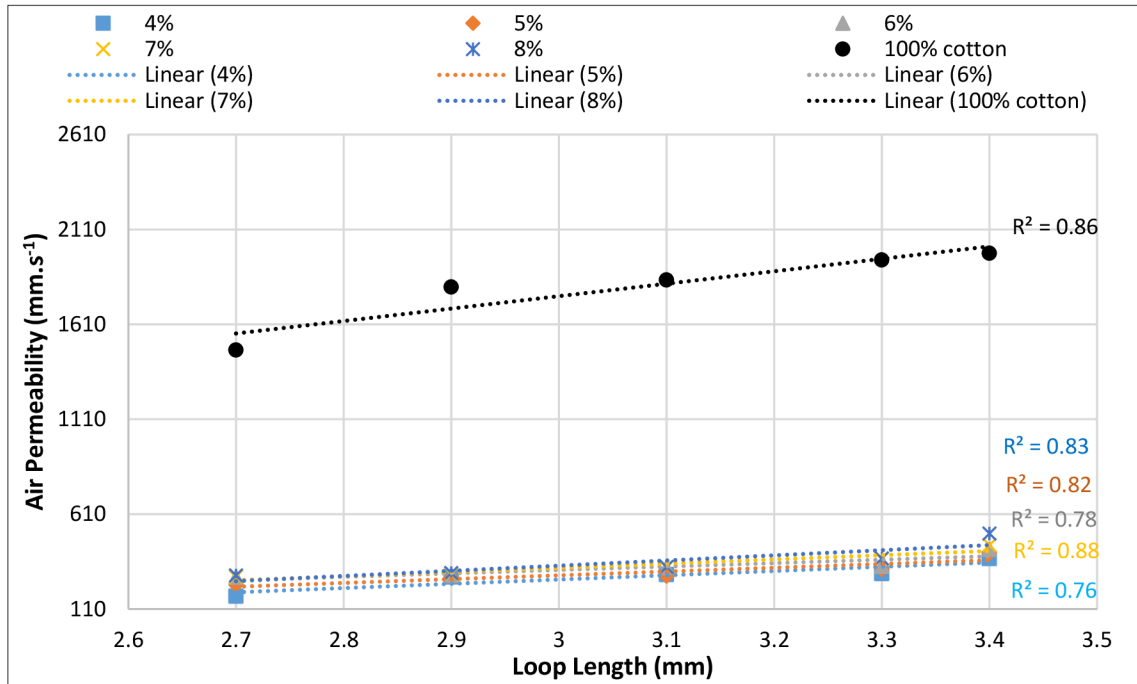
a-   Full plaited (35 Ne)
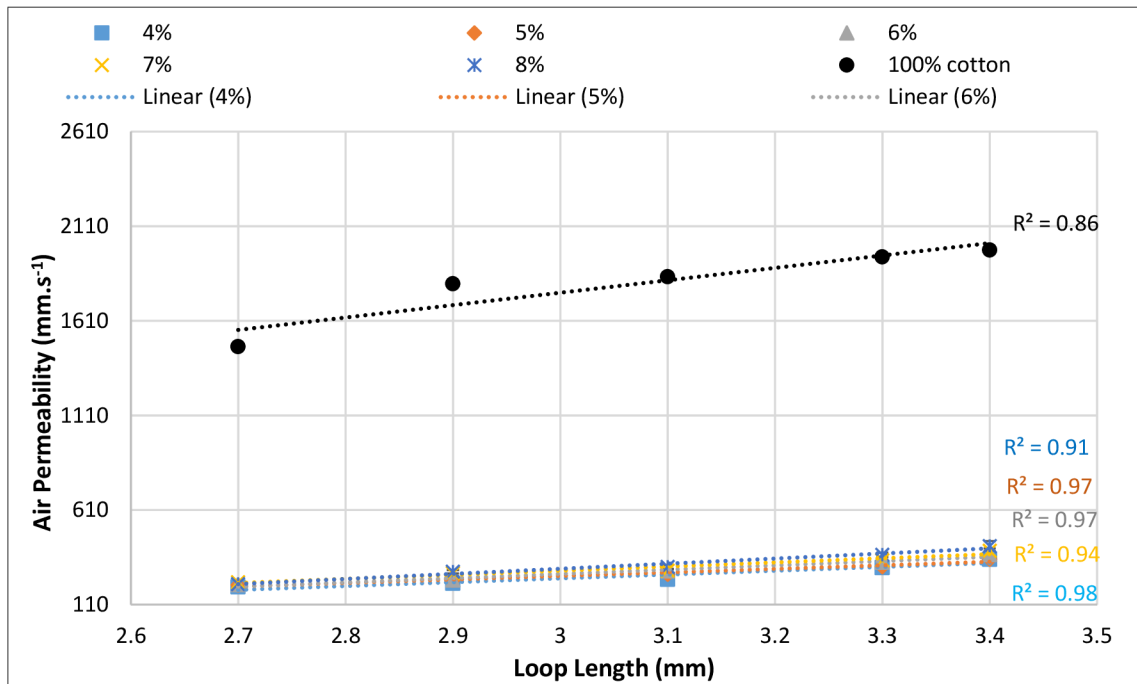
b-   Half plaited (35 Ne)

Figure 5.18. Effect of loop length on the air permeability

Air flow passes through three paths, the first one is through the pores between yarns, and this is the easiest way. The second path of air flow is through pores of single yarns. The third path is through yarn crossing, and it is considered the hardest path of air flow. Generally, air permeability of both *fp* and *hp* elastic knitted fabrics went up with the increase of loop length and *SWP,* as shown in figure 5.18, because of the decrease in the stitch density. Therefore, the pores size increased, and the rate of airflow through the fabric went up. The air permeability of *fp* samples was less than 100% cotton samples by 82% at 3.1 mm loop length and 5% *SWP.* For the elastic *SJKF,* the stitch density was higher than 100% cotton samples and there was stitch overlapping, therefore; the pores volume of elastic samples was lower than 100% cotton samples. The statistical analysis showed that *SWP* and loop length had a significant effect on the air permeability, as shown in table 5.1.

5.2.6 *Fabric growth and fabric stretch*

Stretch fabrics improve comfort through freedom of body movement by providing the necessary elasticity for a garment to respond to every movement of the body and return to its original size and shape[51][22]. Therefore, it was necessary to investigate the fabric stretch and fabric growth.

5.2.7 *Fabric growth*

a-　Wales direction (35 Ne)　　　　　　b-　Courses direction (35 Ne)
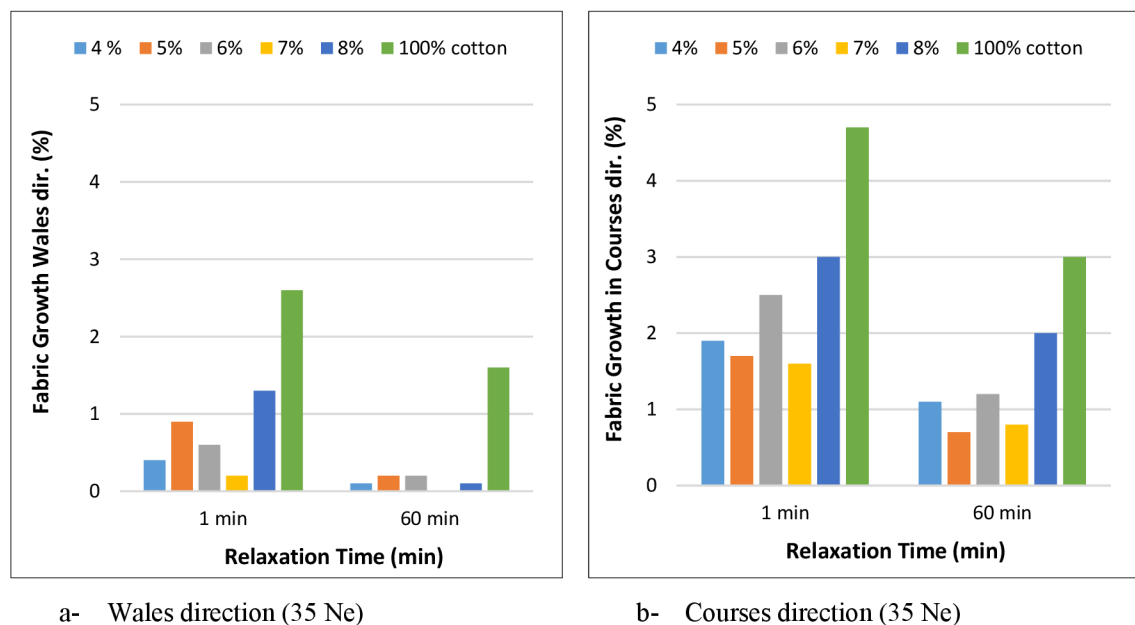
Figure 5.19. Effect of *SWP* on fabric growth (35 Ne)

Figure 5.19 shows the fabric growth after 1 and 60 min of relaxation time in wales

(*FGW*) and courses (*FGC*) directions at loop length 2.9 mm for both 100% cotton fabric and elastic fabrics produced from yarn count 35 Ne with 5 levels of *SWP*. In both directions, the 100% cotton fabric growth was higher than elastic fabric because of the presence of spandex. *FGW* was lower than *FGC*. 95% and 99% of extension in wales direction recovered after 1 and 60 min, respectively, while in 100% cotton 79 and 89 % of extension recovered after 1 and 60 min, respectively. The *FGW* and *FGC* of samples produced from yarn count 35 Ne were less than samples produced from yarn count 25 Ne as shown in figure 5.20. The effect of yarn count and *SWP* were significant on the growth of elastic fabric see table 5.2.

a- Wales direction (25 Ne)   b- Courses direction (25 Ne)
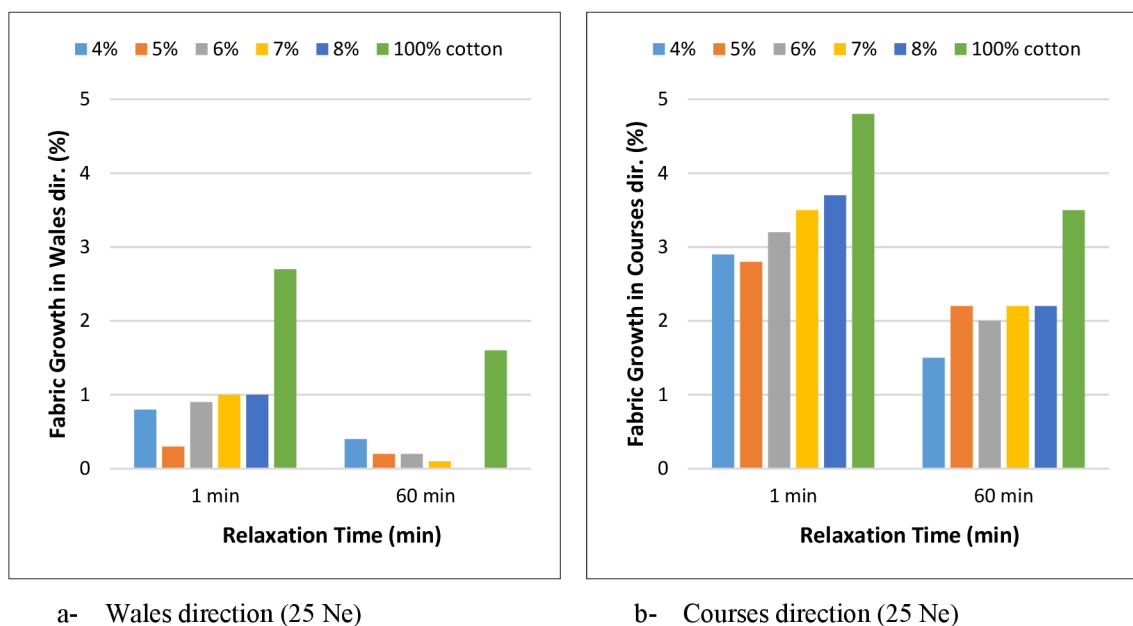
Figure 5.20. Effect of *SWP* on fabric growth (35 Ne)

Table 5.2. The significant levels of yarn count and *SWP* on fabric growth and stretch

Dependent property	P value, (Independent variable)			
	SWP		Yarn count	
	Wales direction	Courses direction	Wales direction	Courses direction
Fabric growth	<0.001	<0.001	<0.001	<0.001
Fabric stretch	<0.001	<0.001	<0.001	<0.001

5.2.8   *Fabric stretch*

Figures (5.21-a) and (5.21-b) illustrate the fabric stretch in wales (*FSW*) and courses (*FSC*) directions at different extension forces. *FSW* is lower than *FSC*. When tension is applied in

the course's direction, the needle loop, sinker loop, and loop legs straighten, as shown in figure (5.22-c), and wale density increases. When the applied tension is in the wale's direction, there is no opportunity to straighten the needle loop, sinker loop and loop leg, but it started to change the overlap structure to the normal structure as shown in figure (5.22- d). The fabric stretch went up with decreasing in *SWP* because of stitch overlapping and stitch density increasing. *FSW* of elastic fabric was higher than 100% cotton.
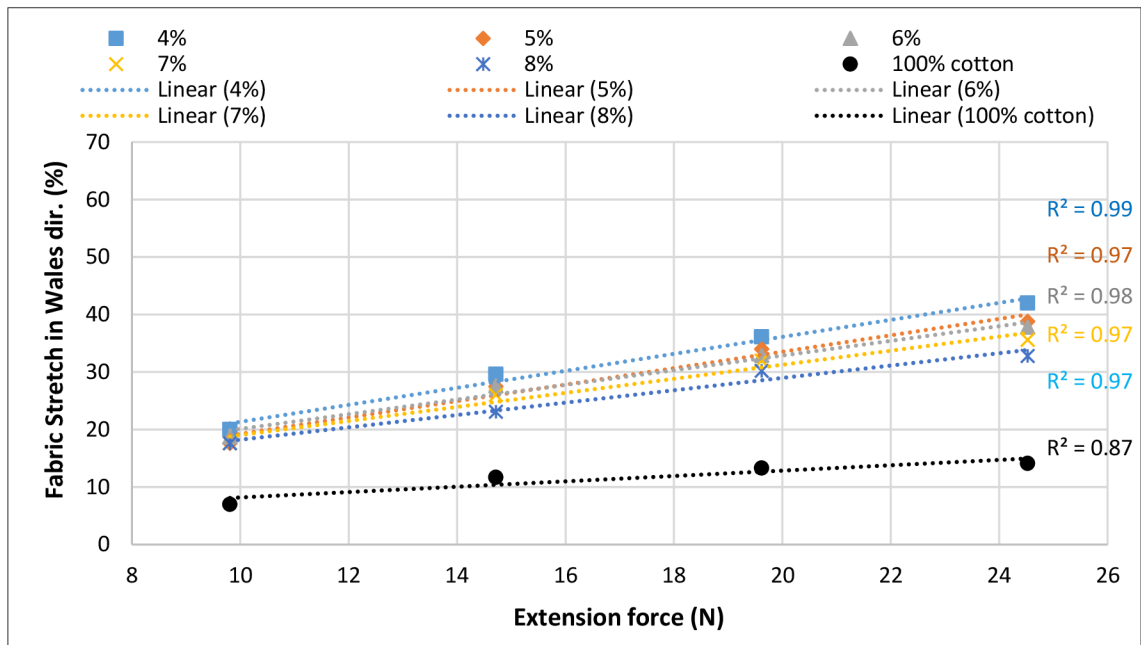
a-   Wales direction (35 Ne)
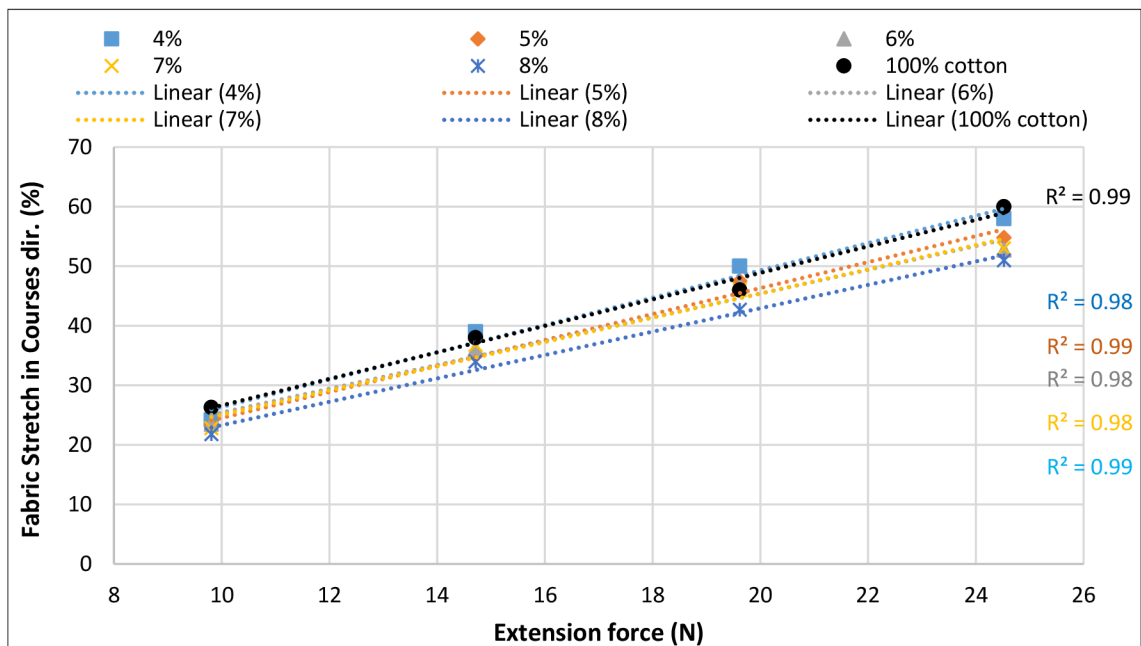
b-   Courses direction (35 Ne)

Figure 5.21. Effect of *SWP* on the fabric stretch (35 Ne)
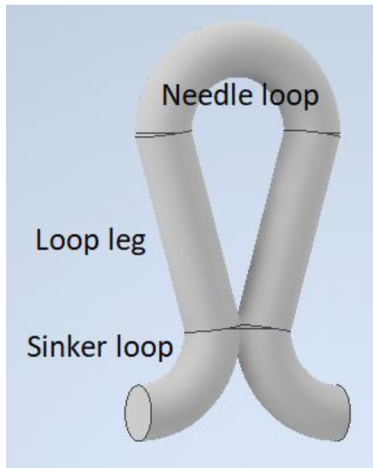
a- 3D loop
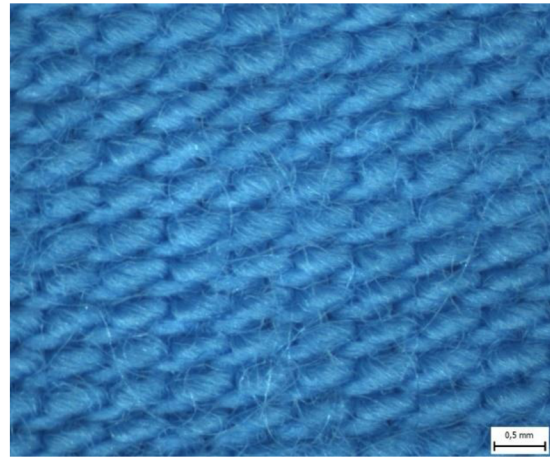
b- Sample image at *SWP* 4% without extension
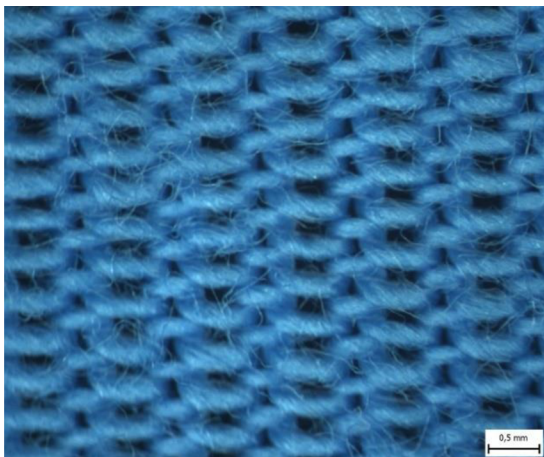
c- Sample image at 30% extension in course direction
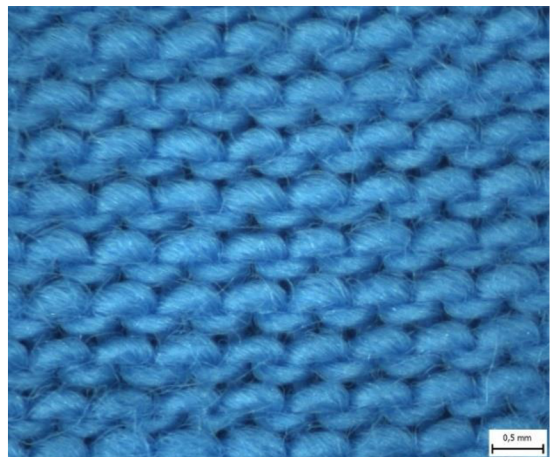
d- Sample image at 15% extension in warp direction

Figure 5.22. Sample images at different extensions in wales and course direction

FSW and *FSC* of samples produced from yarn count 35 Ne were higher than *FSW* and *FSC* of samples produced from yarn count 25 Ne as shown in figure 5.23. The yarn count and *SWP* had a significant effect on the growth of elastic fabric see table 5.2.
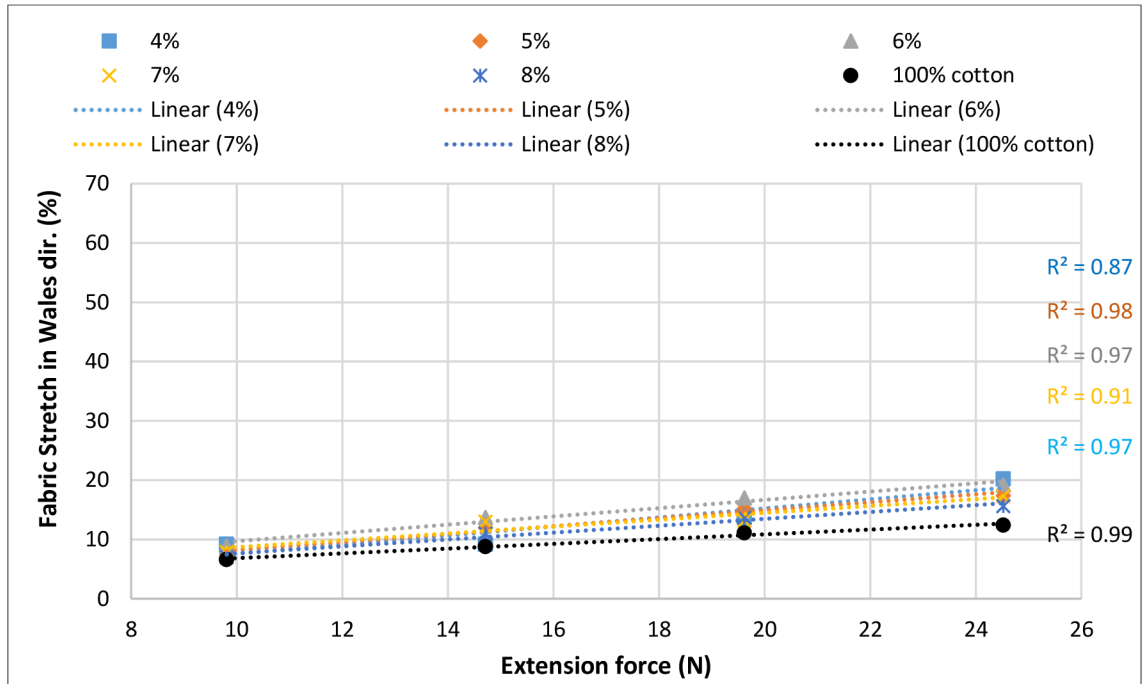
a- Wales direction (25 Ne)
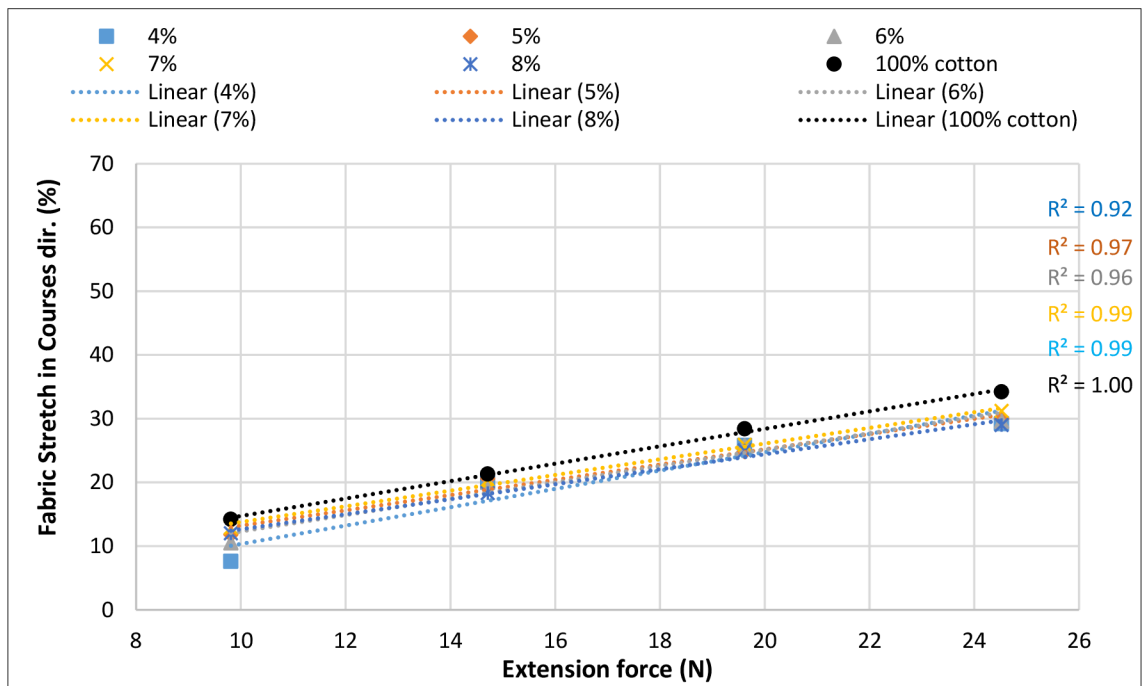
b- Courses direction (25 Ne)

Figure 5.23. Effect of *SWP* on the fabric stretch (35 Ne)

5.2.9   *Fabric thickness and thermal properties under extension*

Thermal properties were measured at two levels of extensions 15, and 30% in both warp and weft directions which were applied on elastic *SJKF* which were produced from yarn count 35 Ne at 2.9 mm loop length and five levels of *SWP*. Due to applied extension, the fabric thickness decreased by 5 and 15% for 15 and 30% extension, respectively, at *SWP* 4%, as shown in figure 5.24. When the extension was applied, the stitch overlapping disappeared gradually, as shown in figure 5.25, therefore; the fabric thickness decreased.
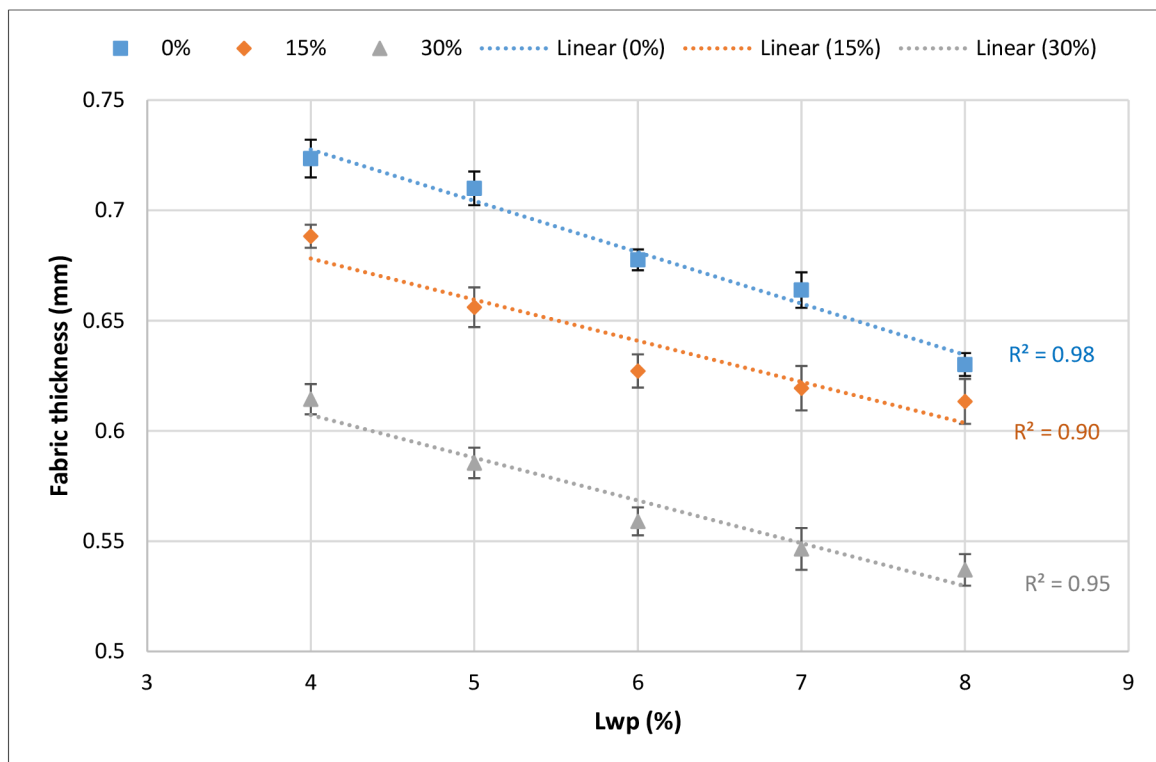
Figure 5.24. Fabric thickness after extension
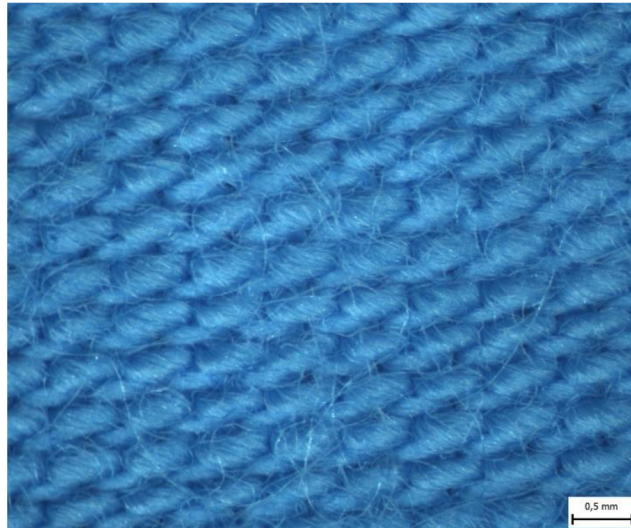
a-   Without extension
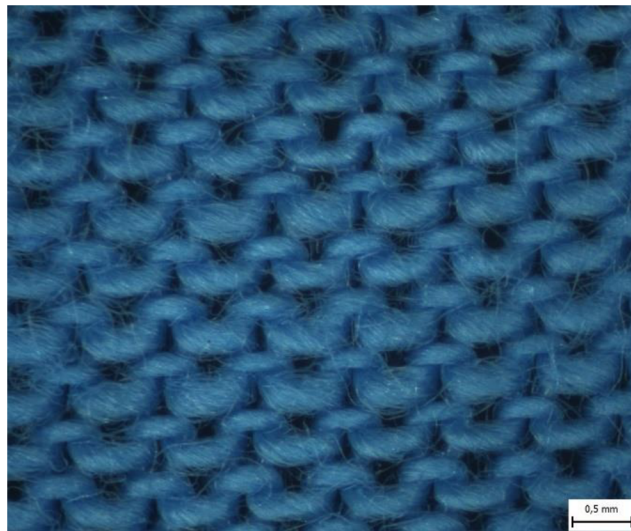
b-   With 15% extension
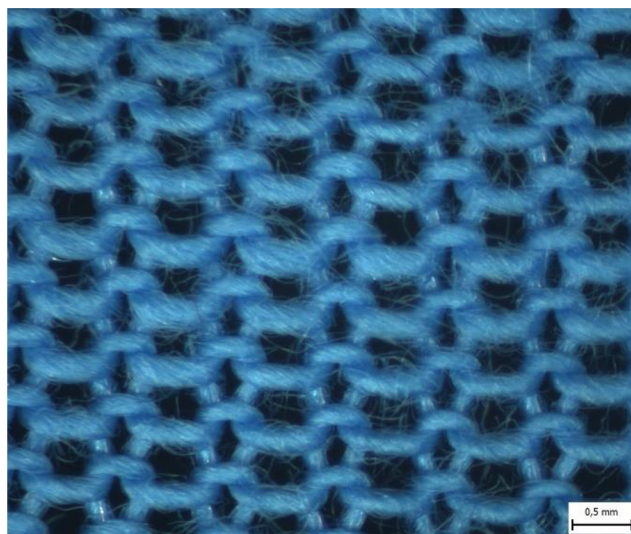
c-   With 30% extension

Figure 5.25. Sample images with and without an extension at loop length 2.9 mm and SWP 4%

The thermal conductivity increased due to the increase of extension from 0 to 15% at *SWP* 4, 5 and 6% and decreased at *SWP* 7 and 8% as shown in figure 5.26. When the extension reached to 15 % at *SWP* 4, 5, and 6%, the amount of heat flow increased due to the radiation because of the porosity increasing, as shown in figure (5.25-b). At extension 30%, the thermal conductivity went down due to a reduction in the number of fibres, as shown in figure (5.25-c).
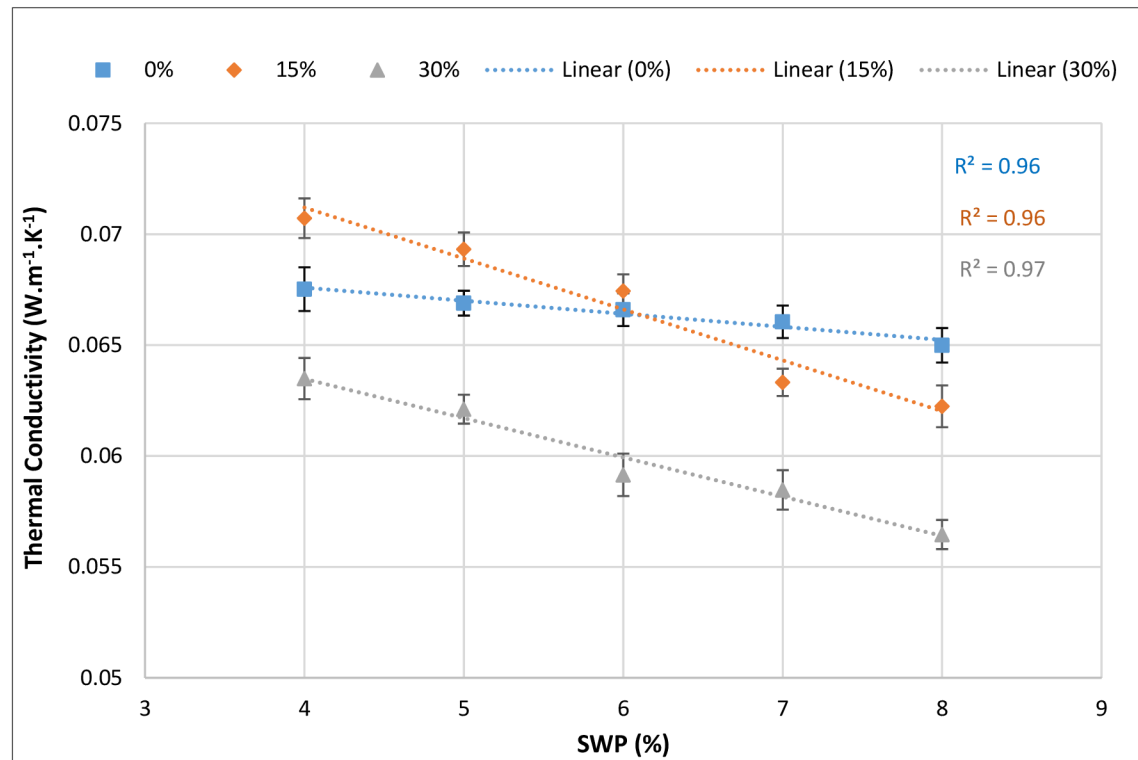
Figure 5.26. Thermal conductivity after extension

Figure 5.27 shows that the thermal resistance went down after applied extension 15 and 30% by 14 and 16 %, respectively, due to the fabric porosity and pore's size increased, as shown in figure 5.25, therefore, the amount of entrapped air increased, and the thermal conductivity decreased. Figure 5.28 shows that thermal absorptivity decreased with extension increasing due to a decrease in the thermal conductivity, the number of contact points per unit area and stitch density, as shown in figure 5.25.
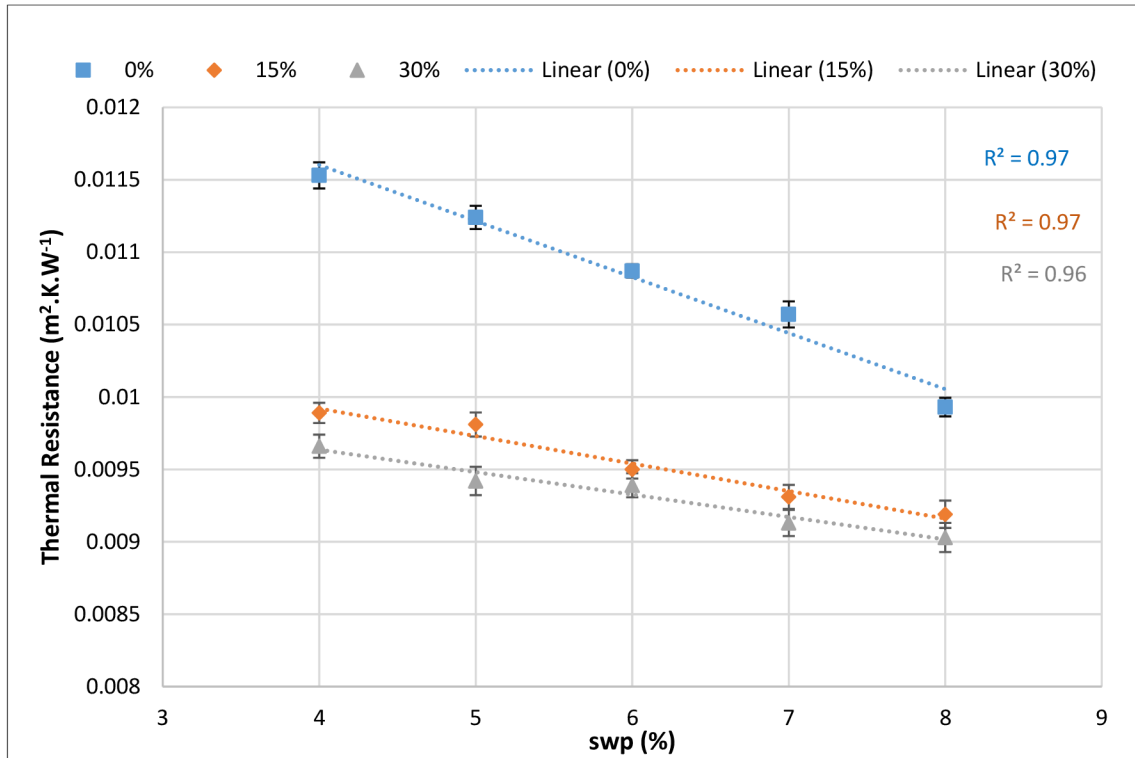
Figure 5.27. Thermal resistance after extension
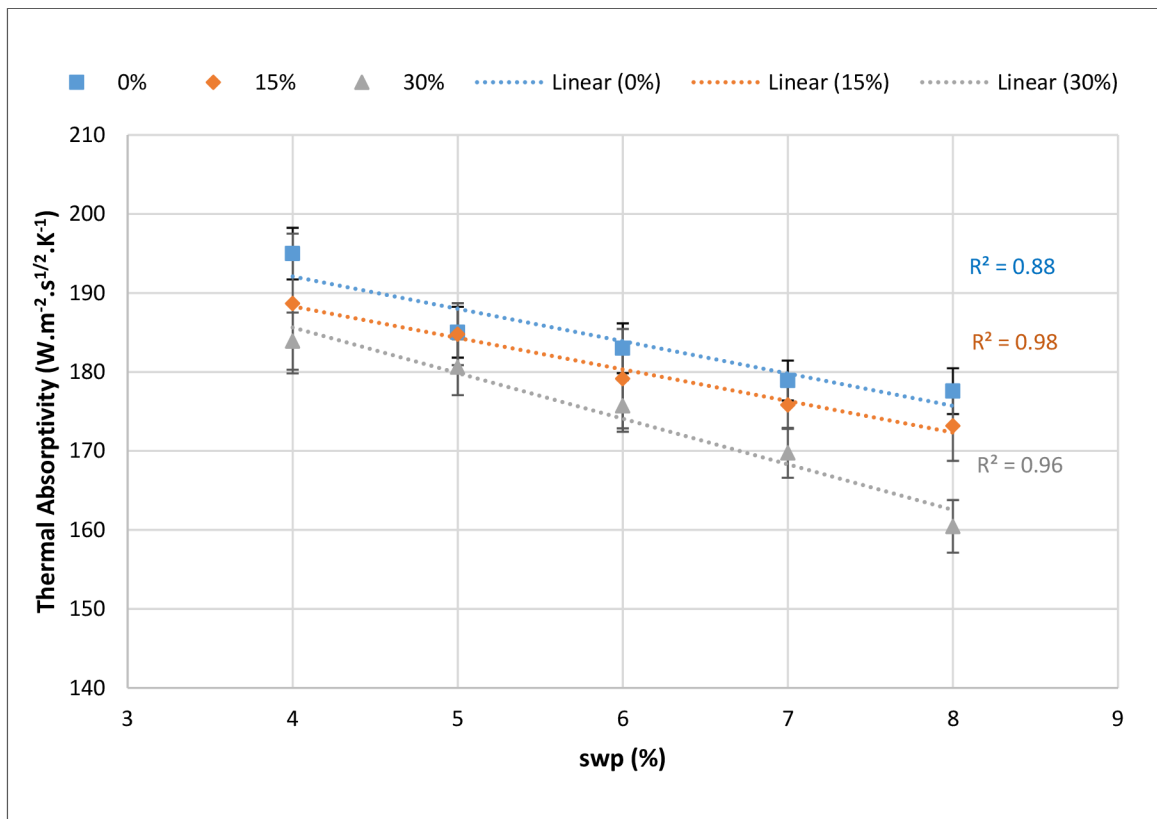
Figure 5.28. Thermal absorptivity after extension

6. CHAPTER 6: 3D GEOMETRICAL MODEL OF STITCH OVERLAPPING

The stitch overlapping phenomena of the elastic *SJKF* with high stitch density changes the conventional dimensions of *SJKF*; therefore, the physical properties in terms of the heat and moisture transfer. Hence the need to study the change occurring within the fabric structure and the distribution of pores size within the structure in the hope that this study could contribute to the interpretation of the relationships between structural parameters and physical properties.

The fabric porosity of elastic *SJKF* was relatively lower than 100% cotton by 7% as shown in figure 5.9. The stitch density, fabric thickness and thermal resistance of elastic *SJKF* were higher than 100% cotton samples by up to 80, 47 and 23% respectively at loop length 2.7 mm and *SWP* 4%. Also, air permeability of elastic *SJKF* was lower than 100% cotton samples by up to 85% at loop length 2.7 mm and *SWP* 4%, as the pores size and distribution inside the structure played an important role in heat and air flow. There were problems to analyse the pores size, distribution and porosity of elastic *SJKF* by Micro CT. Therefore, loop geometry model of *SJKF* was needed to investigate the pores size, distribution and porosity inside the structure.

In this chapter, 3D geometrical model based on different *SJKF* structures (open, max set, and stitch overlapping) was established to describe the pore's size, pores' distribution, and the fabric porosity through the different structures based on the actual geometrical parameters of the loop by using AutoCAD software. Then, the fabric thickness was divided into several sections, and the theoretical pore's size at each section of fabric thickness was analysed and calculated.

It is known that the fabric porosity influences the physical and thermal properties and hence, the fabric end-use. Fabric porosity can give a clue about thermal resistance, air permeability, and water vapour resistance. The heat, liquid sweat generation, and water vapour must also be transferred and dissipated from the body to the environment [52]. The water vapour moves primarily through fabric pores by a diffusion process in the air from one fabric side to the other [53]. The fabric porosity depends on pore size, volume, and pore distribution. These factors in turn, are influenced by fabric construction parameters such as yarn count, fabric structure, machine setting, and finishing process. According to

Guidoin [54], [55] porosity is '*the ratio of void space within the boundaries of a solid material to the total volume occupied by this material, including void spaces*'.

Mostly, the fabric porosity is investigated using three methods, image processing, air permeability, and geometrical modelling [56]. A lot of research investigated the pore size and its distribution for woven and knitted fabric by using image processing techniques and based on yarn and fibre parameters from fabric cross-section images [52], [56]–[58]. The surface porosity of single jersey knitted fabrics was investigated by many researchers using image analysis techniques with and without yarn hairiness consideration. Inter pores between yarns were measured by computing the equivalent pores diameter, while intra pores inside yarns were calculated from Neckar's theoretical equation [59].

Since air permeability has a direct relationship to pore size [52], some research linked air permeability and knitted fabric porosity based on geometrical parameters such as fibre density, yarn count, stitch length, courses density, wales density, and fabric thickness [53], [56], [60], [61].

Furthermore, geometrical modelling was conducted using the geometry of the unit cell of a single loop. Fabric porosity was estimated from a 2D knitted fabric model by calculating the area covered by yarn and the total area of one repeat [62], [63]. Few models for 3D porosity are available that investigated weft knitted fabric, such as the Benltoufa and Karaguzel theoretical models and the Guidoin empirical model [64]. Benltoufa calculated the knitted fabric porosity from the geometrical representation of the elementary loop geometry, assuming a circular yarn cross-section [56]. In addition to this method, Benltoufa used the air permeability and image processing method and concluded that geometrical modelling is the most appropriate and easiest way to evaluate porosity.

Karaguzel's model predicted pore volume in addition to inter yarn pore size for simple weft knitted fabric structures, from fabric parameters, such as courses and wales density, yarn linear density, and fabric thickness, which characterize the structure [65]. A plug-in was developed using Python script to predict the plain knitted fabric porosity by using the actual parameters of the fabric. 3D solid and multifilament models of knitted fabric were generated automatically with two alternatives of models (Peirce and parametric). It was assumed that the yarn cross-section was circular that is swept around the yarn's central axis [54]. Adam K. et al. Modelled the air permeability of knitted fabric by using three-dimensional models of knitted fabrics and mapping the geometry in the microscale [66].

It is known that spandex yarns are incorporated with yarns in knitting machines to enhance the dimensional stability of knitted fabric during usage and after repeated stresses, which is considered the main defect of knitted fabrics, particularly single jersey knitted fabric [67]. Adding Spandex turns the knitted structure from an open and normal structure into a very compact structure, and causes stitch overlapping where the courses spacing becomes less than $2\sqrt{3}d$, wales spacing becomes less than $4d$, and fabric thickness becomes higher than $3d$, where d is yarn diameter [62], [68], [69]. Since the stitch overlapping effect was not studied earlier using the above-mentioned geometrical modelling method, this research presents a 3D modelling of the stitch overlap geometry to calculate the fabric porosity. The research developed a novel method of calculating porosity by making several sections of fabric thickness and calculating the accumulative volume of fibres in a unit cell of single jersey knitted fabric. The results are compared to porosity calculated by using the Guidoin model.

6.1.1 *Basis of the presented model*

This model was based on the actual fabric parameters (yarn diameter and loop length) and theoretical assumptions.

6.1.2 *Actual parameters*

To obtain the overlapping structure, the produced full plaited *SJKF* sample from yarn count 35 Ne (d = 0.1662 mm) at the loop length 2.9 mm and *SWP* 8% was chosen. To obtain an open structure, 100% cotton *SJKF* (without spandex) was chosen at the same yarn count and loop length. Moreover, one more fabric structure called "maximum set" or normal structure was not produced, but instead, it was drawn since the maximum set is the transitional case between open and overlapping structures.

6.1.3 *Mathematical model design*

A 3-dimensional multi-fibre model (rather than a solid cylindrical model) was developed taking into consideration the following parameters: loop length (2.9 mm), yarn diameter (0.1662 mm) as actual and experimental parameters. Yarn cross-section inside the fabric was closed to circular as shown in figure 6.1, fibre length in a single loop, fibre diameter, fibre cross-section shape, the total number of fibres in yarn cross-section, and yarn twist. The model was constructed to simulate fabric structures.
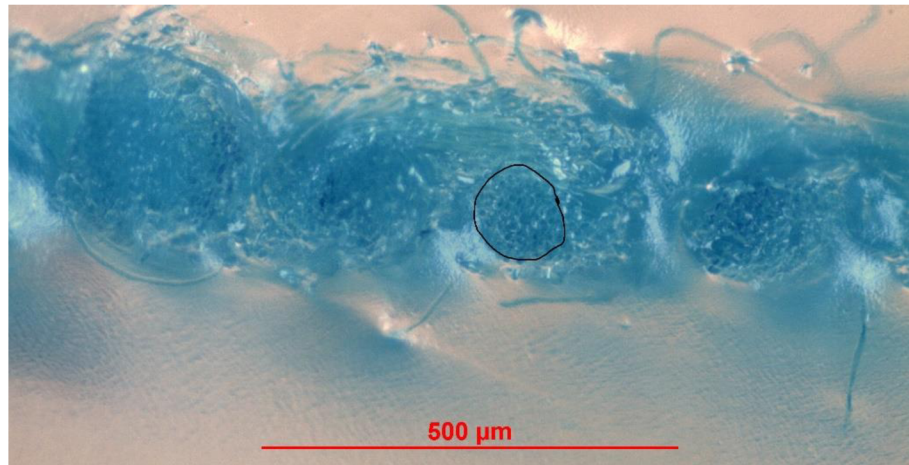
a-   Image of yarn cross section in courses direction
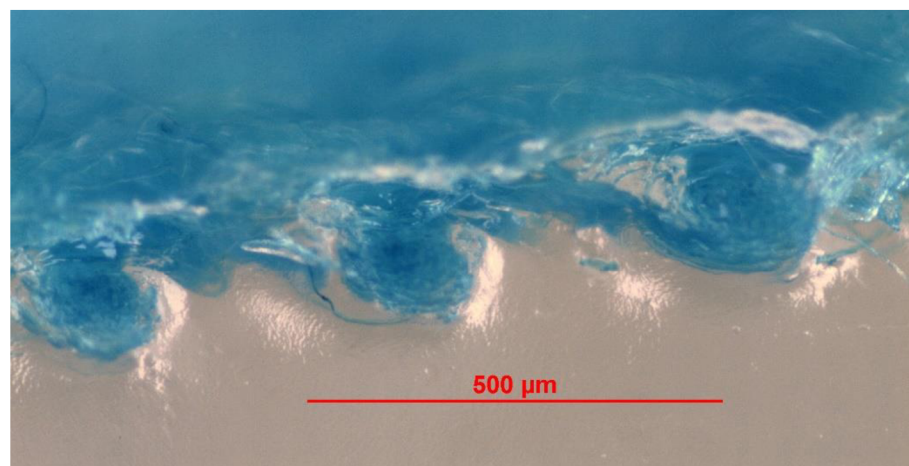
b-   Image of yarn cross section in wales direction

Figure 6.1. Cross-section images of 100% cotton sample

6.1.3.1 *Assumptions*

1. The following assumptions were used to describe the fabric structure:

2. Fibres have kidney shape and their cross-section areas are equal.

3. The yarn cross-section is circular based on Peirce model [70].

4. Fibres are evenly distributed along the yarn cross-section.

5. Yarns forming the loops were fully flexible, touched, but not compressed [71].

6. Yarn hairiness is neglected.

7. Individual fibres are continuous.

8. Theoretical fabric thickness for open structure $2d$, for maximum set $2d$, and for overlapping $3d$.

9. Wales spacing is constant and equal to $4d$.

6.1.3.2 *Yarn structure*

The total number of fibres in the yarn cross-section, N was calculated according to equation (6.1):

$$N = \frac{T}{t} \qquad \dots \dots \dots \dots \qquad (6.1)$$

Where T is yarn count (tex), t is cotton fibre fineness (tex). Cotton fibre diameter, D (mm) was obtained according to equation (6.2) [72]:

$$D = \sqrt{\frac{4\,t}{\pi\,\rho_f}} \qquad \dots \dots \dots \dots \qquad (6.2)$$

Where ρ_f is fibre density (kg/m³). The cotton fibre cross-section area, A was obtained according to equation (6.3).

$$A = \frac{\pi D^2}{4} \qquad \dots \dots \dots \dots \qquad (6.3)$$

The circular cross-section that had an area A shown in Figure (6.2-a) was converted into a kidney shape with the same area to imitate the cotton fibre as shown in Figure (6.2-b). The number of twists per inch of that yarn, TPI was calculated according to equation (6.4).

$$TPI = \alpha_e \sqrt{Ne} \qquad \dots \dots \dots \dots \qquad (6.4)$$

Based on loop length, the number of twists in one loop of fabric was calculated. Spandex yarn diameter was calculated according to equation (6.2).

| **a.** Fibres disrtibution inside yarn with circle cross section | **b.** Fibres disrtibution inside yarn with kidney cross section | **c.** Real yarn cross-section |
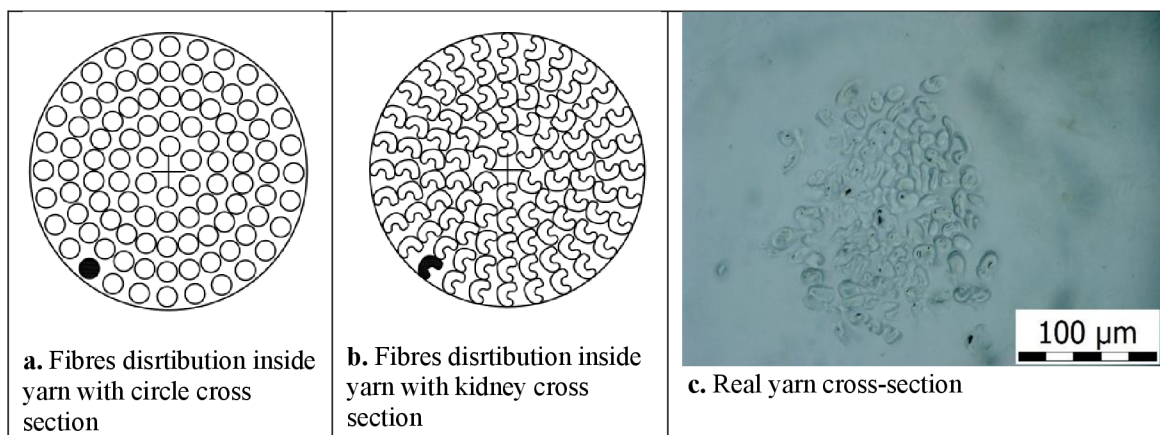
Figure 6.2. Yarn cross-section.

6.1.3.3 *Fabric geometry*

To present the *SJKF* 3D model using AutoCAD software, a two-dimensional sketch of a single loop was carried out based on the Peirce model (the yarn axis follows a path composed of circular arcs and straight lines) [70], as shown in figure 6.3 and actual yarn diameter, wales, and courses density as shown in Figure 6.3. The actual loop parameters are shown in Table 6.1.

0.64 mm / d / 0.67 mm	0.58 mm / 0.67mm	0.45 mm / 0.67 mm
Open structure (100% cotton)	Maximum set	Overlapping at *SWP* 8%
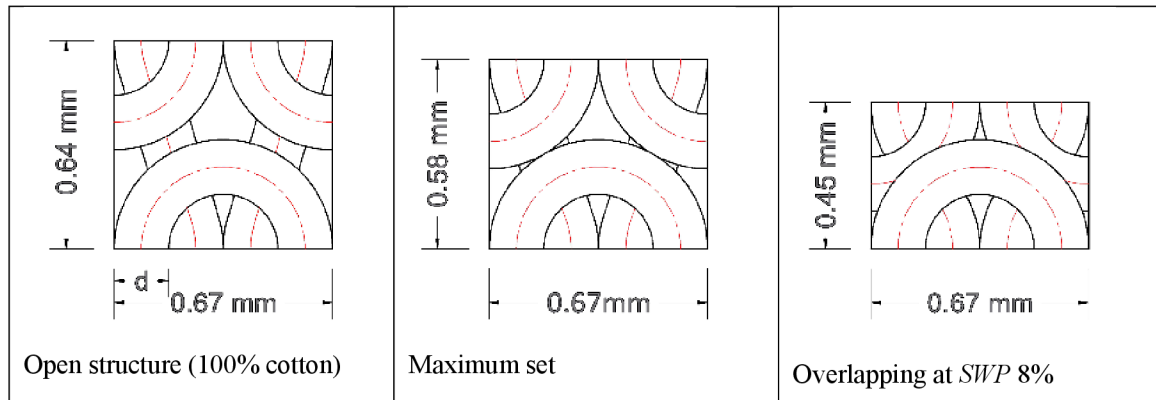
Figure 6.3. 2D Scheme of the knitted fabric structure.

Table 6.1. Actual loop geometrical parameters

Parameters	Single jersey knitted fabrics	
	Open Structure (100% Cotton)	Overlapping (elastic sample)
Wales/cm	14.63	15.92
Courses/cm	15.75	22.37
Stitch density/cm^2	230.4	356.1
Yarn diameter (mm)	0.16642	0.16642

As the inclusion of inter-fibre spacing is one of the important factors that determine the utility of the model for theoretical predictions of the porosity of textiles, a cross-sectional sketch of the yarn based on individual fibres was drawn, as shown in figure (6.2- b). Then, a sketch describing the profile of the loop in a 3D view was created consisting of a continuous spline as shown in Figure 6.4 [73]. For spandex yarn, it follows a shorter trajectory than in the case of 100% cotton yarn since more tension is applied while feeding, as shown in Figure 6.4. Therefore, the loop length in the 3D model varied slightly from the actual loop length, where the loop length of open, maximum set, and overlapping structures were 3.07 mm, 2.9 mm, and 2.85 mm, respectively. Finally, the 3D loop was obtained using the sweep operation of the fibre cross-sections.
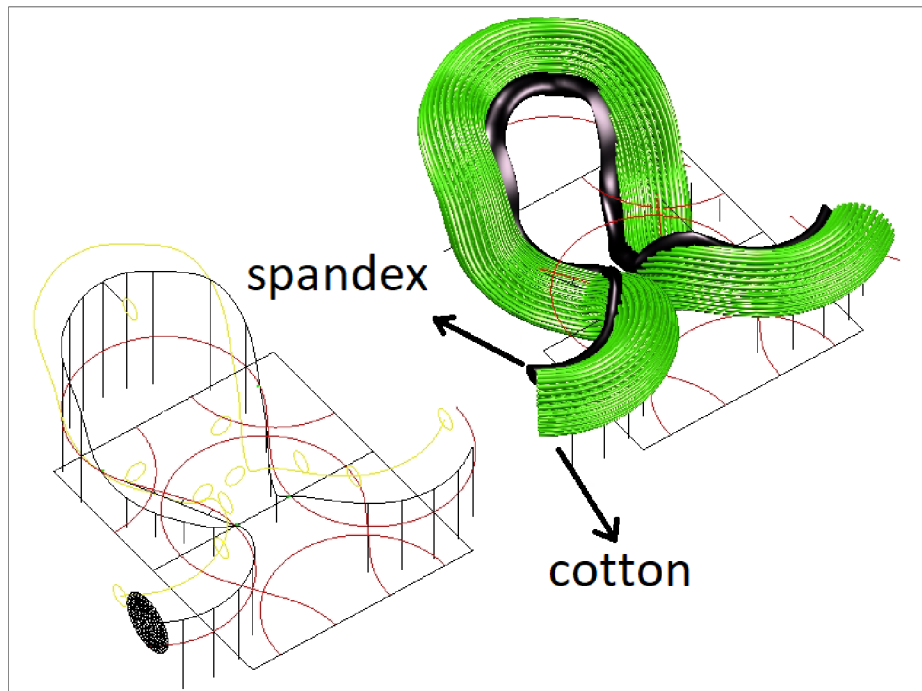
Figure 6.4. Stages of designing the 3D geometrical model of stitch overlapping.

Afterwards, the loop was repeated to demonstrate the final fabric appearance. Figure 6.5 shows the different views for each structure. Figures (6.5-a), (6.5-e), and (6.5- h) show the 3D isometric projection of open *SJKF*, maximum set, and overlapping structures, respectively. Figures (6.5-b), (6.5-f), and (6.5-i) show the side view, and figures (6.5-c), (6.5-g), and (6.5-j) show the front views. Finally, figures (6.5-d) and (6.5-k) show the optical microscopic images of the produced open and overlapping *SJKF* structures, respectively.
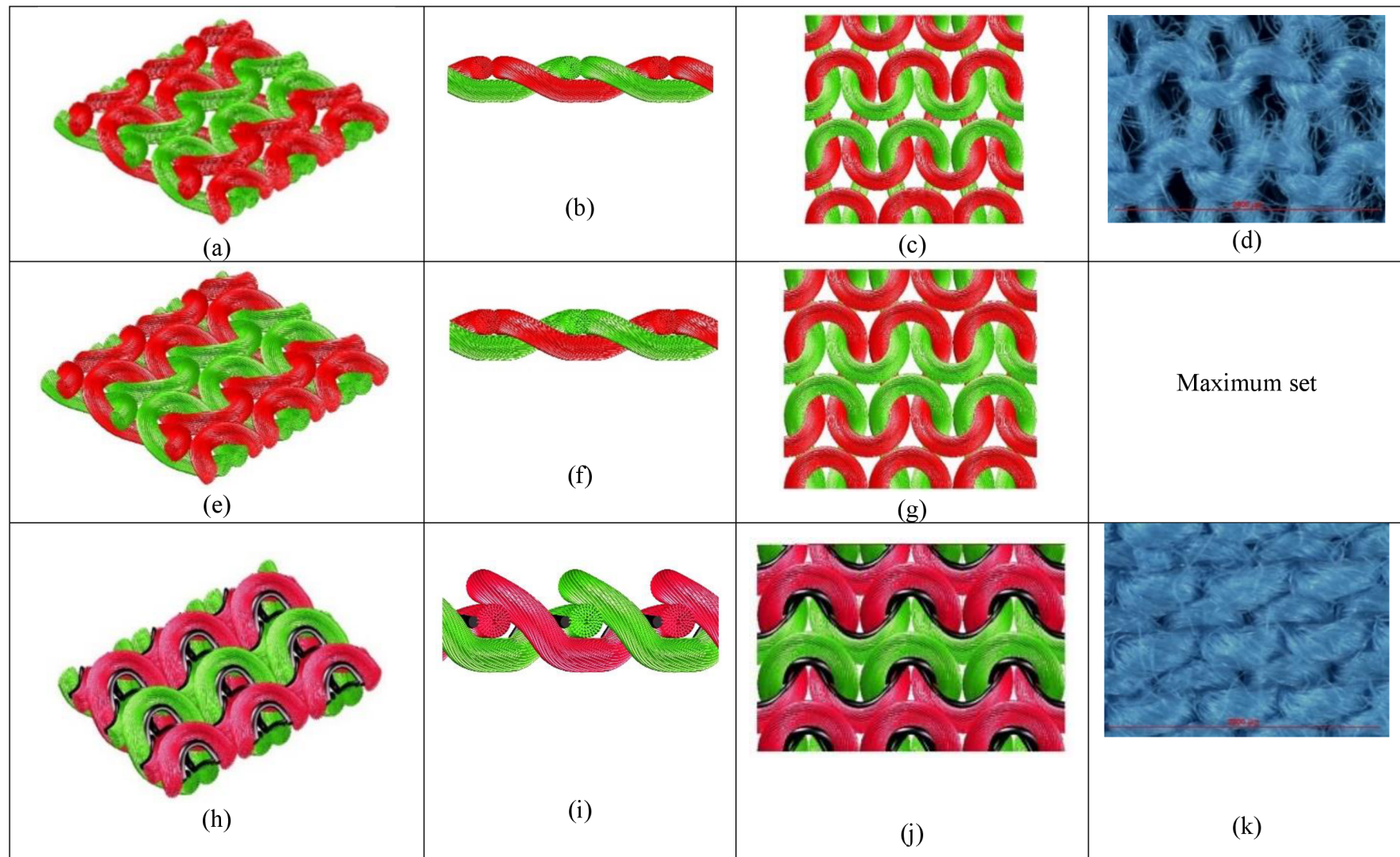
Figure 6.5. Optical microscopic images of fabric along with its corresponding 3D model

6.1.4   *Determining pore's size, volume, and distributions*

An enclosure was drawn around the repeat of the knitted fabric structure to simulate the surrounding air, as shown in figure 6.6. The pore's volume was obtained by calculating the fibre's volume and total enclosure volume of progressive growing sections of the fabric (top to bottom), using a 0.033 mm increment value, as shown in Figure 6.7. The open structure and maximum set fabrics were divided into 10 sections, while overlapping was divided into 15 sections because its thickness was greater.

Figure 6.6. A volume enclosing the repeat of the knitted fabric structure.

The pores volume at i^{th} section, V_{pi} can be calculated according to equation (6.5), as shown in table 6.2 for deferent structures.

$$V_{pi} = V_{xi} - V_{fi} \qquad \dots \dots \dots \dots \qquad (6.5)$$

Where V_{xi} is enclosure volume of the ith section, and V_{fi} is fibre volume of the ith section. The theoretical porosity in the ith section, ε_i can be calculated according to equation (6.6).

$$\varepsilon_i = \frac{100V_{pi}}{V_{xi}} * 100 \qquad \dots \dots \dots \dots \qquad (6.6)$$
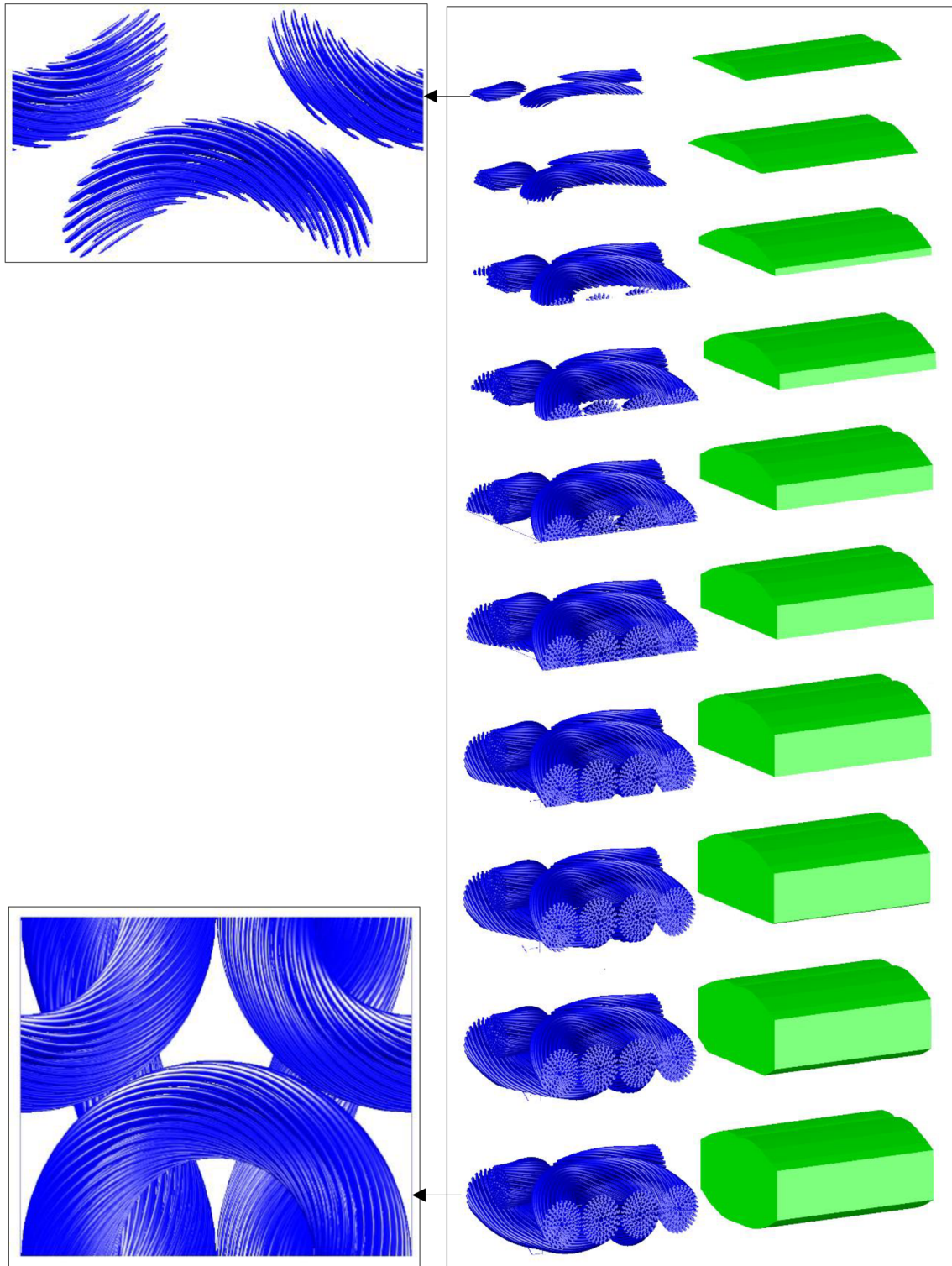
Figure 6.7. Progressive enclosure volume used to calculate fabric porosity (maximum set).

Table 6.2. Theoretical pore's volume values of different fabric structures at different sections

Open structure					
Section number	Fabric thickness (mm)	V_{xi} (mm³)	V_{fi} (mm³)	V_{pi} (mm³)	ε_i (%)
1	0.033	0.008	0.001	0.006	82.7
2	0.067	0.020	0.004	0.015	78.1
3	0.100	0.034	0.009	0.025	74.6
4	0.133	0.049	0.013	0.036	72.8
5	0.166	0.062	0.018	0.044	71.4
6	0.200	0.076	0.022	0.054	71.2
7	0.233	0.091	0.026	0.065	71.2
8	0.266	0.105	0.030	0.075	71.7
9	0.300	0.117	0.032	0.085	72.5
10	0.333	0.126	0.033	0.093	73.7
Maximum set					
Section number	Fabric thickness (mm)	V_{xi} (mm³)	V_{fi} (mm³)	V_{pi} (mm³)	ε_i (%)
1	0.033	0.007	0.001	0.006	81.4
2	0.067	0.018	0.004	0.013	75.1
3	0.100	0.031	0.008	0.022	72.5
4	0.133	0.043	0.013	0.030	69.1
5	0.166	0.056	0.018	0.038	68.0
6	0.200	0.069	0.022	0.047	68.3
7	0.233	0.082	0.026	0.056	68.6
8	0.266	0.094	0.029	0.066	69.4
9	0.300	0.106	0.031	0.075	70.4
10	0.333	0.113	0.032	0.081	71.6
Overlapping					
Section number	Fabric thickness (mm)	V_{xi} (mm³)	V_{fi} (mm³)	V_{pi} (mm³)	ε_i (%)
1	0.033	0.002	0.0004	0.001	77.8
2	0.067	0.005	0.002	0.003	69.4
3	0.100	0.009	0.003	0.006	62.6
4	0.133	0.014	0.006	0.009	61.0
5	0.166	0.020	0.008	0.012	62.1
6	0.200	0.028	0.010	0.019	65.5
7	0.233	0.038	0.013	0.025	65.5
8	0.266	0.048	0.017	0.031	64.4
9	0.300	0.058	0.021	0.037	64.2
10	0.333	0.068	0.024	0.044	64.9
11	0.366	0.078	0.027	0.052	65.9
12	0.400	0.088	0.030	0.058	65.8
13	0.433	0.098	0.033	0.065	66.2
14	0.466	0.107	0.035	0.072	67.0
15	0.500	0.113	0.036	0.077	67.9

The total pores volume at each section of fabric thickness is shown in figure 6.8. It is obvious that the open structure has the highest pore volume at all sections followed by the maximum set followed by the overlapping structure. At the fabric thickness is equal to d, the total pores volume of overlapping structure is less than open and the maximum set, structures by 72 and 68%, respectively. Also, when fabric thickness is equal to 2d, the total pores volume of the overlapping structure is less than open and maximum set structures by 74 and 70%, respectively. So, adding spandex has a great effect in pore size and distribution of *SJKF*
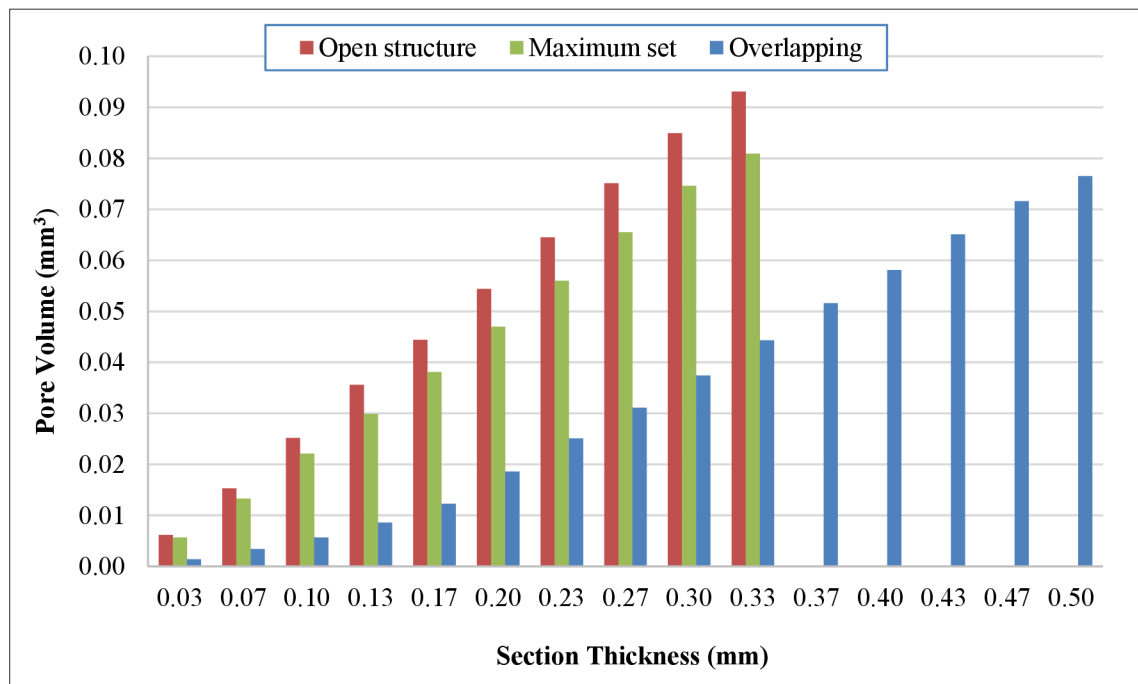
Figure 6.8. Total pore volume at ith fabric section

Figure 6.9 shows the theoretical values of fabric porosity at the ith fabric section (top to bottom) for different fabric structures. The porosity at the first section (top) is maximum and it significantly decreases with the increase in fabric thickness until the fabric centre line, then it increases again until the final section (bottom). This trend was almost the same for all structures. Based on the results of the 3D model, in all fabric sections, the fabric porosity of 100% cotton is the highest, followed by the maximum set, followed by overlapping.
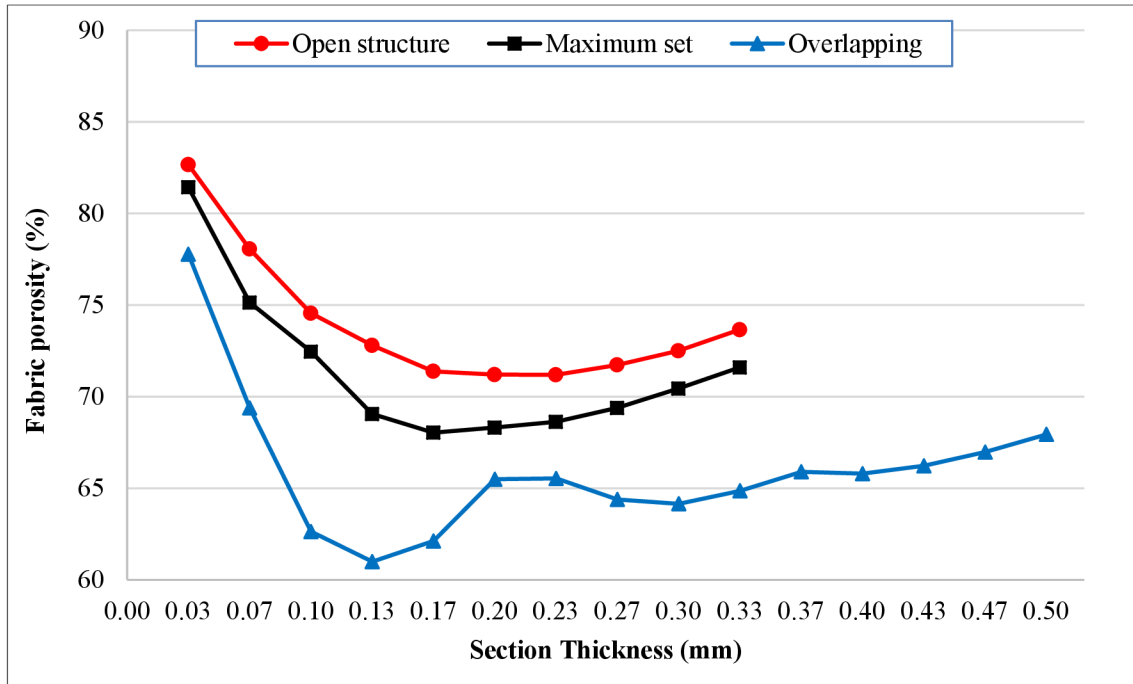
Figure 6.9. Fabric porosity at i^th fabric section (top to bottom)

7. CHAPTER 7: PREDICTION OF THERMAL CONDUCTIVITY OF ELASTIC SJKF

Generally, the mathematical models are needed to interpret experimental relations, estimate the expected properties, and to assist in designing and developing of a new fabric to achieve a certain property. As there are several theoretical models to predict the thermal conductivity and resistance of textile fabrics by mathematical equations, empirical equations, neural network, finite element method, and multiple regression models. Still, there is a need to investigate if some of these models can be valid to elastic *SJKF* and is it possible to derive a new model that can predict the thermal conductivity of elastic *SJKF*.

The thermal resistance and conductivity of the fabrics can be predicted by means of experimental (empirical), analytical and numerical methods [74]. The preference of selection depends on the requisite precision and nature of the solution. Thermal conductivity and resistance were also predicted by using an Artificial Neural Network (ANN) [75]–[78]. The thermal conductivity of knitted fabrics made from cotton, viscose and spandex fibres was investigated by using an Artificial Neural Network [76], where the fabric structure and weight, yarn count and composition, gauge, spandex percent and count, fabric thickness, and loop length were used as input parameters. There are research that predicted thermal resistance by regression model [79]–[81]. The thermal resistance of fabric and socks was predicted by modelling in the wet state [74], [82]–[84].

Some researchers have predicted the thermal resistance and conductivity of fabrics with mathematical approaches. Several research presented a mathematical models of thermal conductivity and resistance of woven fabric based on actual construction parameters of repeat by using finite element method [85] and theoretical unit cell geometry [86][87].

Schuhmeister summarized the relationship between the thermal conductivity of a fabric and fabric structural parameters and assumed that one-third of fibres are parallel and two-third are in series with a homogeneous distribution in all directions as shown in figure 7.1 by the empirical equation as following [88]:

$$\lambda_{fab} = 0.33\,(F_f\lambda_f + F_a\lambda_a)\quad + 0.67\,\frac{\lambda_f \times \lambda_a}{\lambda_f\,F_a + \lambda_a\,F_f} \qquad \ldots\ldots\ldots \qquad (7.1)$$

Where λ_{fab}, λ_f, λ_a are thermal conductivity coefficients of fabric, fibres, and air respectively, and F_f, F_a are the volume fractions of fibres and air respectively.
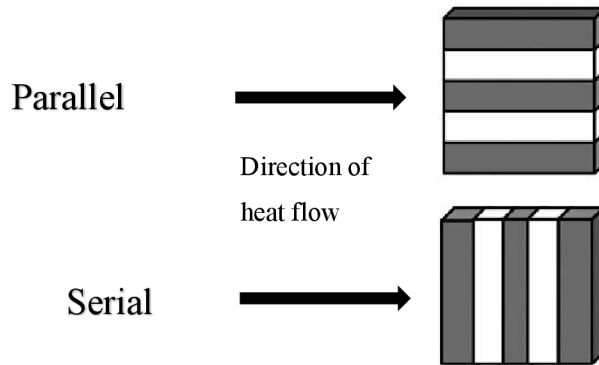
Figure 7.1. The direction of fibres compared to heat flow direction

Other researchers [89][90] have confirmed the equation and interpreted the first term as an ideal model for a fabric construction that fibres are parallel to the heat flow. The second term has been treated as an ideal model for a fabric construction where fibres lie in series to the heat flow. Bogaty [91] found that the percent of fibres in series and parallel is 21% and 79%, respectively, for wool fabric. Militky [33] considered that 50% fibres in series and 50% in parallel to the heat flow, as shown in the following equation:

$$\lambda_{fab} = 0.5 * \left[((F_f \lambda_f + F_a \lambda_a) + \frac{\lambda_f \times \lambda_a}{\lambda_f F_a + \lambda_a F_f} \right] \qquad \dots \dots \dots \qquad (7.2)$$

Maxwell introduced the two-phase concept (continuous and dispersed phase) for the determination of electrical conductivity. Later on, Eucken used the same concept for thermal conductivity evaluation [92]. Maxwell–Eucken (ME) model can be used to describe the thermal conductivity of a two-component material with simple physical structures. The phase that is present in form of droplets is the dispersed phase, and the phase in which droplets are suspended is called the continuous phase. Thermal conductivity models require the naming of a continues and dispersed phase. The materials with exterior porosity, individual solid particles are surrounded by a gaseous matrix, and hence the gaseous component (air) forms the continuous phase, and the solid component (fibres) forms the dispersed phase (ME2) [93][94]. The Maxwell–Eucken 2 (ME2) model equation is as follows:

$$\lambda_{fab} = \frac{\lambda_a F_a + \lambda_f \ F_f \frac{3\lambda_a}{2\lambda_a + \lambda_f}}{F_a + F_f \frac{3\lambda_a}{2\lambda_a + \lambda_f}} \qquad \ldots \ldots \ldots \qquad (7.3)$$

7.1 Applying three simple mathematical models (Maxwell–Eucken 2, Schuhmeister, Militky)

Schuhmeister, Militky, and Maxwell–Eucken 2 were applied on elastic *SJKF* to calculate predicted values of the thermal conductivity and then compared to experimental values and see if one of them is valid to the elastic *SJKF*. The predicted values from ME2 was very low compared to the experimental values as shown in figure 7.2. the predicted values from Schuhmeister model (one-third of fibres are parallel and two-third are in series) was lower than experimental values. When the percent of fibres in parallel increased to fifty percent, the predicted values from Militky model were higher than experimental values as shown in figure 7.2. Therefore, the predicted thermal conductivity increased when the parallel component increased. So, a new model is needed to be valid for the elastic *SJKF* and this the aim is of this chapter.
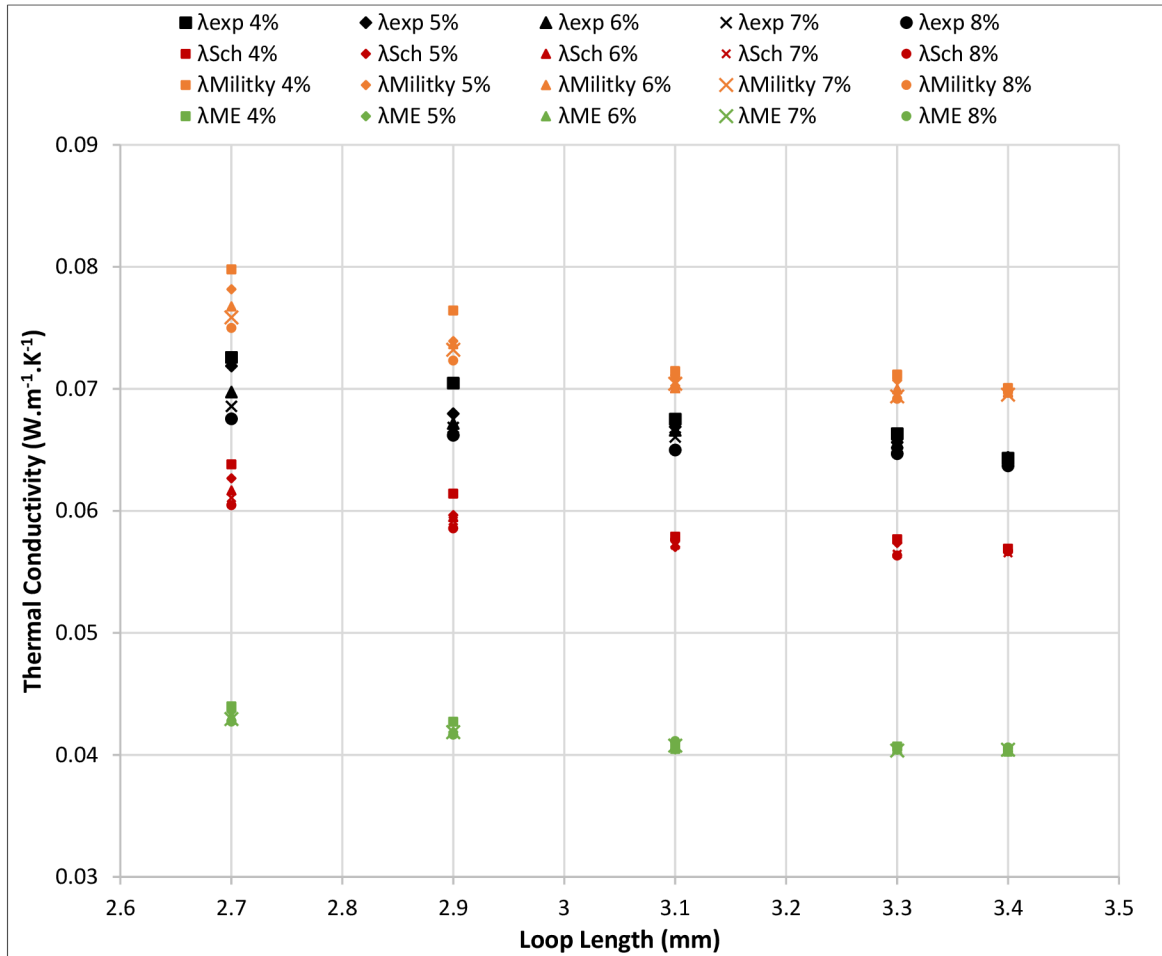
Figure 7.2. Experimental and predicted values from Schuhmeister, Militky, and ME 2 of thermal conductivity of elastic knitted fabric produced from yarn count 35 Ne

7.2 Assumptions and equations of a new model

7.2.1 *Assumptions*

A new model was derived based on the loop geometry and fabric construction parameters, namely wales and courses spacing, yarn diameter, fibres density, fabric thickness. It was assumed that:

- Yarn in one repeat was a cylinder with diameter d and its length equal to loop length (l).

- Fibres was divided to equal three components

- One third of fibres was in the same direction of heat flow (parallel to heat flow)

- Two third of fibres were in series with heat flow direction as shown.

7.2.2 *Equations*

7.2.2.1 *Thermal conductivity of fibres in one repeat*

$$Total\ volume\ of\ one\ repeat,\ mm^3 = w * c * h$$

Where w is wales spacing (mm) = (1/wales density), c is courses spacing (mm) = (1/courses density), h is fabric thickness (mm) as shown in figure 7.3.
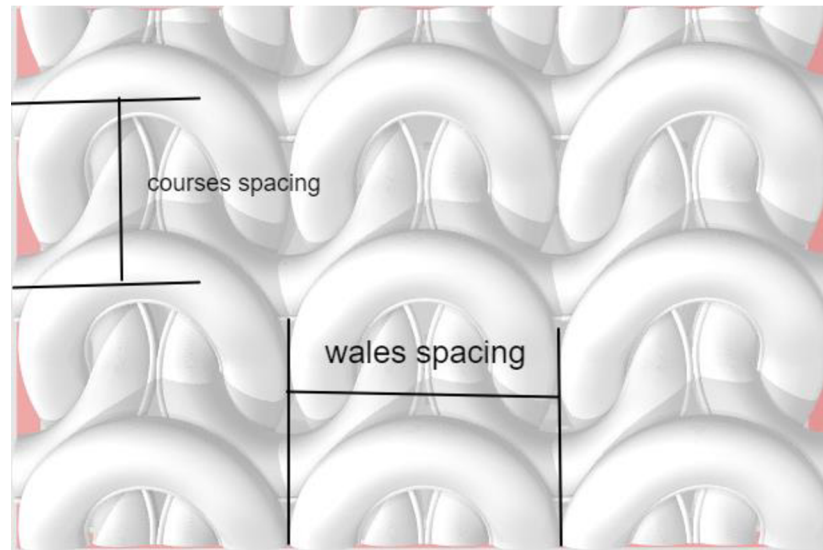
Figure 7.3. Theoretical image of elastic knitted fabric with the overlapping

$$Cotton\ yarn\ volume\ in\ one\ repeat\ (mm^3) = \frac{\pi}{4} * d^2 * l$$

$$Cotton\ fibres\ weight\ in\ one\ repeat\ (gm) = \frac{l}{1000 * Nm}$$

Where Nm is yarn metric count, l is the loop length (mm), and d is yarn diameter (mm).

$$Cotton\ fibres\ volume\ in\ one\ repeat\ (mm^3) = \frac{1000 * l}{Nm * \rho_c}$$

$$Cotton\ fibres\ volume\ fraction, F_c = \frac{1000 * l}{Nm * w * c * h * \rho_c}$$

$$Thermal\ conductivity\ of\ cotton\ fibres\ in\ one\ repeat, \lambda_{cotton} = F_c * \lambda_c$$

Where λ_c is the thermal conductivity coefficient of cotton fibres (0.5 W.m^{-1}.K[-1]) [42].

$$\lambda_{cotton} = \frac{1000*l}{Nm*w*c*h*\rho_c} * \lambda_c \qquad \dots \dots \dots \qquad (7.4)$$

$$Spandex\ weight\ in\ one\ repeat, gm = Cotton\ fibre\ weight\ in\ one\ repeat * \frac{SWP}{100}$$

$$Spandex\ weight\ in\ one\ repeat, gm = \frac{l*SWP}{10^5 * Nm}$$

$$Spandex\ volume\ in\ one\ repeat, mm^3 = \frac{Spandex\ weight\ in\ one\ repeat}{\rho_s}$$

$$Spandex\ volume\ in\ one\ repeat, mm^3 = \frac{10*l*SWP}{Nm*\rho_s}$$

$$Spandex\ volume\ fraction, F_s = \frac{10*l*SWP}{w*c*h*Nm*\rho_s}$$

$$Thermal\ conductivity\ of\ spandex\ in\ one\ repeat, \lambda_{spandex} = F_s * \lambda_s$$

Where λ_s is the thermal conductivity coefficient of spandex fibres (0.15 W.m^{-1}.K^{-1}) [42].

$$\lambda_{spandex} = \frac{10*l*SWP}{w*c*h*Nm*\rho_s} * \lambda_s \qquad \dots \dots \dots \qquad (7.5)$$

$$Total\ thermal\ conductivity\ of\ fibres, \lambda_f = \lambda_{cotton} + \lambda_{spandex} \ \dots \dots \ (7.6)$$

By substituting with the equation 7.4 and 7.5 on equation 7.6, λ_f can be calculated as follow:

$$\lambda_f = \frac{1000*l}{Nm*w*c*h*\rho_c} * \lambda_c + \frac{10*l*SWP}{w*c*h*Nm*\rho_s} * \lambda_s$$

$$\lambda_f = \left[\frac{l}{Nm*w*c*h}\right]\left[\frac{1000*\lambda_c}{\rho_c} + \frac{10*SWP*\lambda_s}{\rho_s}\right] \quad \dots \dots . \dots \qquad (7.7)$$

7.2.2.2 *Thermal conductivity of air in one repeat*

Inter air volume between yarns

$\quad = Total\ volume\ of\ one\ repeat$

$\quad - (Cotton\ yarn\ volume\ in\ one\ repeat$

$\quad + Spandex\ \ volume\ in\ one\ repeat)$

$$Inter\ air\ volume\ between\ yarns = w * c * h - \left(\frac{\pi}{4} * d^2 * l + \frac{10 * l * SWP}{Nm * \rho_s}\right)$$

Intra air volume inside cotton yarn

$\quad = Cotton\ yarn\ volume\ in\ one\ repeat$

$\quad - Cotton\ fibres\ \ volume\ in\ one\ repeat$

$$Intra\ air\ volume\ inside\ cotton\ yarn\ = \frac{\pi}{4} * d^2 * l - \frac{1000 * l}{Nm * \rho_c}$$

Total air volume inside one repeat

$\quad = Inter\ air\ volume\ between\ yarns$

$\quad + Intra\ air\ volume\ inside\ cotton\ yarn$

Total air volume inside one repeat

$$= \left(w * c * h - \left(\frac{1000 * l}{Nm * \rho_c} + \frac{10 * l * SWP}{Nm * \rho_s}\right)\right) + \left(\frac{\pi}{4} * d^2 * l - \frac{1000 * l}{Nm * \rho_c}\right)$$

Total air volume fraction, F_a

$$= \frac{\left(w * c * h - \left(\frac{\pi}{4} * d^2 * l + \frac{10 * l * SWP}{Nm * \rho_s}\right)\right) + \left(\frac{\pi}{4} * d^2 * l - \frac{1000 * l}{Nm * \rho_c}\right)}{w * c * h}$$

Thermal conductivity of air in one repeat, $\lambda_{air} = F_a * \lambda_a$

Where λ_a is the thermal conductivity coefficient of air (0.026 W.m^{-1}.K^{-1})

$$\lambda_a = \frac{\left(w*c*h - \left(\frac{\pi}{4}*d^2*l + \frac{10*l*SWP}{Nm*\rho_s}\right)\right) + \left(\frac{\pi}{4}*d^2*l - \frac{1000*l}{Nm*\rho_c}\right)}{w*c*h} * \lambda_a \qquad \ldots \ldots \ldots \quad (7.8)$$

7.2.2.3 *Thermal conductivity of fabric*

In this model, λ_f was divided to equal three components, one-third was in the same direction of heat flow (parallel to heat flow), and two third were in series with the heat flow direction, as shown in figure 7.4.
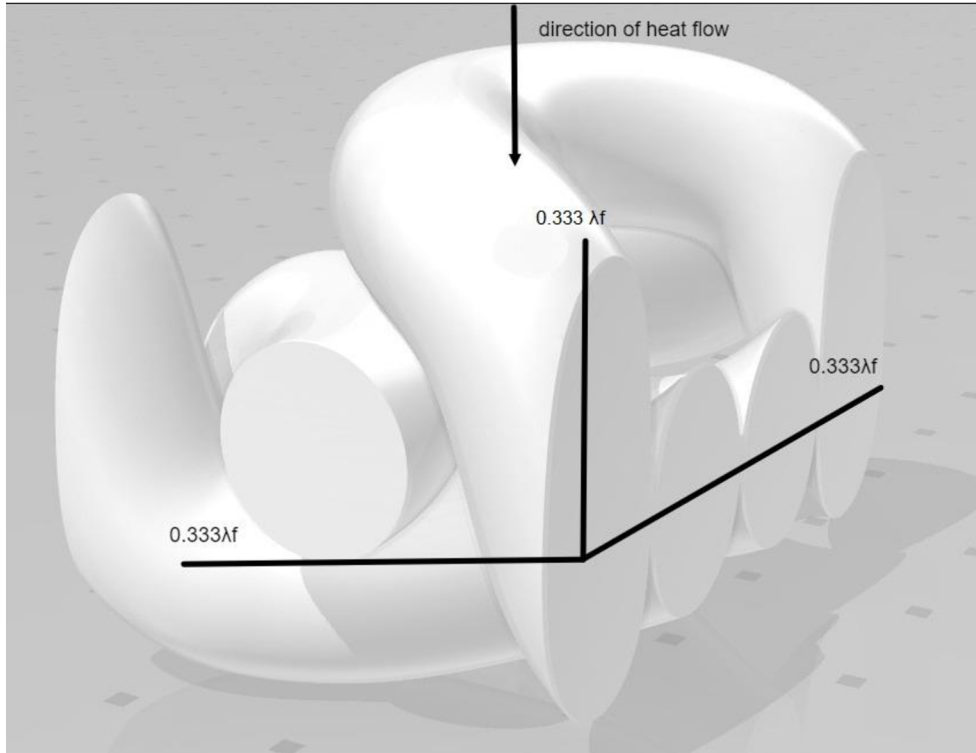
Figure 7.4. Fibres thermal conductivity components to heat flow direction

$$Thermal\ conductivity\ of\ fibres\ in\ series, \lambda_{ser} = \frac{0.333\lambda_f \times 0.333\lambda_f}{0.333\lambda_f + 0.333\lambda_f}$$

$$\lambda_{ser} = \frac{0.333\lambda_f}{2} \qquad \dots \dots \dots \quad (7.9)$$

$$Thermal\ conductivity\ of\ fibres\ in\ parallel, \lambda_p = 0.333\lambda_f \qquad \dots \dots \dots \quad (7.10)$$

$$Total\ thermal\ conductivity\ of\ fabric, \lambda_{fab} = \lambda_{ser} + \lambda_p + \lambda_a \quad \dots \dots \quad (7.11)$$

7.3 *Validation of the new model*

A new model, Schuhmeister, Militky, and ME 2 were applied on elastic *SJKF* to compare between predicted values from a new model, Schuhmeister, Militky, ME 2 and

experimental values and see if a new model can express the thermal conductivity of elastic *SJKF*.
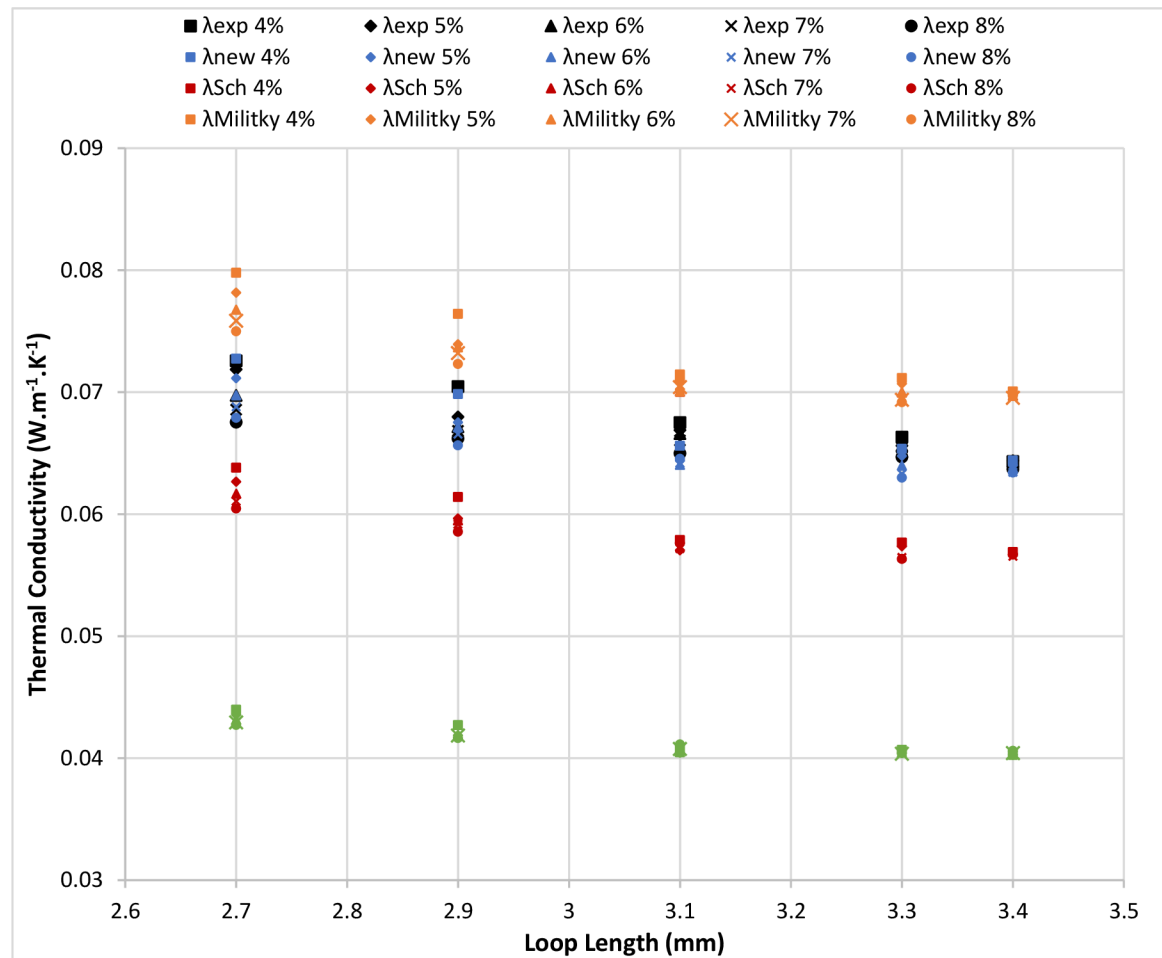
Figure 7.5. Experimental and predicted values of thermal conductivity of elastic knitted fabric produced from yarn count 35 Ne

Figure 7.5 shows the experimental and predicted values of thermal conductivity of elastic knitted fabric produced from yarn count 35 Ne. the predicted values from a new model were very closed to the experimental values of thermal conductivity at most points compared to the predicted values from Schuhmeister, Militky, and Maxwell–Eucken 2 models. For the elastic *SJKF* samples produced from yarn count 25 Ne, the predicted values of thermal conductivity from a new model were also closed to the experimental values, as shown in figure 7.6.
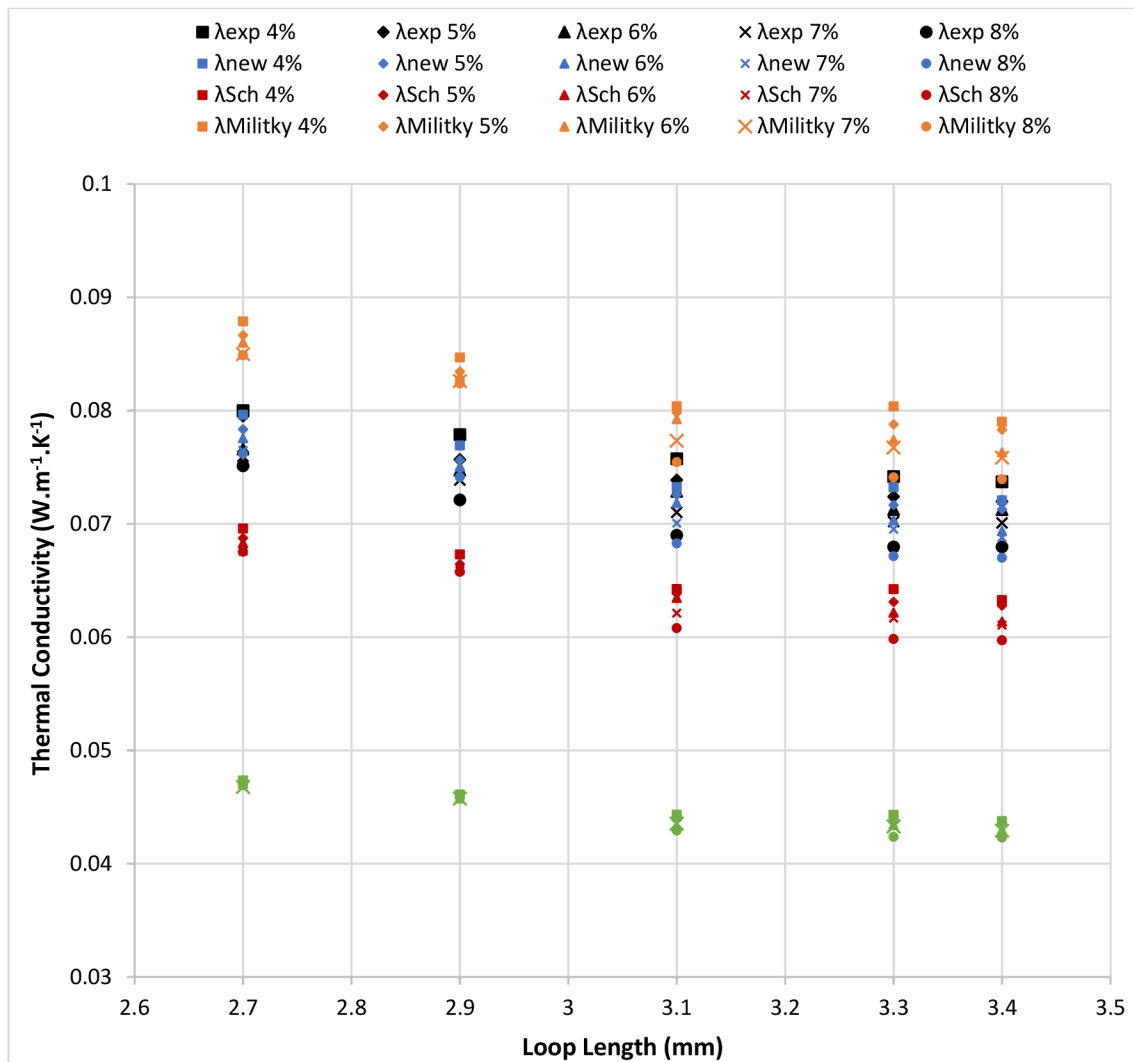
Figure 7.6. Experimental and predicted values of thermal conductivity of elastic knitted fabric produced from yarn count 25 Ne

For more clear presentation, the predicted values from the new model of elastic *SJKF* produced from yarn count 25 and 35 Ne vs experimental values were represented as shown in figure 7.7. Therefore, it can be said that the new model can be used to predict the thermal conductivity of the elastic *SJKF* compared to Schuhmeister, Militky, and ME 2 models.
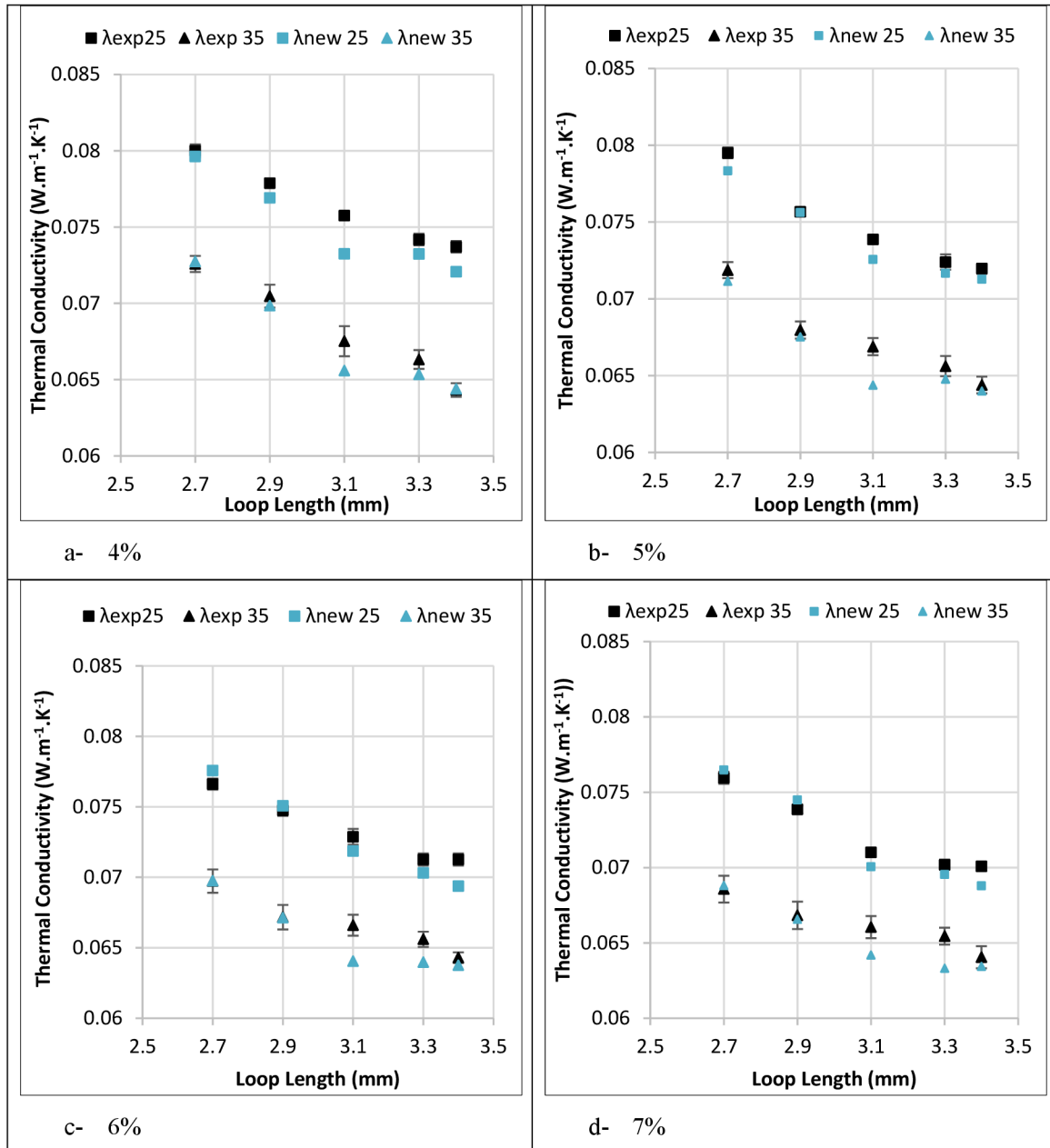
Figure 7.7. Predicted thermal conductivity values from the new model vs experimental values at different levels of *SWP* and yarn count.

Figure 7.8 shows the coefficient of determination (R^2) 0.95 between the predicted values from a new model and experimental values of the thermal conductivity of elastic *SJKF* samples produced from yarn count 25 and 35 Ne.
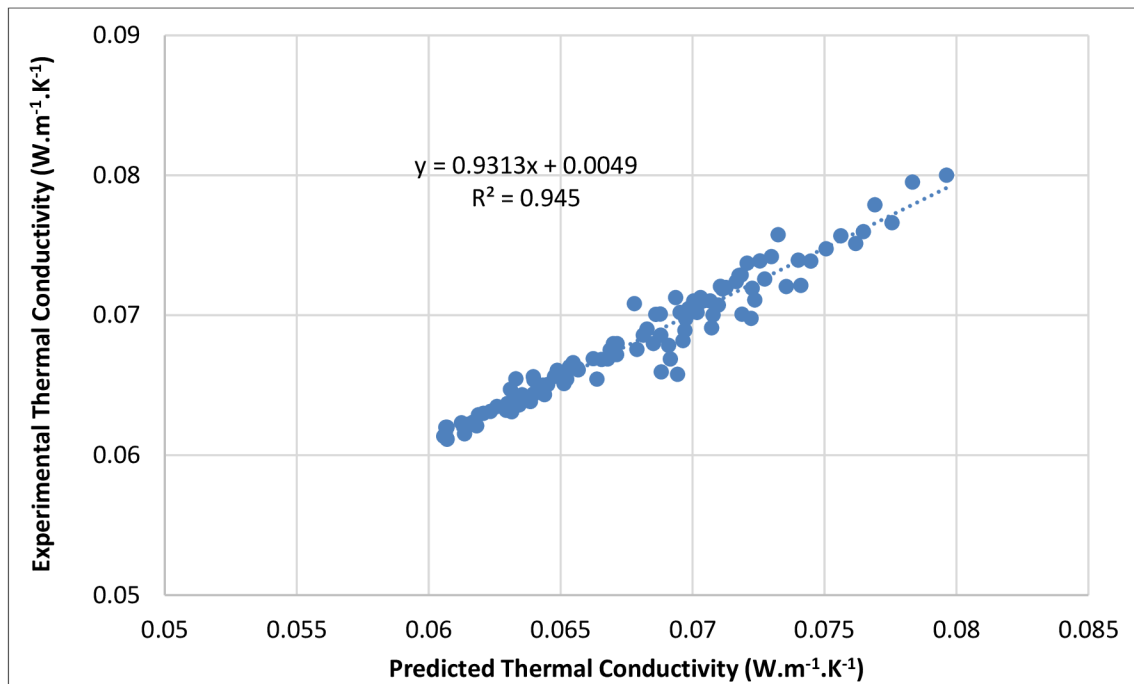
Figure 7.8. Experimental thermal conductivity vs predicted thermal conductivity from a new model

7.4 An attempt to determine structural parameters to obtain a desired thermal conductivity

At designing textiles, construction parameters are chosen in order to reach the appropriate physical properties for the specific end-use. Practically, these parameters are chosen based on previous experience in this field with the required adjustment within the competitive cost limitation. In this field, there are few mathematical models and equations that start with the desired property and end with the selection of the appropriate construction parameters, especially with the interference of the required properties.

In this part, an attempt to determine one property, which is thermal conductivity by selecting the appropriate structural parameters, namely yarn count, *SWP*, and the loop length as independent structural parameters is proposed, and vice versa. So that, the designers of elastic knitted fabric can choose the construction parameters for these fabrics based on knowing their thermal conductivity value.

To achieve this purpose, the equations 7.11, 7.10, 7.9, 7.8, and 7.7 were used to obtain the predicted value of thermal conductivity, which is the dependent variable, considering that the yarn count, *SWP*, and the loop length are independent variables, and the wales spacing, courses spacing, and the fabric thickness are considered as dependent

variables. The predicted values of thermal conductivity of elastic *SJKF* produced from yarn count 25 and 35 Ne versus loop length are illustrated in figure 7.9. The relation between thermal conductivity (y) and loop length (x) was presented by using polynomial equations as listed in table 7.1 at different levels of *SWP* and yarn count. This figure could be used to determine the structural parameters of elastic *SJKF* by knowing the desired value of the thermal conductivity.
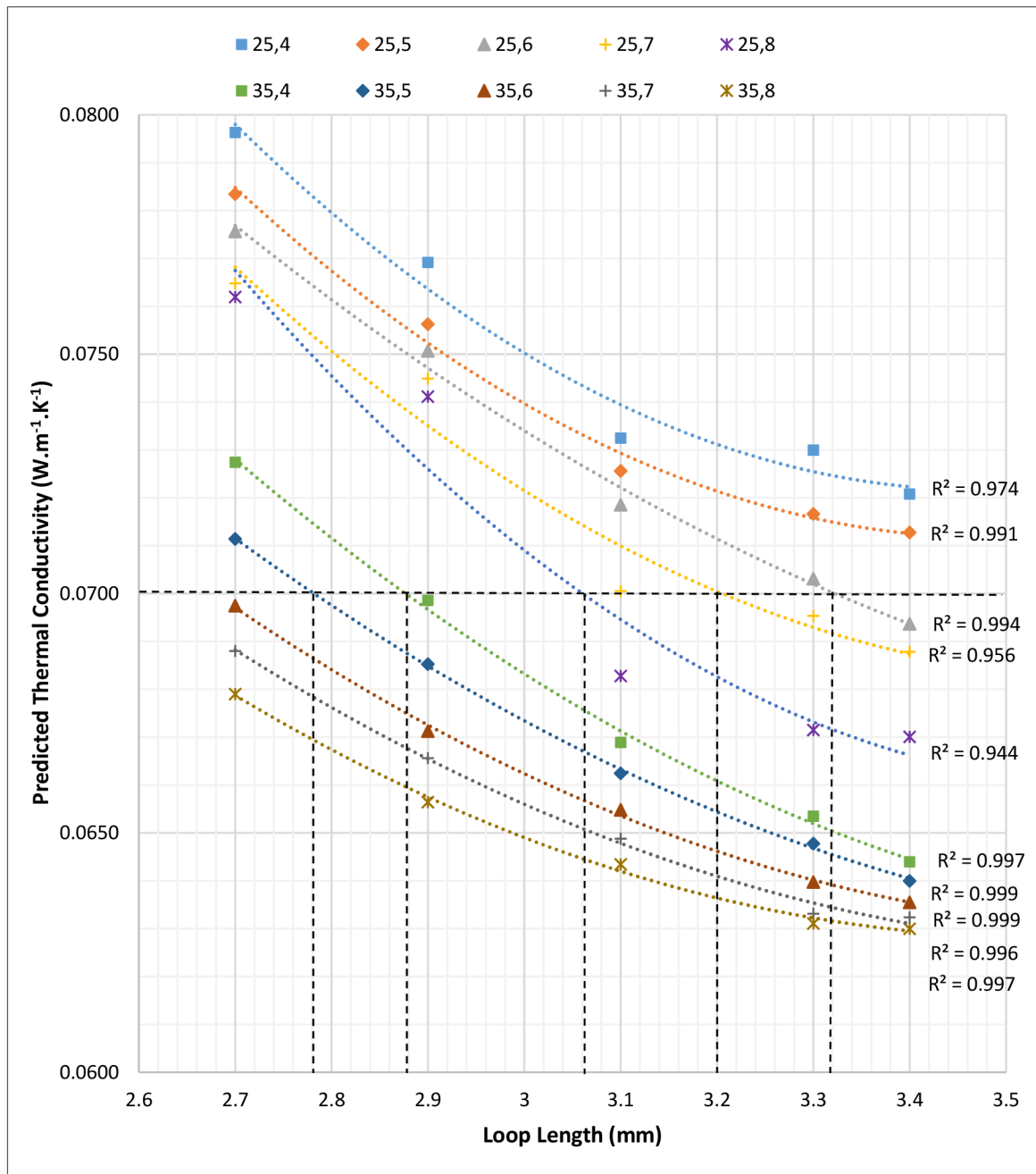
Figure 7.9. The predicted values of thermal conductivity of elastic *SJKF* versus loop length

Table 7.1. Curve fitting equations for the relation between thermal conductivity and loop length

Yarn count (Ne)	SWP (%)	Coefficient of determination (R^2)	Curve equation
25	4	0.974	$y = 0.013x^2 - 0.089x + 0.226$
	5	0.991	$y = 0.012x^2 - 0.082x + 0.215$
	6	0.994	$y = 0.006x^2 - 0.048x + 0.165$
	7	0.956	$y = 0.010x^2 - 0.073x + 0.200$
	8	0.944	$y = 0.013x^2 - 0.091x + 0.231$
35	4	0.997	$y = 0.008x^2 - 0.058x + 0.174$
	5	0.999	$y = 0.006x^2 - 0.049x + 0.157$
	6	0.999	$y = 0.007x^2 - 0.051x + 0.157$
	7	0.996	$y = 0.006x^2 - 0.047x + 0.150$
	8	0.997	$y = 0.007x^2 - 0.051x + 0.153$

For example, if the desired value of thermal conductivity of elastic *SJKF* is $0.07 \ W.m^{-1}.K^{-1}$, this value could be achieved in case of:

1. Yarn count 35 Ne, loop length 2.78 mm, and *SWP* 5%.
2. Yarn count 35 Ne, loop length 2.88 mm, and *SWP* 4%.
3. Yarn count 25 Ne, loop length 3.06 mm, and *SWP* 8%.
4. Yarn count 25 Ne, loop length 3.2 mm, and *SWP* 7%.
5. Yarn count 25 Ne, loop length 3.32 mm, and *SWP* 6%.

These results are related to the used material (cotton), yarn count range 25- 35 Ne, and *SWP* 4 - 8 %, however, this attempt can be generalized and achieved practically and industrially by expanding the range of the yarn count, *SWP* and the type of raw material.

8.   CHAPTER 8: EVALUATION OF RESULTS AND NEW FINDINGS

8.1 conclusion

First, the effect of construction parameters, namely yarn count, loop length, spandex weight percent, and plaiting technique on the geometrical and thermo-physiological comfort properties of full and half plaited *SJKF* was investigated. Elastic *fp* and *hp* samples were produced at five levels of loop length five level of *SWP*, and two levels yarn count (25 and 35 Ne). For comparison. 100% cotton samples were produced at the same levels of loop length and yarn count. The geometrical properties (thickness, weight, stitch density, fabric bulk density), thermal conductivity and absorptivity, water vapour resistance, air permeability were measured. By using flexi frame, the fabric growth and stretch of *fp* knitted samples were measured, and the thermal properties were measured under two levels of extension 15 and 30%.

The results showed that:

- **The *fp* thickness was higher than 100% cotton samples by up to 69% at 3.4 mm loop length and 8% *SWP*.**
- **The elastic *SJKF* thickness was ranged between 3.6 *d* to 4.4 *d* where *d* is the yarn diameter because of stitch overlapping**. The elastic fabric thickness decreased with increasing of *SWP* and increased with loop length increase for both *fp* and *hp*.
- **The thermal conductivity and *WVR* were higher than 100% cotton samples by 24 and 55%, respectively, at 2.7 mm loop length and 4% *SWP*.**
- **The thermal resistance and absorptivity were higher than 100% cotton samples by 60 and 42%, respectively, at 3.4 mm loop length and 4% *SWP*.**
- The thermal conductivity, thermal absorptivity, and water vapour resistance of both *fp* and *hp* decreased with increasing of *SWP*, **so the elastic *SJKF* could be used in summer and winter with comfort feeling.**
- **For all elastic *SJKF* samples, the *WVR* values were less than 5 and it is within excellent level of *WVR* transfer ability which gives comfort during wearing**.
- Yarn count had a significant effect on the geometrical and thermo-physiological properties. The thickness of elastic fabric decreased with increased yarn count from 25 to 35 Ne. The fabric weight went down with increasing of yarn count. **Thermal**

conductivity and absorptivity of elastic *SJKF* went down with yarn count increase.

- The thermal conductivity and absorptivity, and water vapour resistance values of elastic single jersey samples indicated to comfort, so adding spandex to *SJKF* had a good impact to geometrical and thermo-physiological properties.

- **Adding spandex enhanced the elastic recovery of *SJKF*. Fabric growth of elastic samples were less than 100% cotton samples and *FGW* was less than *FGC*.**

- Fabric stretch of elastic samples decreased when *SWP* increased and *FSW* of elastic samples was higher than 100% samples.

- **Thermal conductivity, resistance and absorptivity and fabric thickness of elastic fabrics decreased when the extension was up to 30%.**

- **Adding spandex from 4 to 8% to *SJKF* samples had a great effect on the geometrical and thermo-physiological properties** compared to 100% cotton samples.

- **Adding spandex leads to stitch overlapping therefore, the open structure converts to maximum set (normal structure) and overlapping (compact structure)**

Second, AutoCAD software was used to present **an innovated 3D modelling of stitch overlapping, maximum set, and open structures** to **investigate the pore size and distribution** for different *SJKF* structures. The fabric thickness was divided to several sections to calculate the pore size at each section. It was marked that the open structure had the highest pore volume at all sections, followed by maximum set, followed by overlapping structure.

Third, a new geometrical model to predict thermal conductivity of elastic *SJKF* was derived based on geometrical parameters of loop and the fibres direction to the direction of heat flow. Then the predicted values from a new model and three theoretical model and experimental values were compared. **The predicted values from the new model was very closed to experimental values. Therefore, the new model can be used to investigate the thermal conductivity of elastic *SJKF*** and vice versa**, where an attempt to determine structural parameters to obtain a desired thermal conductivity** was proposed.

8.2 Recommendations for continuing work

Based on this thesis, it was recommended that:

1. The effect of construction parameters on the thermo-physiological properties on the elastic knitted fabric with changing the raw material, fabric structure and increase the range of yarn count.
2. Tabulated information can be prepared to help the knitted fabric manufacturers to predict thermal conductivity from the construction parameters and vice versa
3. The thermal conductivity can be predicted by using the finite element method and 3 D geometrical model by using AutoCAD software.

9. CHAPTER 9: REFERENCES

[1]   R. Apurba Das, Alagirusamy, *Science in Clothing Comfort*, vol. 53, no. 9. India: WOODHEAD PUBLISHING INDIA PVT LTD, 2010.

[2]   B. P. Saville, *physical testing of textiles*. North and South America: Woodhead publishing Ltd and CRC press LLC, 2000.

[3]   M. O. R. Siddiqui and D. Sun, "Conjugate heat transfer analysis of knitted fabric," *J. Therm. Anal. Calorim.*, vol. 129, no. 1, pp. 209–219, 2017, doi: 10.1007/s10973-017-6166-y.

[4]   M. Matusiak, "Thermal comfort index as a method of assessing the thermal comfort of textile materials," *Fibres Text. East. Eur.*, vol. 79, no. 2, pp. 45–50, 2010.

[5]   A. R. R. Aboalasaad, Z. Skenderi, K. S. Brigita, and A. A. S. Khalil, "Analysis of Factors Affecting Thermal Comfort Properties of Woven Compression Bandages," *Autex Res. J.*, 20(2), pp.178-185.

[6]   A. M. Gözde Ertekin, Nida Oğlakcioğlu, "Strength and Comfort Characteristics of Cotton/Elastane Knitted Fabrics," *J. Text. Eng.*, pp. 140–145, 2018, doi: 10.7216/1300759920182511009.

[7]   R. Sadek, El-Hossini.A.M, A. . S. Eldeeb, and A. . Yassen, "Effect of Lycra Extension Percent on Single Jersey Knitted Fabric Properties," *J. Eng. Fiber. Fabr.*, vol. 7, no. 2, pp. 11–16, 2012.

[8]   M. Senthilkumar, N. Anbumani, and J. Hayavadana, "Elastane fabrics - A tool for stretch applications in sports," *Indian J. Fibre Text. Res.*, vol. 36, no. 3, pp. 300–307, 2011.

[9]   M. K. Bardhan and A. D. Sule, "Anatomy of sportswear and leisurewear: Scope of spandex fibres," *Man Made Text India*, vol. 3, no. 81, 2001.

[10]   K. Singha, "Analysis of Spandex/Cotton Elastomeric Properties: Spinning and Applications," *Int. J. Compos. Mater.*, vol. 2, no. 2, pp. 11–16, 2012, doi: 10.5923/j.cmaterials.20120202.03.

[11]   G. Bhat, S. Chand, and S. Yakopson, "Thermal properties of elastic fibers,"

Thermochim. Acta, vol. 367–368, pp. 161–164, 2001, doi: 10.1016/S0040-6031(00)00673-0.

[12]   S. B. Abdessalem, Y. B. Abdelkader, S. Mokhtar, and S. Elmarzougui, "Influence of Elastane Consumption on Plated Plain Knitted Fabric Characteristics," *J. Eng. Fiber. Fabr.*, vol. 4, no. 4, pp. 30–35, 2009.

[13]   A. Majumdar, S. Mukhopadhyay, and R. Yadav, "Thermal properties of knitted fabrics made from cotton and regenerated bamboo cellulosic fibres," *Int. J. Therm. Sci.*, vol. 49, no. 10, pp. 2042–2048, 2010, doi: 10.1016/j.ijthermalsci.2010.05.017.

[14]   S. Pant and R. Jain, "Comfort and Mechanical Properties of Cotton and Cotton Blended Knitted Khadi Fabrics," *Stud Home Com Sci*, vol. 8, pp. 69–74, 2014.

[15]   E. Onofrei, A. M. Rocha, and A. Catarino, "Thermal comfort properties of knitted fabrics made of elastane and bioactive yarns," *Fiber Soc. Spring 2010 Int. Conf.*, vol. 1, pp. 428–435, 2010.

[16]   Y. Jhanji, D. Gupta, and V. . . Kothari, "Effect of fibre , yarn and fabric variables on heat and moisture transport properties of plated knit," vol. 42, no. September, pp. 255–263, 2017.

[17]   A. Bivainytė, D. Mikučionienė, and P. Kerpauskas, "Investigation on Thermal Properties of Double-Layered Weft Knitted Fabrics," vol. 18, no. 2, 2012.

[18]   B. Marmarali, "Dimensional and Physical Properties of Cotton/S pandex Single Jersey Fabr," *Text. Res. J.*, vol. 73, pp. 11–14, 2003.

[19]   A. Yousuf, M. Anwarul, K. Sowrov, and M. Ahmed, "Effect of Elastane on Single Jersey Knit Fabric Properties - Physical & Dimensional Properties," *Int. J. Text. Sci.*, vol. 3, no. 1, pp. 12–16, 2014, doi: 10.5923/j.textile.20140301.03.

[20]   C. N. Herath, B. C. Kang, and H. Y. Jeon, "Dimensional stability of cotton-spandex interlock structures under relaxation," *Fibers Polym.*, vol. 8, no. 1, pp. 105–110, 2007, doi: 10.1007/BF02908167.

[21]   S. Tezel and Y. Kavusturan, "Experimental Investigation of Effects of Spandex Brand and Tightness Factor on Dimensional and Physical Properties of Cotton/Spandex Single Jersey Fabrics," *Text. Res. J.*, vol. 78, no. 11, pp. 966–976, 2008, doi: 10.1177/0040517507087685.

[22]   M. Senthilkumar, N. Anbumani, and M. De Araujo, "Elastic Properties of Spandex Plated Cotton Knitted Fabric," *J. Inst. Eng.*, no. August, 2011.

[23]   Z. Değirmenci and E. Çoruh, "Comparison of the performance and physical properties of plain, pique, double-pique and fleeced knitted fabrics," *Tekst. ve Konfeksiyon*, vol. 26, no. 2, pp. 159–165, 2016.

[24]   E. Eltahan, "Effect of Lycra Percentages and Loop Length on the Physical and Mechanical Properties of Single Jersey Knitted Fabrics," *J. Compos.*, vol. 2016, pp. 1–7, 2016, doi: 10.1155/2016/3846936.

[25]   N. Kizildag, N. Ucar, and B. Gorgun, "Analysis of some comfort and structural properties of cotton/spandex plain and 1×1 rib knitted fabrics," *J. Text. Inst.*, vol. 107, no. 5, pp. 606–613, 2016, doi: 10.1080/00405000.2015.1054143.

[26]   F. Fayala, H. Alibi, A. Jemni, and X. Zeng, "A New Hybrid Artificial Intelligence Approach to Predicting Global Thermal Comfort of Stretch Knitted Fabrics," vol. 16, no. 6, pp. 1417–1429, 2015, doi: 10.1007/s12221-015-1417-7.

[27]   H. A. El-dessouki, "The Thermal Comfort Properties of Certain Egyptian Stretched Knitted Fabrics," *Int. Des. J.*, vol. 5, no. 1, pp. 69–72, 2014.

[28]   G. Ertekin, N. Oğlakcioğlu, and A. Marmarali, "Strength and Comfort Characteristics of Cotton/Elastane Knitted Fabrics," *J. Text. Eng.*, vol. 25, no. 110, 2018, doi: 10.7216/1300759920182511010.

[29]   ASTM D2594 − 04, *Standard Test Method for Stretch Properties of Knitted Fabrics Having Low Power*. 2016.

[30]   B. Striz, "Internal Standard No.22-201-01/01 (in Czech)," *Tech. Univ. Lib. Fac. Text.*, pp. 1–17, 2004.

[31]   B. Striz, I. Mertova, and B. Sirkova, "Application of Equation of Deflection Curve to Determination of Yarn Bending Rigidity," *4 th Cent. Eur. Conf. 7-9 Sept. Lib. Czech Repub.*, 2005.

[32]   A. A. Salama, A. S. El-Deeb, and I. M. El-shahat, "Evaluation of Bed Cover Properties Produced from Double Fabric Based on Honeycomb," *J. Text.*, vol. 2015, pp. 1–7, 2015, doi: 10.1155/2015/470456.

[33]   J. Militký and D. Křemenáková, *THERMAL CONDUCTIVITY PREDICTION OF*

TEXTILE MATRIALS, Selected topics of textile and material Science. Czech Republic: Publishing House of WBU, Pilsen (responsible J. Vojtěchová), 2011.

[34] L. Hes and I. Dolezal, "New Method Thermal and Equipment for Measuring Properties of Textiles," *J. Text. Mach. Soc. Japan*, vol. 42, pp. 71–75, 1989.

[35] I. standarad I. 8301, *Thermal insulation- determination of steady-state thermal resistance and related properties—heat flow meter apparatus*. 1991.

[36] L. Hes and I. Dolezal, "A new computer-controlled skin model for fast determination of water vapour and thermal resistance of fabrics," 2003.

[37] L. Hes, "Non-destructive determination of comfort parameters during marketing of functional garments and clothing," *Indian J. Fibre Text. Res.*, vol. 33, no. 3, pp. 239–245, 2008.

[38] International Standard ISO 11092, *Textiles - Physiological effects - Measurement of thermal and water-vapour resistance under steady-state conditions (sweating guarded-hotplate test)*. 1993.

[39] I. stansard ISO9237, *Textiles — Determination of the permeability of fabrics to air*. 1995.

[40] D. Gupta, R. Chattopadhyay, and M. K. Bera, "Comfort properties of pressure garments in extended state," *Indian J. Fibre Text. Res.*, vol. 36, pp. 415–421, 2011.

[41] H. F. Siddique, A. A. Mazari, A. Havelka, and R. Laurinová, "ANALYSIS OF THERMAL PROPERTIES AFFECTED BY DIFFERENT EXTENSION LEVELS OF COMPRESSION SOCKS," *Fibers Text.*, pp. 64–69, 2019.

[42] K. Herlinger, *Ullmann's Fibers Volume 1*, vol. 1. Fritz Schultze-Gebhardt,D¨usseldorf, Federal Republic of Germany, 2008.

[43] C. Prakash and G. Ramakrishnan, "Effect of blend ratio, loop length, and yarn linear density on thermal comfort properties of single jersey knitted fabrics," *Int. J. Thermophys.*, vol. 34, no. 1, pp. 113–121, 2013, doi: 10.1007/s10765-012-1386-7.

[44] I. S. Čubrić and Z. Skenderi, "Geometry of Weft Knitted Structures - Influence on Heat Resistance," no. 66, pp. 1–4, 2014.

[45] A. Afzal, S. Ahmad, A. Rasheed, F. Ahmad, F. Iftikhar, and Y. Nawab, "Influence

of fabric parameters on thermal comfort performance of double layer knitted interlock fabrics," *Autex Res. J.*, vol. 17, no. 1, pp. 20–26, 2017, doi: 10.1515/aut-2015-0037.

[46]   L. Hes, M. de Araujo, and V. V. Djulay, "Effect of Mutual Bonding of Textile Layers on Thermal Insulation and Thermal Contact Properties of Fabric Assemblies," *Text. Res. J.*, vol. 66, no. 4, pp. 245–250, 1996, doi: 10.1177/004051759606600410.

[47]   R. S. Rengasamy, B. R. Das, and Y. B. Patil, "Thermo-physiological comfort characteristics of polyester air-jet-textured and cotton-yarn fabrics," *J. Text. Inst.*, vol. 100, no. 6, pp. 507–511, 2009, doi: 10.1080/00405000801977183.

[48]   A. E. Mangat, L. Hes, V. Bajzik, and A. Mazari, "Thermal Absorptivity Model of Knitted Rib Fabric and its Experimental Verification," *Autex Res. J.*, vol. 18, no. 1, pp. 20–27, 2018, doi: 10.1515/aut-2017-0003.

[49]   L. Hes, K. Bal, and I. Dolezal, "Principles of Clothing Comfort and Their Use in Evaluation of Sensorial and Thermal Comfort of Men's Casual Jacket," *Fibers Polym.*, vol. 0, no. 0, pp. 1–7, 2021, doi: 10.1007/s12221-021-0425-z.

[50]   G. Song, *Improving Comfort in Clothing*. The Textile Institute and Woodhead Publishing, 2011.

[51]   R. Shishoo, *Textiles in sports*. England: Woodhead Publishing Limited and CRC Press LLC, 2005.

[52]   R. Kumar and S. Sood, "A study on porosity related aspects of cotton knitted fabric with single jersey structure for improved comfort application for garment," *J. Text. Eng. Fash. Technol.*, vol. 6, no. 5, pp. 199–204, 2020, doi: 10.15406/jteft.2020.06.00251.

[53]   S. Mezarciöz and R. T. Oğulata, "Modelling of Porosity in Knitted Fabrics," *J. Fash. Technol. &Textile Eng.*, no. 1, pp. 1–3, 2015.

[54]   M. O. R. Siddiqui and D. Sun, "Porosity prediction of plain weft knitted fabrics," *Fibers*, vol. 3, no. 1, pp. 1–11, 2015, doi: 10.3390/fib3010001.

[55]   P. B. Robert Guidoin, Martin King, Daniel Marceau, Alain Cardou, Dominique De La Faye, Jean-Michel Legendre, "Textile arterial prostheses: Is water permeability

equivalent to porosity?," *J. Biomed. Mater. Res.*, vol. 21, no. 1, pp. 65–87, 1987, doi: https://doi.org/10.1002/jbm.820210111.

[56] S. Benltoufa, F. Fayala, M. Cheikhrouhou, and B. Nasrallah, "Porosity determination of jersey structure," *Autex Res. J.*, vol. 7, no. 1, pp. 63–69, 2007.

[57] R. B. Turan, A. Okur, R. Deveci, and M. Açikel, "Predicting the intra-yarn porosity by image analysis method," *Text. Res. J.*, vol. 82, no. 16, pp. 1720–1728, 2012, doi: 10.1177/0040517511427971.

[58] M. K. Imrith, R. Unmar, and S. Rosunee, "Determination of Knitted Fabric Porosity Using Digital Imaging Techniques," *Adv. Mater. Sci. Eng.*, vol. 2016, no. 1, 2016, doi: 10.1155/2016/6470351.

[59] M. Havlová and J. Špánková, "Porosity of knitted fabrics in the aspect of air permeability-discussion of selected assumptions," *Fibres Text. East. Eur.*, vol. 25, no. 3, pp. 86–91, 2017, doi: 10.5604/12303666.1237242.

[60] R. T. Ogulata and S. Mavruz, "Investigation of porosity and air permeability values of plain knitted fabrics," *Fibres Text. East. Eur.*, vol. 18, no. 5, pp. 71–75, 2010.

[61] E. A. Elnashar, "Volume porosity and air permeability in knitting fabrics," *Int. J. Res. Adv. Eng. Technol.*, vol. 3, no. 1, pp. 75–80, 2017.

[62] A. Fouda, A. El-Hadidy, and A. El-Deeb, "Mathematical Modeling to Predict the Geometrical and Physical Properties of Bleached Cotton Plain Single Jersey Knitted Fabrics," *J. Text.*, pp. 1–10, 2015, doi: 10.1155/2015/847490.

[63] A. Fouda and M. Eldeeb, "Mathematical Modeling to Predict the Geometrical Properties of Float Stitches in Single Jersey Knitted Fabrics," *MANSOURA Eng. J.*, vol. 45, no. 2, 2020.

[64] S. Abdolmaleki, A. A. A. Jeddi, and M. Amani, "Estimation on the 3D porosity of plain knitted fabric under uniaxial extension," *Fibers Polym.*, vol. 13, no. 4, pp. 535–541, 2012, doi: 10.1007/s12221-012-0535-8.

[65] B. Karaguzel, "CHARACTERIZATION AND ROLE OF POROSITY IN KNITTED FABEIC," 2004.

[66] A. K. Puszkarz and I. Krucińska, "Modeling of Air Permeability of Knitted Fabric Using the Computational Fluid Dynamics," *Autex Res. J.*, vol. 18, no. 4, pp. 364–

376, 2018, doi: 10.1515/aut-2018-0007.

[67] A. Khalil, A. Fouda, P. Těšinová, and A. S. Eldeeb, "Comprehensive assessment of the properties of cotton single Jersey knitted fabrics produced from different Lycra States," *Autex Res. J.*, vol. 21, no. 1, pp. 71–78, 2021.

[68] A. Khalil, P. Těšinová, and A. R. R. Aboalasaad, "Thermal comfort properties of cotton/spandex single jersey knitted fabric," *Ind. Textila*, vol. 72, no. 3, pp. 244–249, 2021, doi: 10.35530/IT.072.03.1760.

[69] A. Khalil, P. Těšinová, and A. R. R. Aboalasaad, "Effect of Lycra Weight Percent and Loop Length on Thermo-physiological Properties of Elastic Single Jersey Knitted Fabric," *Autex Res. J.*, Jul. 2021, doi: 10.2478/aut-2021-0030.

[70] F. T. Peirce, "Geometrical Principles Applicable to the Design of Functional Fabrics," *Text. Res. J.*, no. 3, pp. 123–147, 1947.

[71] K. F. Choi and T. Y. LO, "An Energy Model of Plain Knitted Fabric," *Text. Res. J.*, vol. 73, no. 8, pp. 739–748, 2003.

[72] H. Abou-Taleb and H. El-Fowaty, "Theoretical Development of Mathematical Model to Predict Vertical Wicking Behavior of Flow through Terry Towels.," *MEJ. Mansoura Eng. J.*, vol. 41, no. 4, pp. 1–15, 2016.

[73] A. Demiroz and T. Dias, "A Study of the Graphical Representation of Plain-knitted Structures Part I : Stitch Model for the Graphical Representation of Plain-knitted Structures A Study ofthe Graphical Representation of Plain-knitted Structures Part I : Stitch Model for the Graphic," *J. Text. Inst.*, vol. 91, no. 4, pp. 463–480, 2000, doi: 10.1080/00405000008659121.

[74] T. Mansoor *et al.*, "Conductive Heat Transfer Prediction of Plain Socks in Wet State," *Autex Res. J.*, pp. 1–13, 2021, doi: 10.2478/aut-2021-0032.

[75] A. E. Mangat, V. Bajzik, L. Hes, and F. B. Mazari, "The use of artificial neural networks to estimate thermal resistance of knitted fabrics," *Tekst. ve Konfeksiyon*, vol. 25, no. 4, pp. 304–312, 2015.

[76] H. Alibi, F. Fayala, A. Jemni, and X. Zeng, "Modeling of thermal conductivity of stretch knitted fabrics using an optimal neural networks system," *Journal of Applied Sciences*, vol. 12, no. 22. pp. 2283–2294, 2012, doi:

10.3923/jas.2012.2283.2294.

[77]   F. Fayala, H. Alibi, S. Benltoufa, and A. Jemni, "Neural Network for Predicting Thermal Conductivity of Knit Materials," *J. Eng. Fiber. Fabr.*, vol. 3, no. 4, p. 155892500800300, 2008, doi: 10.1177/155892500800300407.

[78]   A. Majumdar, "Modelling of thermal conductivity of knitted fabrics made of cotton-bamboo yarns using artificial neural network," *J. Text. Inst.*, vol. 102, no. 9, pp. 752–762, 2011, doi: 10.1080/00405000.2010.516929.

[79]   K. Shaker *et al.*, "Effect of fabric structural design on the thermal properties of woven fabrics," *Therm. Sci.*, 2018, doi: 10.2298/TSCI170707003S.

[80]   X. Qian and J. Fan, "Prediction of clothing thermal insulation and moisture vapour resistance of the clothed body walking in wind," *Ann. Occup. Hyg.*, vol. 50, no. 8, pp. 833–842, 2006, doi: 10.1093/annhyg/mel050.

[81]   A. Afzal, T. Hussain, M. Mohsin, A. Rasheed, and S. Ahmad, "Statistical models for predicting the thermal resistance of polyester/cotton blended interlock knitted fabrics," *Int. J. Therm. Sci.*, vol. 85, pp. 40–46, 2014, doi: 10.1016/j.ijthermalsci.2014.06.016.

[82]   M. M. Mangat and L. Hes, "Thermal resistance of denim fabric under dynamic moist conditions and its investigational confirmation," *Fibres Text. East. Eur.*, vol. 22, no. 6, pp. 101–105, 2014.

[83]   R. S. Hollies and H. Bogaty, "Some thermal properties of fabrics: part II: The influence of water content," *Text. Res. J.*, vol. 35, no. 2, pp. 187–190, 1964.

[84]   F. L. Zhu, "Investigating the effective thermal conductivity of moist fibrous fabric based on Parallel-Series model: A consideration of material's swelling effect," *Mater. Res. Express*, vol. 7, no. 4, 2020, doi: 10.1088/2053-1591/ab8541.

[85]   J. J. Wu, H. Tang, and Y. X. Wu, "A predictive model of thermal conductivity of plain woven fabrics," *Therm. Sci.*, vol. 21, no. 4, pp. 1627–1632, 2017, doi: 10.2298/TSCI160805045W.

[86]   M. I. Ismail, A. S. A. Ammar, and M. El-Okeily, "Heat transfer through textile fabrics: mathematical model," *Math. Comput. Model.*, vol. 12, no. 9, p. 1187, 1988, doi: 10.1016/0895-7177(89)90268-9.

[87]   D. Bhattacharjee and V. K. Kothari, "Heat transfer through woven textiles," *Int. J. Heat Mass Transf.*, vol. 52, no. 7–8, pp. 2155–2160, 2009, doi: 10.1016/j.ijheatmasstransfer.2008.09.035.

[88]   J. Schuhmeister, "Ber. K. Akad. Wien (Math-Naturw. Klasse)," *Ber. K. Akad. Wien (Math-Naturw. Klasse)*, vol. 76, p. 283, 1877.

[89]   N. Mao and S. J. Russell, "The Thermal Insulation Properties of Spacer Fabrics with a Mechanically Integrated Wool Fiber Surface," *Text. Res. J.*, vol. 77, no. 12, pp. 914–922, 2007, doi: 10.1177/0040517507083524.

[90]   S. T. Baxter, "The thermal conductivity of textiles," *Proc. Phys. Soc.*, vol. 85, no. 1, 1946.

[91]   H. Bogaty, N. R. S. Hollies, and M. Harris, "Some Thermal Properties of Fabrics: Part I: The Effect of Fiber Arrangement," *Text. Res. J.*, vol. 27, no. 6, pp. 445–449, 1957, doi: 10.1177/004051755702700605.

[92]   A. Eucken, "General laws for the thermal conductivity of various types of material and states of matter," *Res. F. Eng.*, vol. 11, no. 1, pp. 1488–1497, 1940.

[93]   P. Kumar and F. Topin, "Simultaneous determination of intrinsic solid phase conductivity and effective thermal conductivity of Kelvin like foams," *Appl. Therm. Eng.*, vol. 71, no. 1, pp. 536–547, 2014, doi: 10.1016/j.applthermaleng.2014.06.058.

[94]   J. K. Carson, "Use of simple thermal conductivity models to assess the reliability of measured thermal conductivity data," *Int. J. Refrig.*, vol. 74, pp. 456–462, 2017, doi: 10.1016/j.ijrefrig.2016.10.024.

10. CHAPTER 10: APPENDICES

10.1 Appendix (I) for results and discussion

Table 10.1. Stitch density (cm^{-2}) of *SJKF*

Yarn count			100% cotton	Full plaited					Half plaited				
		SWP (%)	0	4	5	6	7	8	4	5	6	7	8
35 Ne	Loop length (mm)	2.7	272	486	448	411	391	371	414	395	383	367	358
		2.9	230	437	403	379	366	356	371	362	340	323	315
		3.1	190	371	353	334	328	315	343	332	312	310	302
		3.3	177	353	340	321	309	293	319	310	301	287	281
		3.4	169	323	327	312	301	297	312	293	282	281	272
25 Ne	Loop length (mm)	2.7	287	399	373	340	331	309	345	338	321	315	301
		2.9	250	362	339	323	315	285	319	316	294	284	273
		3.1	220	315	302	289	273	266	295	285	291	269	261
		3.3	201	298	283	268	262	245	282	276	267	254	243
		3.4	189	284	272	255	251	238	264	257	253	239	229

Table 10.2. Fabric weight (g.m^{-2}) of *SJKF*

Yarn count	Loop length (mm)	SWP (%)	100% cotton	Full plaited					Half plaited				
			0	4	5	6	7	8	4	5	6	7	8
35 Ne	Loop length (mm)	2.7	118	231	207	199	194	189	199	195	194	193	191
		2.9	103	222	199	191	186	183	188	183	181	180	178
		3.1	97	207	197	191	184	183	180	178	174	172	168
		3.3	92	197	188	184	181	177	171	169	166	164	160
		3.4	90	179	174	164	162	157	168	167	161	157	158
25 Ne	Loop length (mm)	2.7	181	255	254	248	242	238	263	262	262	258	253
		2.9	170	249	249	241	240	231	261	258	252	249	244
		3.1	157	239	231	222	220	214	238	236	234	228	226
		3.3	146	227	222	218	217	215	227	226	223	220	216
		3.4	145	223	216	210	210	207	221	213	212	211	211

Table 10.3. Fabric thickness (mm) of *SJKF*

Yarn count	Loop length (mm)	SWP (%)	100% cotton	Full plaited					Half plaited				
			0	4	5	6	7	8	4	5	6	7	8
35 Ne	Loop length (mm)	2.7	0.4742	0.6986	0.6671	0.6326	0.6144	0.5957	0.6832	0.6697	0.6589	0.6402	0.6333
		2.9	0.453	0.719	0.7013	0.6657	0.652	0.6091	0.7053	0.6903	0.6603	0.6492	0.6383
		3.1	0.4494	0.7235	0.71	0.6776	0.6639	0.6301	0.7083	0.6928	0.6796	0.6745	0.6586
		3.3	0.4396	0.7368	0.7212	0.6958	0.6807	0.6513	0.7171	0.7011	0.6909	0.6804	0.6673
		3.4	0.4362	0.7389	0.728	0.6989	0.6989	0.6805	0.7324	0.7043	0.6887	0.6847	0.6644
25 Ne	Loop length (mm)	2.7	0.5631	0.7013	0.6711	0.621	0.6166	0.58	0.6763	0.6697	0.6589	0.6402	0.6333
		2.9	0.5511	0.7196	0.6912	0.6647	0.657	0.5991	0.7053	0.6915	0.6603	0.6402	0.6326
		3.1	0.5454	0.7216	0.7009	0.6807	0.67	0.6802	0.7083	0.6928	0.6796	0.6745	0.6586
		3.3	0.5394	0.7263	0.7126	0.6967	0.6928	0.6852	0.7262	0.7185	0.7052	0.6772	0.6608
		3.4	0.5324	0.7297	0.7132	0.6972	0.6948	0.6882	0.7474	0.7154	0.7109	0.7027	0.6923

Table 10.4. Fabric porosity (%) of *SJKF*

Yarn count		SWP (%)	100% cotton	Full plaited					Half plaited				
			0	4	5	6	7	8	4	5	6	7	8
35 Ne	Loop length (mm)	2.7	83.7	78.0	79.3	79.0	78.8	78.8	80.6	80.6	80.4	79.8	79.7
		2.9	85.7	79.5	81.1	80.9	80.9	79.8	82.3	82.3	81.7	81.4	81.3
		3.1	85.8	81.0	81.5	81.2	81.5	80.6	83.1	82.9	82.9	83.0	82.9
		3.3	86.3	82.2	82.6	82.3	82.2	81.7	84.2	83.9	84.0	83.9	83.9
		3.4	86.2	83.9	84.1	84.3	84.5	84.5	84.8	84.2	84.4	84.6	84.1
25 Ne	Loop length (mm)	2.7	78.9	75.9	74.8	73.3	73.7	72.5	74.1	73.9	73.5	73.0	73.2
		2.9	79.8	77.0	76.1	75.8	75.6	74.1	75.4	75.2	74.6	74.0	74.2
		3.1	81.1	78.0	78.1	78.2	78.0	79.0	77.6	77.3	77.1	77.3	77.0
		3.3	82.2	79.3	79.2	79.1	79.0	79.0	79.3	79.1	78.9	78.3	78.1
		3.4	82.1	79.7	79.8	79.9	79.8	79.8	80.3	80.2	80.1	79.9	79.6

Table 10.5. Thermal conductivity (W.m^{-1}. K^{-1}) of *SJKF*

Yarn count		SWP (%)	100% cotton	Full plaited					Half plaited				
			0	4	5	6	7	8	4	5	6	7	8
35 Ne	Loop length (mm)	2.7	0.0584	0.0726	0.0719	0.0697	0.0686	0.0676	0.0669	0.0661	0.0651	0.0650	0.0644
		2.9	0.0566	0.0705	0.0680	0.0672	0.0668	0.0662	0.0654	0.0638	0.0631	0.0629	0.0623
		3.1	0.0551	0.0675	0.0669	0.0666	0.0661	0.0650	0.0636	0.0632	0.0622	0.0620	0.0615
		3.3	0.0550	0.0663	0.0656	0.0656	0.0655	0.0647	0.0635	0.0631	0.0621	0.0620	0.0613
		3.4	0.0539	0.0643	0.0644	0.0643	0.0641	0.0637	0.0630	0.0623	0.0620	0.0612	0.0611
25 Ne	Loop length (mm)	2.7	0.0651	0.0800	0.0795	0.0766	0.0760	0.0751	0.0739	0.0720	0.0711	0.0701	0.0691
		2.9	0.0648	0.0779	0.0757	0.0747	0.0739	0.0721	0.0728	0.0719	0.0707	0.0700	0.0689
		3.1	0.0637	0.0758	0.0739	0.0729	0.0710	0.0690	0.0721	0.0710	0.0698	0.0678	0.0659
		3.3	0.0629	0.0742	0.0724	0.0713	0.0702	0.0680	0.0710	0.0702	0.0682	0.0669	0.0658
		3.4	0.0619	0.0737	0.0720	0.0713	0.0701	0.0680	0.0708	0.0701	0.0686	0.0654	0.0654

Table 10.6. Thermal resistance (m^2.K.W^{-1}) of *SJKF*

Yarn count	Loop length (mm)	SWP (%)	100% cotton	Full plaited					Half plaited				
			0	4	5	6	7	8	4	5	6	7	8
35 Ne		2.7	0.0081	0.0100	0.0099	0.0087	0.0085	0.0084	0.0108	0.0106	0.0101	0.0099	0.0098
		2.9	0.0080	0.0112	0.0108	0.0101	0.0099	0.0088	0.0114	0.0111	0.0107	0.0101	0.0100
		3.1	0.0079	0.0115	0.0112	0.0109	0.0106	0.0099	0.0118	0.0113	0.0110	0.0108	0.0106
		3.3	0.0079	0.0127	0.0120	0.0117	0.0115	0.0112	0.0121	0.0114	0.0112	0.0109	0.0108
		3.4	0.0078	0.0125	0.0119	0.0115	0.0113	0.0112	0.0119	0.0116	0.0112	0.0110	0.0108
25 Ne		2.7	0.0085	0.0096	0.0089	0.0088	0.0087	0.0086	0.0104	0.0100	0.0098	0.0098	0.0095
		2.9	0.0085	0.0100	0.0096	0.0094	0.0090	0.0087	0.0106	0.0103	0.0101	0.0099	0.0098
		3.1	0.0084	0.0104	0.0103	0.0102	0.0095	0.0093	0.0112	0.0111	0.0103	0.0101	0.0100
		3.3	0.0083	0.0104	0.0104	0.0103	0.0096	0.0093	0.0113	0.0112	0.0104	0.0102	0.0100
		3.4	0.0083	0.0104	0.0104	0.0103	0.0096	0.0093	0.0114	0.0112	0.0104	0.0102	0.0100

Table 10.7. Thermal absorptivity (W. s$^{1/2}$ m^{-2}. K^{-1}) of *SJKF*

Yarn count	Loop length (mm)	SWP (%)	100% cotton	Full plaited					Half plaited				
			0	4	5	6	7	8	4	5	6	7	8
35 Ne		2.7	177	212	206	203	201	198	202	200	199	198	191
		2.9	166	198	193	188	187	183	194	187	181	179	178
		3.1	145	195	185	183	179	178	188	182	180	179	176
		3.3	135	186	182	177	175	173	179	176	174	172	171
		3.4	126	179	177	176	174	167	178	175	174	171	169
25 Ne		2.7	200	255	251	248	246	235	241	238	233	232	215
		2.9	197	247	241	238	235	227	229	223	220	215	211
		3.1	192	232	228	217	212	207	222	219	215	208	200
		3.3	186	232	228	215	210	205	216	210	209	204	199
		3.4	181	230	226	213	205	201	209	208	205	199	188

Table 10.8. Water vapour resistance (Pa.m^2. W^{-1}) of *SJKF*

Yarn count	Loop length (mm)	SWP (%)	100% cotton	Full plaited					Half plaited				
			0	4	5	6	7	8	4	5	6	7	8
35 Ne	Loop length (mm)	2.7	2.4	3.72	3.62	3.44	3.38	3.22	3.28	3.24	3.2	3.18	3.04
		2.9	2.32	3.64	3.52	3.4	3.28	3.22	3.2	3.18	3.06	2.96	2.86
		3.1	2.28	3.36	3.26	3.16	3.18	3.04	3.14	2.94	2.84	2.82	2.68
		3.3	2.24	3.3	3.22	3.14	3.1	3.06	3.06	2.9	2.88	2.86	2.64
		3.4	2.2	3.26	3.1	3.14	3.12	3	2.98	2.9	2.82	2.84	2.66
25 Ne	Loop length (mm)	2.7	2.94	3.82	3.63	3.57	3.47	3.43	3.67	3.57	3.52	3.43	3.43
		2.9	2.92	3.70	3.57	3.47	3.38	3.28	3.63	3.53	3.43	3.38	3.32
		3.1	2.88	3.48	3.37	3.32	3.`28	3.22	3.52	3.43	3.42	3.27	3.23
		3.3	2.82	3.38	3.33	3.28	3.22	3.17	3.47	3.37	3.28	3.27	3.08
		3.4	2.78	3.33	3.32	3.27	3.13	3.12	3.37	3.28	3.22	3.18	3.07

Table 10.9. Air permeability (mm.s^{-1}) of *SJKF*

Yarn count	Loop length (mm)	SWP (%)	100% cotton	Full plaited					Half plaited				
			0	4	5	6	7	8	4	5	6	7	8
35 Ne	Loop length (mm)	2.7	1470	173	236	273	280	287	204	213	216	229	219
		2.9	1800	272	277	284	286	284	223	239	240	277	284
		3.1	1840	293	324	329	374	376	244	271	288	290	310
		3.3	1960	274	273	332	318	323	306	310	334	345	374
		3.4	1990	409	447	382	425	511	349	350	374	395	419
25 Ne	Loop length (mm)	2.7	398	89	105	116	122	126	86	88	86	84	88
		2.9	440	109	111	118	125	126	91	93	103	103	108
		3.1	605	154	168	188	190	210	128	131	130	139	150
		3.3	757	178	190	203	204	212	159	163	179	182	193
		3.4	827	204	203	209	225	230	214	243	256	259	265

Table 10.10. Fabric growth (%) of *SJKF* at loop length 2.9 mm

Spandex state		100% cotton		Full plaited									
SWP (%)		0		4		5		6		7		8	
Relaxation time (min)		1	60	1	60	1	60	1	60	1	60	1	60
Yarn count	35 Ne	2.6	1.6	0.4	0.1	0.9	0.2	0.6	0.2	0.2	0	1.3	0.1
	25 Ne	2.7	1.6	0.8	0.4	.3	0.2	0.9	0.2	1	0.1	1	0

Table 10.11. Fabric stretch (%) of *SJKF* at loop length 2.9 mm

Yarn count			100% cotton		Full plaited									
		SWP (%)	0		4		5		6		7		8	
		Direction of applied force	wales	courses	wales	courses	wales	courses	wales	courses	wales	courses	wales	courses
35 Ne	Extension force	10	7	26	20	24	18	23	19	24	18	23	18	22
		15	12	38	30	39	28	35	28	36	26	37	23	34
		20	13	46	36	50	34	48	33	47	32	46	30	43
		25	14	60	42	58	39	55	38	53	36	53	33	51
25 Ne	Extension force	10	7	14	9	8	8	12	9	11	8	13	7	12
		15	9	21	9	20	12	21	14	20	13	20	11	18
		20	11	28	14	26	15	25	17	26	13	26	14	25
		25	12	34	20	29	17	30	19	30	17	31	16	29

Table 10.12. Fabric thickness at three levels of extension and loop length 3.1 mm (mm) of *SJKF*

Yarn count			Full plaited				
	SWP (%)		4	5	6	7	8
35 Ne	Applied extension (%)	0	0.7235	0.71	0.6776	0.6639	0.6301
		15	0.6883	0.6561	0.6272	0.6194	0.6134
		30	0.6144	0.5855	0.559	0.5465	0.537

Table 10.13. Thermal resistance at three levels of extension and loop length 3.1 mm (W.m^{-1}.K^{-1}) of *SJKF*

Yarn count			Full plaited				
	SWP (%)		4	5	6	7	8
35 Ne	Applied extension (%)	0	0.0675	0.0669	0.0666	0.0661	0.0650
		15	0.0707	0.0693	0.0674	0.0633	0.0622
		30	0.0635	0.0621	0.0592	0.0585	0.0565

Table 10.14. Thermal resistance at three levels of extension and loop length 3.1 mm (m.K.W^{-1}) of *SJKF*

Yarn count			Full plaited				
	SWP (%)		4	5	6	7	8
35 Ne	Applied extension (%)	0	0.0115	0.0112	0.0109	0.0106	0.0099
		15	0.0099	0.0098	0.0095	0.0093	0.0092
		30	0.0097	0.0094	0.0094	0.0091	0.0090

Table 10.15. Thermal absorptivity at three levels of extension and loop length 3.1 mm (W. s$^{1/2}$ m^{-2}. K^{-1}) of *SJKF*

Yarn count			Full plaited				
	SWP (%)		4	5	6	7	8
35 Ne	Applied extension (%)	0	195	185	183	179	178
		15	189	185	179	176	173
		30	184	181	176	170	160

Table 10.16. Predicted values of thermal conductivity (W.m^{-1}. K^{-1}) of elastic *SJKF* produced from yarn count 35 Ne

Loop length (mm)			Full plaited					Half plaited				
		SWP (%)	4	5	6	7	8	4	5	6	7	8
	2.7	A new model	0.0727	0.0711	0.0697	0.0688	0.0679	0.0668	0.0657	0.0651	0.0645	0.0640
		Schuhmeister model	0.0638	0.0627	0.0617	0.0611	0.0605	0.0589	0.0581	0.0578	0.0575	0.0572
		Militky's model	0.0798	0.0782	0.0768	0.0759	0.0750	0.0728	0.0718	0.0713	0.0708	0.0704
		ME-2 model	0.0440	0.0436	0.0431	0.0429	0.0427	0.0412	0.0410	0.0410	0.0409	0.0409
	2.9	A new model	0.0699	0.0675	0.0671	0.0666	0.0656	0.0640	0.0639	0.0632	0.0619	0.0617
		Schuhmeister model	0.0614	0.0597	0.0595	0.0592	0.0586	0.0566	0.0566	0.0562	0.0553	0.0552
		Militky's model	0.0764	0.0739	0.0737	0.0732	0.0723	0.0696	0.0696	0.0690	0.0677	0.0676
		ME-2 model	0.0427	0.0419	0.0419	0.0419	0.0416	0.0401	0.0402	0.0401	0.0397	0.0398
	3.1	A new model	0.0656	0.0644	0.0640	0.0642	0.0645	0.0634	0.0630	0.0615	0.0614	0.0614
		Schuhmeister model	0.0579	0.0570	0.0569	0.0572	0.0576	0.0561	0.0559	0.0548	0.0549	0.0550
		Militky's model	0.0715	0.0703	0.0701	0.0704	0.0710	0.0689	0.0686	0.0670	0.0672	0.0673
		ME-2 model	0.0408	0.0404	0.0405	0.0408	0.0411	0.0398	0.0398	0.0393	0.0395	0.0397
	3.3	A new model	0.0653	0.0648	0.0640	0.0633	0.0630	0.0626	0.0623	0.0618	0.0607	0.0606
		Schuhmeister model	0.0577	0.0574	0.0569	0.0565	0.0563	0.0554	0.0554	0.0551	0.0542	0.0543
		Militky's model	0.0712	0.0707	0.0700	0.0694	0.0692	0.0680	0.0679	0.0675	0.0663	0.0663
		ME-2 model	0.0407	0.0406	0.0405	0.0404	0.0404	0.0395	0.0396	0.0395	0.0392	0.0393
	3.4	A new model	0.06432	0.0644	0.0643	0.0641	0.0637	0.0621	0.0612	0.0607	0.0607	0.0607
		Schuhmeister model	0.0644	0.0640	0.0638	0.0634	0.0634	0.0550	0.0545	0.0541	0.0543	0.0544
		Militky's model	0.0569	0.0567	0.0567	0.0566	0.0567	0.0674	0.0666	0.0661	0.0663	0.0665
		ME-2 model	0.0701	0.0698	0.0697	0.0695	0.0697	0.0392	0.0391	0.0390	0.0392	0.0394

Table 10.17. Predicted values of thermal conductivity (W.m^{-1}. K^{-1}) of elastic *SJKF* produced from yarn count 25 Ne

			Full plaited					Half plaited				
		SWP (%)	4	5	6	7	8	4	5	6	7	8
Loop length (mm)	2.7	A new model	0.0796	0.0783	0.0776	0.0765	0.0762	0.0740	0.0736	0.0724	0.0719	0.0707
		Schuhmeister model	0.0696	0.0687	0.0683	0.0676	0.0675	0.0649	0.0647	0.0635	0.0641	0.0629
		Militky's model	0.0879	0.0866	0.0860	0.0850	0.0849	0.0813	0.0810	0.0793	0.0801	0.0784
		ME-2 model	0.0474	0.0471	0.0470	0.0468	0.0469	0.0446	0.0447	0.0442	0.0447	0.0441
	2.9	A new model	0.0769	0.0756	0.0751	0.0745	0.0741	0.0718	0.0723	0.0710	0.0708	0.0697
		Schuhmeister model	0.0673	0.0664	0.0662	0.0659	0.0658	0.0630	0.0636	0.0627	0.0627	0.0620
		Militky's model	0.0847	0.0834	0.0830	0.0826	0.0824	0.0786	0.0795	0.0782	0.0782	0.0772
		ME-2 model	0.0461	0.0458	0.0458	0.0458	0.0458	0.0436	0.0441	0.0437	0.0439	0.0436
	3.1	A new model	0.0733	0.0726	0.0719	0.0701	0.0683	0.0711	0.0704	0.0722	0.0691	0.0688
		Schuhmeister model	0.0642	0.0639	0.0635	0.0621	0.0608	0.0624	0.0621	0.0638	0.0613	0.0613
		Militky's model	0.0804	0.0798	0.0792	0.0773	0.0754	0.0778	0.0773	0.0797	0.0762	0.0761
		ME-2 model	0.0443	0.0442	0.0442	0.0435	0.0429	0.0433	0.0432	0.0443	0.0431	0.0432
	3.3	A new model	0.0732	0.0717	0.0703	0.0695	0.0672	0.0707	0.0702	0.0696	0.0692	0.0694
		Schuhmeister model	0.0642	0.0631	0.0622	0.0617	0.0598	0.0621	0.0619	0.0616	0.0614	0.0609
		Militky's model	0.0804	0.0788	0.0774	0.0767	0.0741	0.0774	0.0770	0.0766	0.0763	0.0756
		ME-2 model	0.0443	0.0438	0.0434	0.0433	0.0424	0.0431	0.0431	0.0431	0.0431	0.0430
	3.4	A new model	0.0721	0.0713	0.0694	0.0688	0.0670	0.0678	0.0686	0.0681	0.0664	0.0652
		Schuhmeister model	0.0633	0.0628	0.0614	0.0611	0.0597	0.0597	0.0606	0.0603	0.0590	0.0582
		Militky's model	0.0790	0.0783	0.0763	0.0758	0.0739	0.0740	0.0752	0.0749	0.0730	0.0718
		ME-2 model	0.0438	0.0436	0.0430	0.0429	0.0423	0.0418	0.0424	0.0424	0.0418	0.0415

10.2 Appendix (II) for factorial design

Table 10.18. Factorial analysis of fabric thickness

Source	DF	Adj SS	Adj MS	F-Value	P-Value	VIF
Model	99	1.15429	0.01166	267.62	0.000	
Linear	10	1.0247	0.10247	2351.99	0.000	
spandex form	1	0.00017	0.00017	3.97	0.047	1
Yarn count	1	0.00125	0.00125	28.79	0.000	1
loop length	4	0.42339	0.10585	2429.51	0.000	1.6
spandex percent	4	0.59988	0.14997	3442.27	0.000	1.6
2-Way Interactions	33	0.07183	0.00218	49.96	0.000	
spandex form*Yarn count	1	0.00061	0.00061	13.89	0.000	1
spandex form*loop length	4	0.0161	0.00403	92.39	0.000	1.6
spandex form*spandex percent	4	0.0188	0.0047	107.88	0.000	1.6
Yarn count*loop length	4	0.00441	0.0011	25.29	0.000	1.6
Yarn count*spandex percent	4	0.00199	0.0005	11.43	0.000	1.6
loop length*spandex percent	16	0.02993	0.00187	42.93	0.000	2.56
3-Way Interactions	40	0.04764	0.00119	27.33	0.000	
spandex form*Yarn count*loop length	4	0.0063	0.00157	36.12	0.000	1.6
spandex form*Yarn count*spandex percent	4	0.00554	0.00138	31.76	0.000	1.6
spandex form*loop length*spandex percent	16	0.02877	0.0018	41.27	0.000	2.56
Yarn count*loop length*spandex percent	16	0.00704	0.00044	10.1	0.000	2.56
4-Way Interactions	16	0.01012	0.00063	14.52	0.000	
spandex form*Yarn count*loop length*spandex percent	16	0.01012	0.00063	14.52	0.000	2.56
Error	900	0.03921	4.4E-05			
Total	99	1.1935				

Table 10.19. Factorial analysis of thermal conductivity

Source	DF	Adj SS	Adj MS	F-Value	P-Value	VIF
Model	99	0.01954	0.0002	685.89	0.000	
Linear	10	0.01874	0.00187	6511.45	0.000	
spandex form	1	0.00364	0.00364	12642.1	0.000	1
Yarn count	1	0.0103	0.0103	35802.1	0.000	1
loop length	4	0.0028	0.0007	2435	0.000	1.6
spandex percent	4	0.00199	0.0005	1732.56	0.000	1.6
2-Way Interactions	33	0.0006	1.8E-05	63.14	0.000	
spandex form*Yarn count	1	0	0	0	0.967	1
spandex form*loop length	4	0.00019	4.8E-05	167.68	0.000	1.6
spandex form*spandex percent	4	1.2E-05	3E-06	10.44	0.000	1.6
Yarn count*loop length	4	6.2E-05	1.6E-05	53.88	0.000	1.6
Yarn count*spandex percent	4	0.00028	0.00007	244.81	0.000	1.6
loop length*spandex percent	16	5.1E-05	3E-06	11.03	0.000	2.56
3-Way Interactions	40	0.00018	5E-06	15.88	0.000	
spandex form*Yarn count*loop length	4	4.4E-05	1.1E-05	37.92	0.000	1.6
spandex form*Yarn count*spandex percent	4	4E-06	1E-06	3.66	0.006	1.6
spandex form*loop length*spandex percent	16	0.00006	4E-06	13.05	0.000	2.56
Yarn count*loop length*spandex percent	16	7.5E-05	5E-06	16.26	0.000	2.56
4-Way Interactions	16	0.00002	1E-06	4.33	0.000	
spandex form*Yarn count*loop length*spandex percent	16	0.00002	1E-06	4.33	0.000	2.56
Error	900	0.00026	0			
Total	999	0.0198				

Model summary

S	R-sq	R-sq(adj)	R-sq(pred)
0.000536	98.69%	98.55%	98.39%

Table 10.20. Factorial analysis of thermal resistance

Source	DF	Adj SS	Adj MS	F-Value	P-Value	VIF
Model	99	0.00085	9E-06	1151.96	0.000	
Linear	10	0.00072	7.2E-05	9628.69	0.000	
spandex form	1	5.3E-05	5.3E-05	7158.94	0.000	1
Yarn count	1	0.00016	0.00016	21945.9	0.000	1
loop length	4	0.00028	7.1E-05	9515.42	0.000	1.6
spandex percent	4	0.00022	5.4E-05	7280.1	0.000	1.6
2-Way Interactions	33	9.7E-05	3E-06	392.21	0.000	
spandex form*Yarn count	1	1.8E-05	1.8E-05	2455.33	0.000	1
spandex form*loop length	4	3.6E-05	9E-06	1218.03	0.000	1.6
spandex form*spandex percent	4	3E-06	1E-06	89.06	0.000	1.6
Yarn count*loop length	4	3.3E-05	8E-06	1092.15	0.000	1.6
Yarn count*spandex percent	4	3E-06	1E-06	115.67	0.000	1.6
loop length*spandex percent	16	3E-06	0	26.76	0.000	2.56
3-Way Interactions	40	3.4E-05	1E-06	114.61	0.000	
spandex form*Yarn count*loop length	4	1.4E-05	4E-06	471.58	0.000	1.6
spandex form*Yarn count*spandex percent	4	4E-06	1E-06	142.13	0.000	1.6
spandex form*loop length*spandex percent	16	5E-06	0	41.1	0.000	2.56
Yarn count*loop length*spandex percent	16	1.1E-05	1E-06	91.98	0.000	2.56
4-Way Interactions	16	2E-06	0	14.34	0.000	
spandex form*Yarn count*loop length*spandex percent	16	2E-06	0	14.34	0.000	2.56
Error	900	7E-06	0			
Total	999	0.00086				

Model summary

S	R-sq	R-sq(adj)	R-sq(pred)
8.64E-05	99.22%	99.13%	99.03%

Table 10.21. Factorial analysis of thermal absorptivity

Source	DF	Adj SS	Adj MS	F-Value	P-Value	VIF
Model	99	518476	5237	281.94	0.000	
Linear	10	501128	50113	2697.78	0.000	
spandex form	1	16908	16908	910.21	0.000	1
Yarn count	1	340074	340074	18307.6	0.000	1
loop length	4	106777	26694	1437.07	0.000	1.6
spandex percent	4	37369	9342	502.93	0.000	1.6
2-Way Interactions	33	13959	423	22.77	0.000	
spandex form*Yarn count	1	4673	4673	251.56	0.000	1
spandex form*loop length	4	1597	399	21.5	0.000	1.6
spandex form*spandex percent	4	687	172	9.25	0.000	1.6
Yarn count*loop length	4	2263	566	30.45	0.000	1.6
Yarn count*spandex percent	4	3696	924	49.74	0.000	1.6
loop length*spandex percent	16	1043	65	3.51	0.000	2.56
3-Way Interactions	40	2748	69	3.7	0.000	
spandex form*Yarn count*loop length	4	695	174	9.35	0.000	1.6
spandex form*Yarn count*spandex percent	4	233	58	3.13	0.014	1.6
spandex form*loop length*spandex percent	16	850	53	2.86	0.000	2.56
Yarn count*loop length*spandex percent	16	972	61	3.27	0.000	2.56
4-Way Interactions	16	640	40	2.15	0.005	
spandex form*Yarn count*loop length*spandex percent	16	640	40	2.15	0.005	2.56
Error	900	16718	19			
Total	999	535194				

Model summary

S	R-sq	R-sq(adj)	R-sq(pred)
4.30994	96.88%	96.53%	96.14%

Table 10.22. Factorial analysis of water vapour resistance

Source	DF	Adj SS	Adj MS	F-Value	P-Value	VIF
Model	99	59.148	0.5975	204.3	0.000	
Linear	10	51.3571	5.1357	1756.13	0.000	
spandex form	1	6.241	6.241	2134.08	0.000	1
Yarn count	1	16.641	16.641	5690.31	0.000	1
loop length	4	16.2186	4.0546	1386.47	0.000	1.6
spandex percent	4	12.2566	3.0641	1047.77	0.000	1.6
2-Way Interactions	33	6.613	0.2004	68.52	0.000	
spandex form*Yarn count	1	5.6852	5.6852	1944.01	0.000	1
spandex form*loop length	4	0.1328	0.0332	11.35	0.000	1.6
spandex form*spandex percent	4	0.0572	0.0143	4.89	0.001	1.6
Yarn count*loop length	4	0.2368	0.0592	20.24	0.000	1.6
Yarn count*spandex percent	4	0.1492	0.0373	12.75	0.000	1.6
loop length*spandex percent	16	0.3518	0.022	7.52	0.000	2.56
3-Way Interactions	40	1.0217	0.0255	8.73	0.000	
spandex form*Yarn count*loop length	4	0.1654	0.0414	14.14	0.000	1.6
spandex form*Yarn count*spandex percent	4	0.0042	0.0011	0.36	0.835	1.6
spandex form*loop length*spandex percent	16	0.612	0.0383	13.08	0.000	2.56
Yarn count*loop length*spandex percent	16	0.24	0.015	5.13	0.000	2.56
4-Way Interactions	16	0.1562	0.0098	3.34	0.000	
spandex form*Yarn count*loop length*spandex percent	16	0.1562	0.0098	3.34	0.000	2.56
Error	900	2.632	0.0029			
Total	999	61.78				

Model summary

S	R-sq	R-sq(adj)	R-sq(pred)
0.054078	95.74%	95.27%	94.74%

Table 10.23. Factorial analysis of air permeability

Source	DF	Adj SS	Adj MS	F-Value	P-Value	VIF
Model	99	9413550	95086	946.71	0.000	
Linear	10	8914392	891439	8875.49	0.000	
spandex form	1	126860	126860	1263.06	0.000	1
Yarn count	1	5675543	5675543	56507.7	0.000	1
loop length	4	2847611	711903	7087.96	0.000	1.6
spandex percent	4	264378	66095	658.06	0.000	1.6
2-Way Interactions	33	248003	7515	74.82	0.000	
spandex form*Yarn count	1	12424	12424	123.7	0.000	1
spandex form*loop length	4	91401	22850	227.51	0.000	1.6
spandex form*spandex percent	4	3443	861	8.57	0.000	1.6
Yarn count*loop length	4	64426	16106	160.36	0.000	1.6
Yarn count*spandex percent	4	34997	8749	87.11	0.000	1.6
loop length*spandex percent	16	41311	2582	25.71	0.000	2.56
3-Way Interactions	40	220157	5504	54.8	0.000	
spandex form*Yarn count*loop length	4	129217	32304	321.63	0.000	1.6
spandex form*Yarn count*spandex percent	4	1931	483	4.81	0.001	1.6
spandex form*loop length*spandex percent	16	59225	3702	36.85	0.000	2.56
Yarn count*loop length*spandex percent	16	29784	1861	18.53	0.000	2.56
4-Way Interactions	16	30998	1937	19.29	0.000	
spandex form*Yarn count*loop length*spandex percent	16	30998	1937	19.29	0.000	2.56
Error	900	90395	100			
Total	999	9503945				

Model summary

S	R-sq	R-sq(adj)	R-sq(pred)
10.0219	99.05%	98.94%	98.83%

Table 10.24. Variance analysis of fabric growth

Source	DF	Adj SS	Adj MS	F-Value	P-Value	VIF
yarn count	1	14.045	14.045	113.03	0.000	1.00
direction of applied tension	1	142.805	142.805	1149.24	0.000	1.00
relaxation time	1	35.28	35.28	283.92	0.000	1.00
SWP	4	8.242	2.061	16.58	0.000	1.60
yarn count*direction of applied tension	1	9.68	9.68	77.90	0.000	1.00
yarn count*relaxation time	1	0.245	0.245	1.97	0.162	1.00
yarn count*SWP	4	4.417	1.104	8.89	0.000	1.60
direction of applied tension*relaxation time	1	3.125	3.125	25.15	0.000	1.00
direction of applied tension*SWP	4	3.207	0.802	6.45	0.000	1.60
relaxation time*SWP	4	1.883	0.471	3.79	0.006	1.60
yarn count*direction of applied tension*SWP	4	2.582	0.646	5.2	0.001	1.60
yarn count*relaxation time*SWP	4	1.667	0.417	3.35	0.011	1.60
Error	169	21	0.124			
Lack-of-Fit	9	1.2	0.133	1.08	0.382	
Pure Error	160	19.8	0.124			
Total	199	248.18				

Table 10.25. Variance analysis of fabric stretch

Source	DF	Adj SS	Adj MS	F-Value	P-value	VIF
Yarn count	1	28291	28291	118497	0.000	1.00
Direction of applied force	1	8968	8968	37563	0.000	1.00
SWP	4	542	136	568	0.000	1.60
Applied force	3	21758	7253	30378	0.000	1.50
Yarn count*Direction of applied force	1	256	256	1072	0.000	1.00
Yarn count*SWP	4	214	53	224	0.000	1.60
Yarn count*Applied force	3	1608	536	2245	0.000	1.50
Direction of applied force*SWP	4	93	23	97	0.000	1.60
Direction of applied force*Applied force	3	1487	496	2076	0.000	1.50
SWP*Applied force	12	144	12	50	0.000	2.40
Yarn count*Direction of applied force*SWP	4	45	11	47	0.000	1.60
Yarn count*Direction of applied force*Applied force	3	32	11	45	0.000	1.50
Yarn count*SWP*Applied force	12	38	3	13	0.000	2.40
Direction of applied force*SWP*Applied force	12	28	2	10	0.000	2.40
Yarn count*Direction of applied force*SWP*Applied force	12	38	3	13	0.000	2.40
Error	320	76	0			
Total	399	63620				

Table 10.26. Variance analysis of fabric thickness versus Extension percent and *SWP*

Source	DF	Adj SS	Adj MS	F-Value	P-Value	VIF
Extension percent	2	0	0	2464.560	0.00	1.3
SWP	4	0	0	487.970	0.00	1.6
Extension perecnt*SWP	8	0	0	9.600	0.00	2.13
Error	135	0	0			
Total	149	0				

Table 10.27. Variance analysis of thermal conductivity versus Extension percent and *SWP*

Source	DF	Adj SS	Adj MS	F-Value	P-Value	VIF
Extension percent	2	0	0	1014.530	0.00	1.3
SWP	4	0	0	255.600	0.00	1.6
Extension percent*SWP	8	0	0	31.830	0.00	2.13
Error	135	0	0			
Total	149	0				

Table 10.28. Variance analysis of thermal resistance versus Extension percent and *SWP*

Source	DF	Adj SS	Adj MS	F-Value	P-Value	VIF
Extension percent	2	0	0	4389.990	0.00	1.3
SWP	4	0	0	596.230	0.00	1.6
Extension percent*SWP	8	0	0	61.030	0.00	2.13
Error	135	0	0			
Total	149	0				

Table 10.28. Variance analysis of thermal absorptivity versus Extension percent and *SWP*

Source	DF	Adj SS	Adj MS	F-Value	P-Value	VIF
Extension percent	2	2479	1239	67.570	0.00	1.3
SWP	4	6543	1636	89.190	0.00	1.6
Extension percent*SWP	8	540	68	3.680	0.00	2.13
Error	135	2476	18			
Total	149	12038				

11. CHAPTER 11: LIST OF PAPERS PUBLISHED BY THE AUTHOR

11.1 List of journal papers

1) **Khalil, A**., Fouda, A., Těšinová, P., & Eldeeb, A. S. (2021). Comprehensive assessment of the properties of cotton single Jersey knitted fabrics produced from different Lycra States. *AUTEX Research Journal, 21*(1), 71-78.

2) **Khalil, A**., Aboalasaad, A. R., & Těšinová, P. (2021). Thermal comfort properties of cotton/spandex single jersey knitted fabric. Industria Textila, 72(3), 244-249. 21.

3) **Khalil, A**., Těšinová, P. & Aboalasaad, A. (2021). Effect of Lycra Weight Percent and Loop Length on Thermo-physiological Properties of Elastic Single Jersey Knitted Fabric. Autex Research Journal, 22(4) 419-426.

4) **Khalil, A**., Eldeeb, M., Těšinová, P., & Fouda, A. (2023). Theoretical Porosity of Elastic Single Jersey Knitted Fabric Based on 3D Geometrical Model of Stitch Overlapping. Journal of Natural Fibers, 20(1). https://doi.org/10.1080/15440478.2023.2181274

5) Aboalasaad, A., Sirková, B., Mansoor, T., Skenderi, Z. & **Khalil, A**. (2020). Theoretical and Experimental Evaluation of Thermal Resistance for Compression Bandages. Autex Research Journal, 22(1) 18-25.

6) Mansoor, T., Hes, L., **Khalil, A.**, Militky, J., Tunak, M., Bajzik, V., Kyosev, Y. (2021). Conductive Heat Transfer Prediction of Plain Socks in Wet State. Autex Research Journal, 22(4) 391- 403.

7) Aboalasaad, A., Skenderi, Z., Brigita Kacavas's. & **Khalil, A**. (2020). Analysis of Factors Affecting Thermal Comfort Properties of Woven Compression Bandages. Autex Research Journal,20(2) 178-185.

8) Fouda, A., Těšinová, P., **Khalil, A.**, & Eldeeb, M. (2022). Thermo-physiological properties of polyester chenille single Jersey knitted fabrics. Alexandria Engineering Journal, 61(9), 7029-7036

11.2 List of Conferences Participation

1) **Khalil, A**., El-Shahat, I.M., Těšinová, P., Eldeeb, A.S. "Estimate Thermal Comfort Properties of Bed Cover Produced from Double Honeycomb", the 9th Central European Conference, Liberec, PhD student day, September 14th, 2017.

2) **Khalil, A**., Tešinová, P., & Aboalasaad, A. R. "Geometrical and Thermal Properties of Stretched Single Jersey   Knitted Fabric". Workshop for PhD student, Liberec, November 2019.

3) **Khalil, A**., Tešinová, P., & Aboalasaad, A. R. "Effect of Some Knitted Fabric Structures on Thermal Comfort Properties". Workshop for PhD student, Liberec, January 2021.

4) **Khalil, A**., Tešinová, P., & Aboalasaad, A. R. (2019). Thermal comfort properties of single jersey knitted fabric produced at different Lycra states. *ICNF 2019-4th International Conference on Natural Fibres*. Porto, Portugal.

5) **Khalil, A.**, Tešinová, P., & Aboalasaad, A. R., "Geometrical and Thermal Properties of Elastic Single Jersey Knitted Fabric", ICNF 5th International Conference on Natural Fibres conference, Portugal, 17-19 May 2021.

6) **Khalil, A**., Tešinová, P., & Aboalasaad, A. R. "Correlation between Geometrical and Thermo-physiological Properties of Elastic Knitted Fabric". Autex 2021 - 20th World Textile Conference, Portugal, 100% online.

7) **Khalil, A**., & Tešinová, P. "Elastic Recovery of Full Plaited Knitted Fabric". Autex 2022 - 21 World Textile Conference, Lodz, Portugal.

12.   CHAPTER 12: CURRICULUM VITAE

Personal Data

Name: Amany Ahmed Salama Khalil.

Sex: Female

Nationality: Egyptian

Date of birth: 02.07.1985, Dakahlia, Egypt.

Permanent Address: 6 Amr Ibn Elaas Street, Mansoura, Egypt.

Mobile number: +420776690508.

Marital status: Married, has three kids.

Email: engamanysalama@gmail.com & amany.khalil@tul.cz

Education

- **M.Sc.** degree in textile engineering "**Comparative Study between Double Honeycomb and Weft Backed Fabric**", 2015.
- Bachelor science in textile engineering, Mansoura University, June 2007, **"Very good with honour degree", Ranked 1ˢᵗ of class**.
- Undergraduate project: "**Quality control of knitted fabric properties**", with grade "**Excellent**".

Employment Experience

1) **PhD scholar** in Technical University of Liberec, Department of Textile Evaluation (15.12.2016) till now.
2) **Lecturer assistant,** from (12-2015) till now, Faculty of Engineering, Textile Department, Mansoura University, Egypt.
3) **Demonstrator,** from (12-2007) until (11-2015), Faculty of Engineering, Textile Department, Mansoura University, Egypt.
4) **Production engineer** in EL GAZZAR CO. for knitwear**,** from (7-2007) till (11-2007), 80 Abdel Salam Aref St. El Mansoura, El Dakahleya, Egypt.

Internship

1) Internship no I in Mansoura University, Egypt (15.05.2017 to 14.06.2017)
2) Internship no II in Mansoura University, Egypt (11.02.2019 to 10.04.2019)
3) Internship III in El Nasr Clothing and Textiles Company (Kabo), Alexandria, Egypt (03.12.2019 to 18.02.2020).

Training

1- Training in "Masr Company for Spinning and Weaving", Mahala El Kobra, Egypt.

From (6:9-2006).

2- Training in "Dakahlia (DTEX) Company for Spinning and Dying" in Mansoura, Egypt. (6:9-2005).

Personal Skills

- **Computer:**
  - Software:
    - Matlab
    - AutoCAD
    - Iventor
    - Internet (Browsing, Searching…).
  - Hardware:
    - Aware of common hardware problems.
- **Languages:**
  - First language   : Arabic (Native)
  - Second language: English (Very good)